Czech Technical University in Prague

Faculty of Electrical Engineering

Doctoral Thesis

June 2017

Rajdi Agalliu

Czech Technical University in Prague

Faculty of Electrical Engineering
Department of Telecommunication Engineering

OPTIMIZATION OF OPTICAL TRANSMISSION SYSTEMS

Doctoral Thesis

Rajdi Agalliu

Prague, *June 2017*

Ph.D. Programme: (P2612) Electrical Engineering and Information Technology
Branch of study: (2601V013) Telecommunication Engineering

Supervisor: ***Ing. Michal Lucki, Ph.D.***

Abstract and Contributions

This doctoral thesis deals with the design and optimization of optical networks. The two main research areas are optimization of network capacity and transmission rate. The primary goal of the research in network capacity is to investigate all possibilities of utilizing in the most efficient way the available bandwidth without any major network hardware upgrade and to propose new solutions that significantly increase the potential number of subscribers in a given transmission system. The goal of the second part of this thesis is to achieve the highest possible transmission rates. Research in optical transceiver design was done primarily in terms of modulation formats, which play the most significant role in signal transmission over optical media and have a direct impact on transmission rates. Both topics are closely related to each other and they represent the key components of optimizing optical networks. In particular, the main contributions of the doctoral thesis are as follows:

- Optimization of the existing solutions in DWDM systems in terms of their transmission rate, network capacity and physical reach.
- Investigation of the most promising modulation formats for transponders operating at 100 Gbps and beyond.
- Design of dynamic solutions which are capable of supporting different bit rates and channel upgrades from a long-term perspective.
- Shrink of the gap between revenues and implementation cost. Maximal utilization of the fiber capacity while minimizing the cost per transmitted data.
- Research on network transparency and potential convergence of networks at the physical layer.
- Optimization of passive optical network component, such as splitters.
- Systematic design of optical networks based on the topology, number of channels, most effective modulation and highest possible throughput.

Keywords:

Optical design, optical fiber communication, hybrid TDM/WDM networks, modulation formats, OptSim.

Abstrakt

Tato disertační práce se zabývá návrhem a optimalizací optických přenosových sítí. Dvě hlavní oblasti výzkumu jsou optimalizace kapacity sítě a přenosové rychlosti. Primárním cílem výzkumu síťové kapacity je prozkoumat všechny možnosti využití dostupné šířky pásma co nejefektivnějším způsobem bez velkých síťových změn a navrhnout nová řešení, která výrazně zvyšují počet účastníků v daném přenosovém systému. Cílem druhé části práce je dosáhnout co nejvyšší možnou přenosovou rychlost. Výzkum v oblasti konstrukce optických přijímačů a vysílačů byl proveden především z hlediska modulačních formátů, které hrají nejvýznamnější roli v přenosu signálu v optických médiích a mají přímý vliv na přenosové rychlosti. Obě témata úzce navazují a představují klíčové prvky optimalizace optických sítí. Hlavní přínosy disertační práce jsou:

- Optimalizace stávajících řešení v DWDM systémech z hlediska jejich přenosové rychlosti, kapacity sítě a fyzického dosahu.
- Výzkum modulačních formátů pro transpondery pracující na rychlosti 100 Gbps a výšší.
- Návrh dynamických řešení, která jsou schopna podporovat různé přenosové rychlosti a optické kanály z dlouhodobého hlediska.
- Snižování rozdílu mezi příjmy a náklady implementace. Maximální využití kapacity vlákna při současné minimalizaci nákladů ve vztahu k objemu přenášených dat.
- Výzkum v oblasti transparentnosti sítě a potenciální konvergence sítí na fyzické vrstvě.
- Optimalizace pasivních komponent optické sítě, jako jsou rozbočovače.
- Systematický návrh optických sítí založených na topologii, počtu kanálů, nejefektivnější modulaci a nejvyšší možnou průchodnost.

Klíčová slova:

Návrh optických sítí, optické komunikační systémy, hybridní TDM/WDM sítě, modulační formáty, OptSim.

Acknowledgement

Research has been supported by the CTU grant under projects SGS13/201/OHK3/3T/13 and SGS16/227/OHK3/3T/13. I would like to express my sincere gratitude to my supervisor Ing. Michal Lucki, Ph.D. for his continuous guidance, support, remarks, motivation and valuable advice.

Special thanks go to the chief of Department of Telecommunication Engineering, Prof. Boris Simak, for ensuring the funding and providing a nice and flexible environment for my research.

Finally, my greatest thanks go to my family members for their support.

Contents

List of Figures

List of Tables

Abbreviations

IPT	Internet Protocol Telephony
CAPEX	Capital Expenditure
OPEX	Operational Expenditure
PMD	Polarization Mode Dispersion
FWM	Four Wave Mixing
BER	Bit Error Rate
SMF	Single Mode Fiber
DSF	Dispersion Shifted Fiber
PDM	Polarization Division Multiplexing
DSP	Digital Signal Processing
PON	Passive Optical Network
TDM	Time Division Multiplexing
10GEPON	10 Gbit/s Ethernet Passive Optical Network
XG-PON	10-Gigabit-capable Passive Optical Network
WDM	Wavelength Division Multiplexing
NE	Network Elements
AON	Active Optical Network
TDSS	Time Domain Split-Step
CWDM	Coarse Wavelength Division Multiplexing
DWDM	Dense Wavelength Division Multiplexing
XPM	Cross-Phase Modulation
OAN	Optical Access Network
GPON	Gigabit Passive Optical Network
OLT	Optical Line Termination
ODN	Optical Distribution Network
ONU	Optical Network Units
NT	Network Termination
ONT	Optical Network Termination
FEC	Forward Error Correction
OA	Optical Amplifier

ITU-T	Telecommunication Standardization Sector of the International Telecommunications Union
DFB	Distributed Feedback laser
EPON	Ethernet Passive Optical Network
ATM	Asynchronous Transfer Mode
BPON	Broadband Passive Optical Network
GEM	GPON Encapsulation Method
EFM	Ethernet in the First Mile
IEEE	The Institute of Electrical and Electronics Engineers
EDFA	Erbium Doped Fiber Amplifier
SSMF	Standard Single Mode Fiber
RZ	Return to Zero
NRZ	Non Return to Zero
DWA	Dynamic Wavelength Allocation
DBA	Dynamic Bandwidth Allocation
FTTx	Fiber To The x
CSRZ	Carrier-Suppressed Return to Zero
OOK	On-Off Keying
CD	Chromatic Dispersion
ASK	Amplitude Shift Keying
OSNR	Optical Signal-to-Noise Ratio
CRZ	Chirped Return to Zero
DB	Duobinary
PSBT	Phase Shaped Binary Transmission
LEAF	Large Effective Area Fiber
DGD	Differential Group Delay
PSK	Phase-Shift Keying
DPSK	Differential Binary Phase-Shift Keying
MZM	Mach-Zehnder Modulator
MZI	Mach-Zehnder Interferometer
DQPSK	Differential Quadrature Phase-Shift Keying
QAM	Quadrature Amplitude Modulation
CO-OFDM	Coherent Optical Orthogonal Frequency Division Multiplexing

DP-MB-OFDM	Dual Polarization Multi-Band Optical Orthogonal Frequency Division Multiplexing
EDC	Electronic Dispersion Compensation
MMF	Multi-Mode Fiber
FFE	Feed-Forward Equalization
LMS	Least Mean Square
MMSE	Minimum Mean Square Error
DFE	Decision Feedback Equalizer
MLSE	Maximum Likelihood Sequence Estimation
ADC	Analog to Digital Converter
SER	Sequence Error Rate
SSB	Single Side-Band
PRBS	Pseudo-Random Binary Sequence
FDSS	Frequency Domain Split Step
FFT	Fast Fourier Transform
IFFT	Inverse Fast Fourier Transform
ISI	Inter-Symbol Interference
VoIP	Voice over Internet Protocol
CW	Continuous Wave
LPF	Low-Pass Filter
SLA	Service Level Agreement
AWG	Arrayed Waveguide Grating

Chapter 1
Introduction

1.1 Motivation

This doctoral thesis summarizes the research work, which was done by the author from September 2013 until March 2017. Research was funded by the Czech Technical University grant projects SGS13/201/OHK3/3T/13 and SGS16/227/OHK3/3T/13, which were focused on photonic transmission media and components for optical telecommunication networks.

Nowadays, the common optical transmission rates can vary from 100 Mbps to 100 Gbps per optical channel. This has been achieved by designing transceivers from the simplest intensity modulated to those very complex ones, which combine simultaneously several techniques, in order to fully utilize the transmission media capabilities.

Current optical networks deal with increasing bandwidth demands for higher transmission rates and capacities due to the growth in data traffic. The emerging services, including Internet Protocol Telephony (IPT), video conferencing, ultra-high-definition television, cloud services and $4^{th}/5^{th}$ Generation mobile Xhaul are gradually consuming the available bandwidth in the existing networks and driving capacity demands beyond any expectation.

Providers, which are planning the deployment of new networks or their expansion, need to evaluate both the required new network investment, i.e. capital expenditure (CAPEX) such as optical infrastructure, network devices or replacement of all residential gateways at subscribers' premises, as well as the potential operational expenditure (OPEX) saving such as lower energy consumption, more efficient service provisioning or better fault management and maintenance. Indeed, one of the reasons that providers are willing to deploy new network solutions is the achievement of Total Cost of Ownership savings by reducing OPEX.

Network technologies have been significantly and continuously improved during the last 20 years, however, besides modern equipment we can find interconnected to them an old infrastructure which is still in use due to the upgrade cost and Return on Investment in the short term. The simplest example can be optical cables which have been installed in the past and need to be reused despite the fact that new enhanced fiber standards have been launched into the market, even if material cost is lower than the original cables.

1.2 Problem Statement

The selection of an efficient modulation format is a key step in the design of optical systems and their future upgrades, which affects not only the transmission rate, but also the overall implementation cost and system output. The design requires detailed knowledge on performance efficiency of modulation formats, as well as clear specification of shortcomings which need to be solved while proposing new solutions.

The upgrade of fiber optic telecommunication systems from transmission rate 10 Gbps to 40 Gbps, 100 Gbps and above, in many cases requires to converge optical systems, such that their frequency channels do not interfere or limit each other, which often requires the use of sophisticated modulation formats and system transparency. Some modulations cannot operate at higher bit rates because of hardware limitations, lower amount of information bits included in a symbol or because of their lower immunity to dispersion and other physical properties that degrade signal quality [1].

Transition to higher bit rates very often requires solving the problem of Polarization Mode Dispersion (PMD) and nonlinear effects, such as Four Wave Mixing (FWM), which can strongly affect system functionality at 10 Gbps and above, and cause increase in Bit Error Rate (BER). For transmission rates higher than 40 Gbps per optical channel, the use of more complex formats is necessary and the design of new modulations is expected, which effectively utilize the available bandwidth, reduce the symbol rate, are more immune to dispersion, and solve at the same time the problem of FWM. The margin created a few years ago for so-called future use, in many cases appears as not sufficient at present. In practice, there is a will to maximize the use of existing infrastructure, installed fibers; mostly Single Mode Fibers (SMF) exhibiting undesired dispersion or Dispersion Shifted Fibers (DSF) causing the origination of FWM at the C band. The upgrade can also require running a new system over an existing frequency grid by using another modulation format.

Transmission schemes for high-density optical systems operating at 40 and 100 Gbps wavelength channels can use phase modulation combined with Polarization Division Multiplexing (PDM), coherent detection and Digital Signal Processing (DSP). PDM halves the symbol rate, introducing higher bit rates, cheaper components and fitting into a proper channel grid at the cost of an increased transceiver complexity [2]. The research on modulation formats above 100 Gbps is usually more important for backbone networks. While moving closer to subscribers' equipment, lower transmission rates per optical channel can be

sufficient and the main focus are multiplexing techniques that accommodate more users within the same shared bandwidth.

Passive Optical Networks (PON), especially those based on Time-Division Multiplexing (TDM), have been extensively deployed in practice as an advantageous scheme for minimizing implementation and operational costs. Despite of trends to increase the total bit rate to 10 $Gbits^{-1}$ such as 10 Gbit/s Ethernet PON (10GEPON) or 10-Gigabit-capable PON (XG-PON), TDM-PONs cannot cope with the expected extensive bandwidth requirements of future networks. Wavelength Division Multiplexing (WDM) PONs can solve this problem. TDM and WDM techniques can be also combined, resulting in enhanced scalability.

Longer physical reaches can be obtained by installing active Network Elements (NE) within the transmission path, which leads to Active Optical Network (AON) schemes. I investigate all of the above mentioned technologies and options by considering also their potential coexistence at the physical layer to find out new solutions that utilize maximum of the fiber capacity. Simulations are done in the OptSim Software Environment version 5.2 from the RSOFT Design Group based on the Time Domain Split-Step (TDSS) method.

1.3 Aims and Contribution of the Thesis

Several topics attract our attention with the goal to investigate and resolve them. Despite of the goal to maximize the use of existing infrastructure, completely new solutions could lead to substantial profits in the long term. Many topics presented challenges during the research. This doctoral thesis deals with scientific problems related to optimization of optical networks and it contributes mainly to the areas of photonics and telecommunication.

The principal contributions of this thesis are the followings:

- Optimization of the capacity and physical reach of Coarse WDM (CWDM) and Dense WDM (DWDM) systems.
- Investigation of transmission rates at 100 Gbps and beyond per optical channel.
- Design of dynamic solutions, capable of supporting simultaneously different bit rates and channel upgrades from a long-term point of view.
- Proposals on how to maximally utilize the fiber capacity meanwhile minimize the cost per transmitted data.
- Investigation of network transparency and potential convergence of network access solutions at the physical layer.

- Optimization of passive optical network component, such as splitters (bilateral cooperation with FHV Vorarlberg University of Applied Sciences, Research Centre for Microtechnology, Austria).
- Recommendation of systematic optical network designs based on topology, number of channels, most effective modulation and highest possible throughput.

In order to experiment, the OptSim platform can be used as a test environment, as well as other software tools available at the Department of Telecommunication Engineering at the Czech Technical University in Prague. Results discussed in this thesis summarize the main scientific achievements from the research, which was done during the first three years of my doctoral studies and published in [1]-[5].

Modulation formats represent a significant research area in this thesis, due to their importance in network design, nevertheless I also analysed many other aspects of optimizing optical transmission networks starting from the negative phenomena, which affect the transmission of optical signals such as dispersion, attenuation and optical nonlinearities e.g. FWM, Cross-Phase Modulation (XPM), to optimal channel spacing, transmission rate, network topology being used and physical reach. Optical Access Networks (OAN) are simulated based on Gigabit PON (GPON) and XG-PON recommendations with triple-play services, i.e. data, voice and video, in terms of optical reach, number of subscribers, transceiver design and modulation, among others.

This thesis addresses also issues from the perspective of signal regeneration. The convergence of multiple systems at the physical layer is simulated and discussed as well. It provides a detailed report on how the existing fiber infrastructures could be combined and maximally utilized regardless of the data traffic.

Simulations in OptiBPM photonic tool deal with optical splitter construction and their optimization. Investigation was done in cooperation with the Research Centre for Microtechnology, part of Vorarlberg University of Applied Sciences in Austria.

Having collected the research from all these different topics in terms of optimizing the optical systems, this doctoral thesis offers not only a new systematic network design in a broader context, but it also introduces new solutions and innovations on the way how optical systems could efficiently increase their performance.

1.4 Structure of the Thesis

A significant part of the thesis is based on the author's articles and conference papers. Thesis contains only the basic mathematical relations in order to be as readable as possible. The rest of network designs, parameters and mathematical equations can be found in the references listed in the end. The thesis is organized in four chapters as follows:

- Chapter 1 – Introduction: in this chapter, the core research problems are stated and then the aim and contribution of the thesis are listed.
- Chapter 2 – State of the Art: the theoretical background and the general overview on the current state of the art are presented.
- Chapter 3 – Methods: design principles, simulation schemes and numerical methods are described in this chapter.
- Chapter 4 – Results and Discussion: the most important results are presented and discussed.

The overview of accomplishments and scientific achievements together with future improvement research ideas is summarized in the last section entitled "Conclusions".

Chapter 2

State of the Art

2.1 Components of Fiber Optic Systems

Figure 1 shows a typical OAN which consists of one Optical Line Termination (OLT), the Optical Distribution Network (ODN) and Optical Network Units (ONU) followed optionally by Network Termination (NT) equipment, as specified in [6]. Optical NT (ONT) generally defines a special, single-user case of ONU.

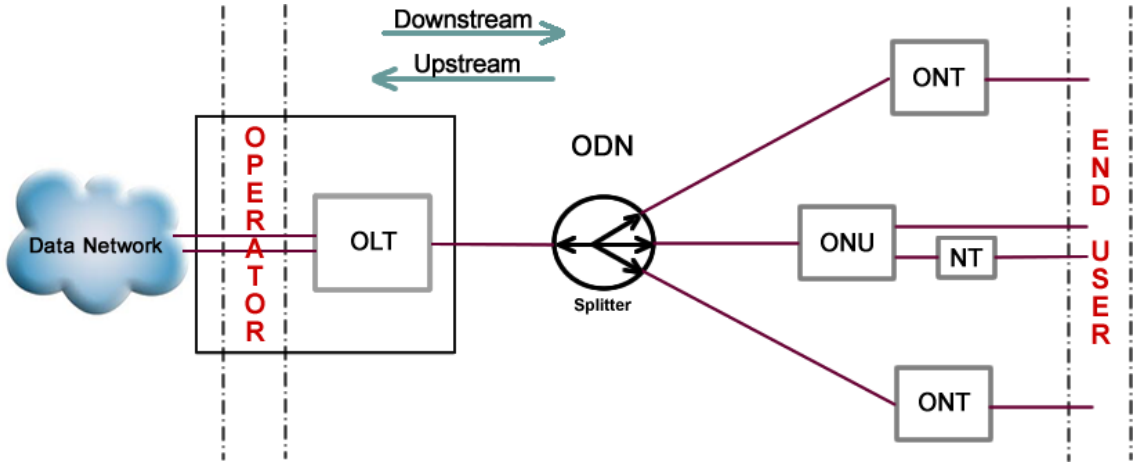

Figure 1: Typical Optical Access Network layout [7]

The current generation of PONs consists of passive NEs in ODN such as fibers, splitters, filters, connectors, couplings, splices etc. PONs are extensively used in practice primarily due their cost effectiveness while satisfying network design parameters to achieve the required quality of service. From the infrastructure point of view, design of such networks is mainly focused on the ODN layout and boundary parameter fulfilment, especially on the attenuation of individual segments. A limiting factor is the optical power budget, which can be overcome by using different techniques, such as Forward Error Correction (FEC) or by deploying optical amplifiers (OA) leading to AONs, which can extend the physical reach between OLT and ONUs and use larger split ratios in the distribution points.

AONs represent the basis of hybrid networks as they form a common platform for other access systems. The disadvantage is their need to ensure power supply for active NEs within ODN. Moving towards the backbone network at providers' premises, a variety of other optical devices can be found such as mux/demux, optical add/drop multiplexers including those reconfigurable ones, optical switches, etc. A detailed description of these devices can be found in [8].

2.2 Optimization of Optical Network Capacity

2.2.1 Wavelength Division Multiplexing

CWDM technique enables simultaneous transmission of several wavelength channels over a single fiber. Wavelength allocation is specified by the Telecommunication Standardization Sector of the International Telecommunications Union (ITU-T) under recommendation G.694.2 [9] for the range between 1270 and 1610 nm [10]. DWDM is characterized by narrower channel spacing, therefore it allows accommodating into the same bandwidth a larger number of wavelength channels than CWDM does. Nevertheless, this comes at the cost of much more expensive devices such as actively cooled optical sources, mainly Distributed Feedback lasers (DFB). Figure 2 graphically summarizes the key differences between CWDM and DWDM.

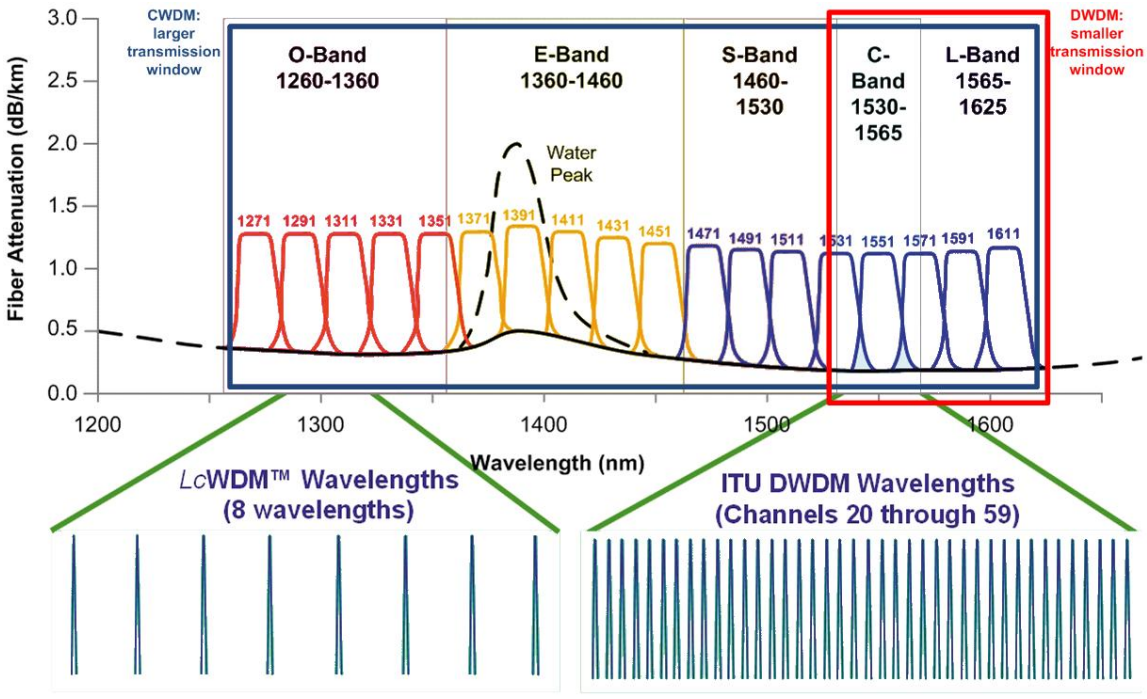

Figure 2: CWDM vs DWDM technique [11]

The 20 nm channel spacing with a tolerance of ± 6-7 nm is specified between CWDM channels in the first place due to the emitted wavelength dependence on temperature of cheap optical sources with low quality. Such dependence can widely vary according to the ambient temperature. CWDM interfaces are specified in the ITU-T G.695 in accordance with various network designs, topologies and fiber types. Table 1 gives a general overview of the common WDM technologies which we find heavily applied in practice.

Table 1: Typically implemented WDM technologies [10]

Technology	**CWDM Access/MAN**	**DWDM MAN/WAN**	**DWDM wide range**
Channels per fiber	4-16	32-80	80-160
Bands	O, E, S, C, L	C, L	C, L, S
Channel spacing	20 nm (2500 GHz)	0.8 nm (100 GHz)	0.4 nm (50 GHz)
Transmission capacity per wavelength	2.5 Gbps	10 Gbps	10-40 Gbps
Fiber transmission capacity	20 – 40 Gbps	100 – 1000 Gbps	> 1 Tbit·s^{-1}
Laser type	Uncooled DFB	Cooled DFB	Cooled DFB
Reach	Up to 80 km	Hundreds of km	Thousands of km
Cost	Low	High	Highest

Further information can be found in [6][10][12]-[14]. Research works in this area are primarily focused on achieving higher transmission rates per wavelength and narrower channel spacing [15][16].

2.2.2 Physical Topology Optimization

Many topologies are suitable for access networks, including tree, tree-and-branch, ring or bus [16]. Redundancy can be achieved by applying double rings, double trees, and so forth. A novel algorithm is introduced in [17] by combining a clustering technique and Steiner tree for optimal deployment of optical cables in ODNs under realistic conditions. Authors in [17] propose an optimized solution for connecting ONUs to OLT through splitters in such a way that the sum of fiber length is close to the shortest possible value for given positions of central offices, subscribers and set of fiber paths.

Proposals for new generation of PONs combine TDM with WDM, leading to hybrid TDM/WDM-PONs. Authors in [18] present a ring-tree ODN, which consists of a WDM

bidirectional ring with cascadable passive “Add&Drop” nodes connected to the TDM access trees. Several benefits come from this topology such as enhanced scalability and granularity. The length of rings may cover longer physical reaches towards a metropolitan range.

For large-scale optical networks, star topology or mesh can be used apart from rings. Mesh offers the highest possible network transmission capacity and a strong redundancy scheme however this comes at the cost of more complex routing algorithms and higher investment cost. The star topology can be more suitable, nevertheless it requires special attention on the proper functionality of the central node. The ring topology has been mostly chosen as an optimal generic solution due to its simpler and cheaper installation although it enables a lower capacity than mesh and star. Its reliability can be increased by applying connected rings.

Each topology optimization relies on good transmission quality at the physical layer between all nodes, hence in this thesis I primarily investigate point to point links which are crucial for any given topology. Star topology is investigated as well since it is a common scheme for OANs.

2.2.3 Recommendations on Optical Access Networks

Figure 3 summarizes the main recommendations of OANs [19].

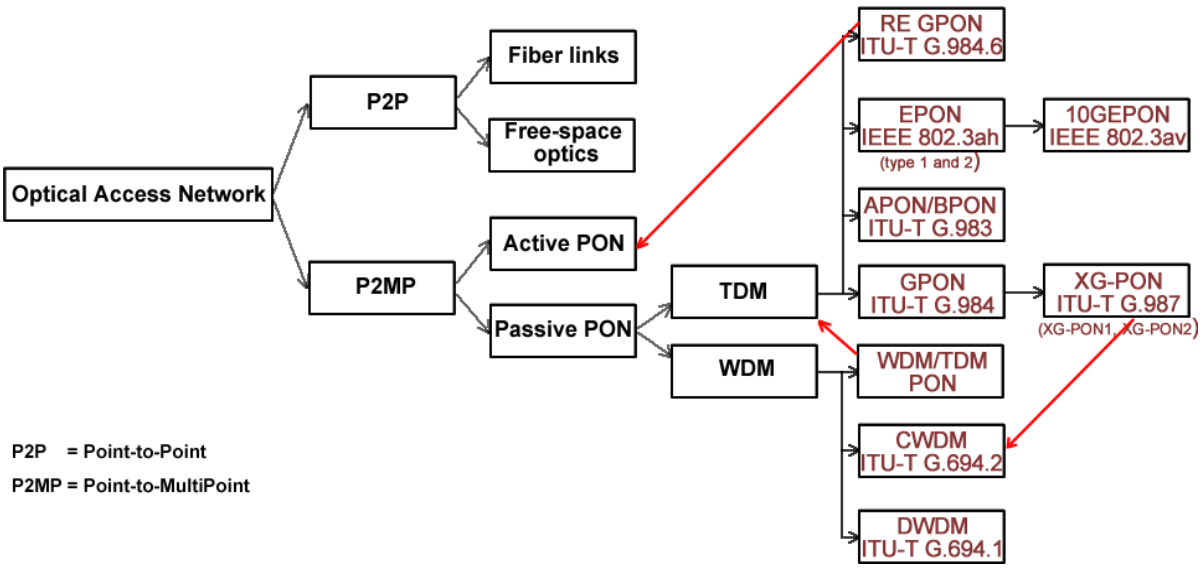

Figure 3: Optical Access Network recommendations

The two main TDM-PONs which have been widely deployed are: GPON mainly in US and Europe; and Ethernet PON (EPON) mainly in Japan and Korea. From users’ perspective,

GPON offers higher bandwidth [13]. From providers' perspective, EPON takes advantage of Ethernet as the most relevant access protocol.

Despite of the newly published standards for 10 Gbps, i.e. 10GEPON [20] and XG-PON [21], TDM-PONs cannot cope with future network evolution due to higher bandwidth and power budget requirements [13]. WDM-PON can utilize more efficiently the available bandwidth by separating ONUs via physical wavelengths. As it will be shown later in this thesis, the most promising solution for next generation optical networks is the combination of both TDM and WDM techniques.

2.2.4 APON/BPON

APON stands for Asynchronous Transfer Mode (ATM) PON. It is described in ITU-T recommendation G.983 [22]. APON consists of the transmission based on ATM cells at 155.52 Mbps in case of symmetric design or 622.08 Mbps of download speed in case of the asymmetric system. On the other hand, for Broadband PON (BPON) were defined the 622.04 Mbps for symmetric systems and downstream line rate of 1244.16 Mbps for the asymmetric ones. Physical and logical reach can be up to 20 km.

2.2.5 GPON

GPON is an evolution of the BPON standard. Table 2 gives an overview of the main GPON parameters, specified in ITU-T recommendation G.984.1 (2008) [23].

Table 2: The main GPON transmission parameters [23]

Downstream	1.244 Gbps, 2.488 Gbps
Upstream	155.52 Mbps, 622.08 Mbps, 1.244 Gbps, 2.488 Gbps
Maximum physical reach	20 km
Maximum logical reach	60 km
Wavelength allocation for downstream	1480 – 1500 nm
Wavelength allocation for upstream	(Originally: 1260 – 1360 nm) 1290 – 1330 nm [24][25]
Maximal mean signal transfer delay	1.5 ms
Max. split ratio	1:64, perspective: 1:128
Data encapsulation mode	GEM/ATM

Besides Gbps speeds, GPON supports also lower data rates like 155.52 Mbps and 622.08 Mbps due to the backward compatibility with earlier PON generations. The common combination is 1.25 Gbps for upstream and 2.5 Gbps for downstream [23]. GPON Encapsulation Method (GEM) protocol is newly introduced in GPON to enable ATM, Ethernet and TDM data transport [23][26].

2.2.6 EPON

Ethernet for access networks is described in [27]. It is known also as Ethernet in the First Mile (EFM). EFM over Copper uses metallic transmission media based on very-high-bit-rate or symmetrical high-speed digital subscriber lines, meanwhile EFM over point-to-point Fiber is aimed for point-to-point fiber connectivity with Ethernet at 100 Mbps (100BASE-BX10-D/U, 100BASE-LX10) and 1 Gbps (1000BASE-BX10-D/U, 1000BASE-LX10). In [27] it is introduced also the concept of EPONs. Its main parameters are summarized in Table 3.

Table 3: The main EPON transmission parameters [19][27]

Transmission rate variants	1G/1G symmetric
Transmission rate at the physical layer	1.25 Gbps
Attenuation classes	PX10, PX20
Wavelength allocation for downstream traffic	1480-1500 nm
Wavelength allocation for upstream traffic	1260-1360 nm
Physical reach	≤10, ≤20 km
Max. split ratio	1:16, 1:32

2.2.7 10GEPON and XG-PON

Recommendation 802.3av [20] from the Institute of Electrical and Electronics Engineers (IEEE) extends the operating speed of EPONs to 10 Gbps, either in symmetric systems with both downstream and upstream at 10 Gbps or asymmetric version with 10 Gbps downstream and 1 Gbps upstream. This recommendation specifies the typical physical reaches and split ratios, however, if the maximum acceptable loss within ODN is satisfied, it is possible to increase a parameter's value at the cost of another one. As an example, if a lower split ratio is applied, it is feasible to extend the physical reach and vice versa. 10GEPON is fully backward compatible with EPON; hence they may run within the same ODN, which benefits in upgrade cost reduction.

In a similar way, ITU-T published a recommendation for a 10 Gigabit capable PON [21], which is backward compatible to its predecessor, i.e. GPON. First world field trial results of XG-PON have been published in [28]. Table 4 compares the main parameters of 10GEPON and XG-PON.

Table 4: Comparison between 10GEPON and XG-PON [20][21][25][27]

	10GEPON – IEEE 802.3av (2009)	**XG-PON – ITU-T G.987.1 (2010)**
Transmission rate variants	10G/10G symmetric	10G/2.5G (XG-PON1) 10G/10G (XG-PON2)
	10G/1G asymmetric	
Transmission rates in physical layer	10.3125 Gbps	9.95328 Gbps
	1.25 Gbps	2.48832 Gbps
Wavelength allocation	Downstream 1575-1580 nm	Downstream 1575-1580 nm
	Upstream 1260-1280 nm or 1260-1360 nm	Upstream 1260-1280 nm
Attenuation classes	PR10, PRX10	Nominal 1
		Nominal 2
	PR20, PRX20	Extended 1
	PR30, PRX30	Extended 2
Physical reach	≤10, ≤20 km	≤20 km (perspective: ≤40 km)
Max. split ratio	1:16, 1:32 (considered higher ratios 1:64, 1:128)	1:64 (1:256 in the logical layer)

2.2.8 Reach Extended GPON

The original specification of GPON in ITU-T G.984 limits the maximum physical reach to 20 km and the split ratio to 1:64. G.984.2 specifies three attenuation ranges (A, B and C), which differ from each other by optical sources and detectors that are being used [29][30]). G.984.2 Amendment 1 [31] defines class B+, which fills the space between B and C classes and Amendment 2 [32] defines class C+. Both B+ and C+ classes work only for the asymmetric version of GPON, i.e. 2.448 Gbps of downstream and 1.244 Gbps of upstream.

A further enhancement of the ODN's attenuation range over class C+ is not possible without using active NEs. For this purpose ITU-T published two amendments, which specify additional modifications such as new attenuation classes and possibility of deploying active NEs to improve GPON limits, named as Reach Extended or Long Reach GPON, specifically: G.984.6 for physical layer parameters [33] and G.984.7 for protocol characteristics [34].

2.2.9 Hybrid PON

Design and deployment activities for OANs are growing to support the exponentially increasing demands and delivery of new multimedia services to the customer premises such as faster internet connectivity, interactive video and voice services.

Fiber to the X (FTTx), where x stands for home, building, office, node, cabinet, etc., employing PON is a standard architecture to deliver triple-play services (data, voice and video) from service providers to subscribers [45]. Both PON standards in FTTx solution area, i.e. GPON and EPON, as well as their 10 Gbps enhanced recommendations are based on TDM [35], which has its limitations. Authors in [36] experimentally demonstrate the 10 Gbps OAN with 256 subscribers and downstream transmission at 1550 nm using a commercial Erbium Doped Fiber Amplifier (EDFA) to reach the maximum distance of 62 km over Standard SMF (SSMF). Besides the deployment of EDFA, modulation formats play also a key factor, which can significantly improve the transmission system. As an example, while comparing Return to Zero (RZ) and Non Return to Zero (NRZ) modulation formats in a co-existing GPON and XG-PON system, the physical reach is greater in case of RZ deployment due to its better immunity to fiber non-linearities [37]. Some solutions beyond 10GEPON/XG-PON are reviewed in [38].

WDM technology is always required as a basis for scalable, future-proof systems, e.g. 100 km x 1000 users x 1000 Mbps. WDM-PON is considered to be the most practical solution for PON capacity expansion. However the 10 Gbps ONUs in pure WDM-PONs are too excessive for next 10 year [39]. Authors in [38] state that there are three options to address 1000 users with a single system: multiple feeder fibers, multi-user wavelength sharing and ultra-dense WDM. The new vision of combining both TDM and WDM techniques seems to be more promising. Authors in [40] propose a hybrid architecture which merges together TDM and WDM capabilities to enable longer optical reach and higher scalability. The main reasons behind the deployment of such networks are to satisfy increasing capacity demand and user density requirements, while ensuring that the cost per unit bandwidth is minimized [41]. TDM/WDM-PON has been recently approved by ITU-T as the primary technology for the second next generation passive optical network (NG-PON2) standard [42].

The most natural combination of TDM and WDM is by cascading them [43]. If each of the wavelength channels operates independently from other ones, then there is no need for any additional medium access control protocol besides the original one from TDM-PON, however this may not utilize the bandwidth efficiently [43]. Dynamic Wavelength Allocation (DWA)

algorithm [43] can be applied to increase the throughput, which in coordination with the Dynamic Bandwidth Allocation (DBA) algorithm enables ONUs to have assigned not only certain times slots, but also specific wavelengths. This combination of DWA and DBA is an important research area in hybrid PONs.

Authors in [13] compare the overall network performance of WDM-PONs and hybrid TDM/WDM-PONs. The lowest ONU link cost of hybrid networks is obtained by combining CWDM and TDM access. On the other hand, DWDM systems require significantly more complex transceivers, among others. The cost and performance of different types of WDM-PONs, including TDM/WDM-PONs, are compared in [44]. In [46] authors evaluate the cost of network migrations starting from GPON to TDM/WDM-PONs. Migration to TDM/WDM-PON turns up as the best solution because of its high bandwidth sharing rate while providing high bandwidth on a per-user basis [47]. Authors in [44]-[46] indicate the cost advantages of network node consolidation due to the more efficient utilization of aggregation networks. Additional physical reach to ONUs can be achieved by using optical amplification as described in [48]-[50].

In this thesis I investigate PONs with triple-play services in terms of optical reach, number of subscribers, transceiver construction, modulation and implementation cost. I search for new solutions to enhance the bandwidth efficiency meanwhile investigating the coexistence of OAN solutions at the physical layer. I consider GPON and XG-PON due to their wider deployment in Europe. GPON and XG-PON are intended to coexist together by applying identical colourless ONUs [51], which brings cost savings, easier network planning and its maintenance. Allocation of the wavelengths is recommended by ITU-T [21] in order to avoid cross-talks between GPON and XG-PON signals, as shown in Figure 4.

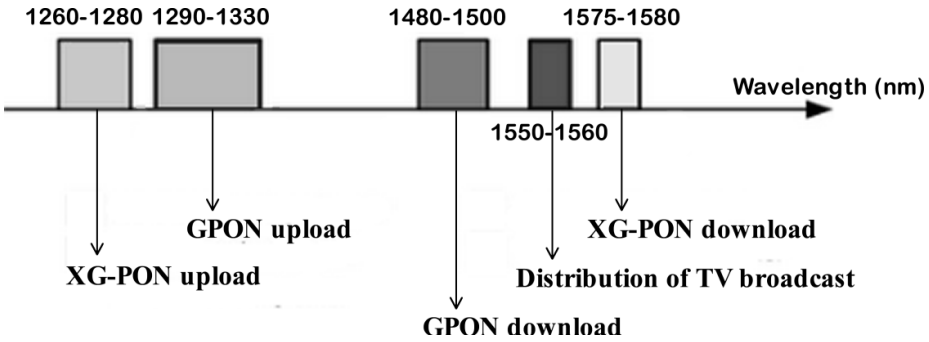

Figure 4: Wavelength ranges for GPON/XG-PON and video components.

2.2.10 Splitter Design

OANs mostly use a tree topology to distribute services from OLTs on providers' edge to ONUs at subscribers' premises. For the design of such networks, one has to consider different aspects like optical linear and nonlinear effects [52], optical attenuation and amplification [50], possible wavelength routing [53], or ageing of network elements [54], among others.

The signal distribution from the OLT to ONUs can be handled by optical splitters, which split the amplitude of one signal into N output signals without applying any other adjustments. Optical splitters are a key component in ODNs not only in pure TDM-PONs or WDM-PONs [55], but also in hybrid broadband access networks [56], as well as in future Ultra-Dense WDM-PONs [57][58]. They are beneficial to reduce the overall network cost implementation, as well as being easy for maintenance and troubleshooting. A splitter can be designed as a cascade of one-by-two waveguide branches, known as Y-branch splitters. The main benefit of this solution is its polarization and wavelength independency, which facilitates signal distribution in the entire operating wavelength window. On the other hand, the fabrication of branching points is demanding and this process generally faces with several problems, such as asymmetry in split ratio.

The core size of waveguides is a key parameter. The commonly used size is 6 μm × 6 μm to match the SMF diameters and minimize the coupling loses. It has been shown that the Y-branch splitter with a smaller waveguide core size can improve the non-uniformity of the power split and enhance the system performance of the network [59]. Authors in [60] analysed the impact of different types of splitter structures in PONs on the resource sharing and power consumption and they pointed out that the combination of cascaded splitters with extended reach is the most beneficial. Authors in [61] proposed a mathematical model for PON planning, where splitter allocation, attenuation and split ratio are considered. Optical splitters can enhance the PON performance efficiency as shown in [62][63]. Many factors have to be considered during their design. For example, the branching angle in Y-branch optical splitters can directly affect the power loss. Authors in [64] showed that the power loss is higher for wider angles. The key parameter remains the split ratio. There is always an interest on finding ways to increase split ratios, because in this manner we could connect more users through the same transmission media. Well-optimized optical splitters are crucial for the long-reach, dense grid, and high split ratio PONs [65]. Authors in [66] described how to design a 1x256 splitter, with an insertion loss below 1.3 dB and channel non-uniformity less than 5 dB within the operating wavelength range from 1530 to 1570 nm.

Asymmetric splitters could be beneficial mainly for balancing the attenuation of ODNs. Three-branch splitter structures can be utilized as a technique to improve the uniformity. Authors in [67] model a novel 1x24 splitter with a three-branch structure and 21 Y-branch elements, which has low insertion loss and good uniformity.

In this thesis, I firstly simulate the standard 1x64 Y-branch splitter with a waveguide core size of 6 μm × 6 μm and then the low-loss length optimized 1x64 splitter with a waveguide core size of 5.5 μm × 5.5 μm. Simulations are based on GPON and XG-PON networks with triple-play services. Bandwidth optimization is obtained by employing CWDM. Data and voice downstream components are transmitted within the wavelength range of 1480-1500 nm for GPON, 1575-1580 nm for XG-PON, and 1550-1560 nm for video services, in accordance with the wavelength allocations shown in Figure 4.

2.3 Optimization of Transmission Rate

2.3.1 Intensity Modulation Formats

NRZ, RZ and Carrier-Suppressed RZ (CSRZ) are well known modulation formats in optical communications [68]. On-Off Keying (OOK) remains the almost exclusively deployed format up to 10 Gbps per optical channel [69] despite the fact that it is the simplest modulation type. Nevertheless, its maximum physical reach at 10 Gbps is strongly limited. The upgrade of existing optical fiber infrastructures to higher bit rates would deal with physical layer constraints, such as Chromatic Dispersion (CD), PMD, fiber nonlinearities, accumulated amplified spontaneous emission noise and filter spectral narrowing [70]. For 10 Gbps DWDM systems, the major sources of optical signal degradation are caused mainly by XPM and FWM [71]. My research was primarily focused on binary intensity formats, due to the significant back-to-back receiver sensitivity penalty of multilevel intensity formats [72][73]. Although a certain combination of Amplitude Shift Keying (ASK) and phase modulation might produce certain benefits, e.g. RZ-DPSK-3ASK format [74], the limited extinction ratios of the ASK modulated levels reduce the Optical Signal-to-Noise Ratio (OSNR) tolerance of the format.

In OOK, binary 1 is represented by an optical carrier and binary 0 by its absence. In RZ-OOK, the transmitted bits don’t occupy the entire bit slot. A duty cycle of 0.5 means the pulses representing binary 1s occupy half of the bit slot. On the other hand, in NRZ-OOK each bit remains at the transmitted value for the entire bit slot and when they are broadened they will leave their desired bit slot. Therefore, NRZ is prone to CD and nonlinear effects,

and it is generally more beneficial because it requires less bandwidth than its counterpart RZ. For basic modulation techniques like RZ and NRZ, the signal can be directly detected using a photodiode. NRZ-OOK has been extensively used in the past as the predominant format in optical communications primarily due to its relatively simple transmitter design and easy signal generation. However its capabilities do not satisfy the rapidly growing network requirements for higher bit rates and high-capacity DWDM transmissions. For such a reason, other formats have to be considered.

Chirped Return to Zero (CRZ) is a variation of RZ, in which each of the pulses is chirped. The most widespread pseudo-multilevel format is CSRZ. In CSRZ, the phase of optical carrier is changed by π every bit regardless of data traffic. As a result, the phases of a given binary sequence are subtracted, the central peak at the carrier frequency is suppressed and the reduced power is distributed over the spectrum where real traffic is carried.

Another important format is Duobinary (DB). It represents correlative coding, a subclass of which is known as partial-response signalling. In DB, the phase changes if there is an odd number of logical zeros between two successive ones. The main benefit of the DB is its high tolerance to CD and narrow-band optical filtering [72]. The study in [75] shows a detailed performance comparison of various options of DB and Phase Shaped Binary Transmission (PSBT) formats for 40 Gbps and mixed 10/40 Gbps long-haul WDM systems based on SSMF and Large Effective Area Fiber (LEAF). Both DB and PSBT formats are more robust to intra-channel Kerr nonlinear effects than NRZ. DB generally offers acceptable compromise between robustness to OSNR degradation and CD immunity. On the other hand, DB's Differential Group Delay (DGD) robustness is roughly similar to that of NRZ. The main goal of using this format at 10 Gbps is to increase dispersion tolerance, whereas at 40 Gbps is to achieve high spectral efficiency in WDM systems. The resistance of DB to nonlinear transmission at 40 Gbps does not differ much from similar duty cycle OOK.

2.3.2 Phase Modulation Formats

Phase-modulated formats generally provide higher spectral efficiency and better OSNR tolerances than intensity formats. In Phase-Shift Keying (PSK) the phase is altered while maintaining constant amplitude. Differential Binary Phase-Shift Keying (DBPSK or simply DPSK) is not limited by the phase stability as the detection is based on the phase difference. DPSK detectors do not need to detect the exact phase of the signal but rather the difference between two adjacent bits. For this reason, DPSK is one of the most PSK variations

implemented in practice. The detection method, which is used with differential phase modulations, is known as differentially coherent phase detection [76].

Since DPSK modulates the signal's phase, transmitters consist of externally modulated laser sources. Mach-Zehnder Modulators (MZM) are used often for this purpose [77]. At a receiver side, signal is demodulated by comparing the phases of sequential bits. Phase differences must be converted into intensity signals, and subsequently transformed into electrical signals by photo-detectors. This can be achieved by splitting the received optical signal into two paths, where one part is delayed by exactly one bit by using a Mach-Zehnder Interferometer (MZI). MZI has two output ports: the constructive and destructive one. At the destructive port, no phase change results in destructive interference while a phase difference of π causes constructive interference. The constructive port yields the opposite results. Each of the ports may be used with a photo-detector to recover the original signal. But, a 3 dB sensitivity improvement is shown when both photo-detectors are used together, which is the main advantage of DPSK over OOK [70][72][78].

Similarly as OOK, DPSK can be implemented in RZ and NRZ versions. Authors in [79] investigate NRZ, RZ, CRZ, CSRZ, DB, RZ-DPSK, NRZ-DPSK in WDM-PONs for link spans up to 50 km. Results in [79] show that DB offers the lowest BER in WDM-PONs with a channel spacing of 100 GHz and bit rates 1.25 Gbps, 2.5 Gbps and 10 Gbps.

Differential Quadrature Phase-Shift Keying (DQPSK) is a multilevel format that has received appreciable attention to achieve narrow signal spectra. In DQPSK, 2-bit symbols are assigned to the four different phases shifted by $\pi/2$. The information is modulated as the phase difference between one and the next symbol period improving receiver's synchronization. DQPSK signals can be produced essentially by combining two DPSK transmitters. Because of this, the laser signal is split into two signals which feed each of the MZMs. Additionally a phase shift of $\pi/2$ is applied optically after the MZMs. A pulse carver may be added at this point to create RZ-DQPSK. DQPSK receivers are made in a similar fashion. The signal is split into two parts which are processed by their own MZI and balanced receiver. The main difference is that the delay is now 2 bits, as the phase is compared to 1 symbol (2 bit duration).

The spectrum shape of DQPSK is similar to that of DPSK, however its compression in frequency enables higher spectral efficiency and increased tolerance to CD [72][80]. DQPSK can be used either to double the bit rate while not requiring more bandwidth, or to halve the required bandwidth for a given bit rate. For this reason, DQPSK has been implemented in many WDM networks. DQPSK is also more immune to PMD due to its longer symbol length,

while comparing it to DPSK [72][76]. DPQSK is primarily limited by XPM and it is more suitable for transmission based on SSMF.

In [81], a part of a 1614 km link has been upgraded to 40 Gbps using DQPSK with live traffic of 10 Gbps OOK and the coexistence of 10 and 40 Gbps channels in the 50 GHz grid of DWDM has been numerically and experimentally confirmed. WDM has been investigated in [82] with different sources of radiation, which strongly influence the channel spacing and bandwidth. Authors in [83] demonstrate that NRZ-DQPSK is promising even for terabit transmission. DQPSK can also operate well at 40 Gbps. Its main limit factor at this speed is CD [84]. In [85], DPSK and DQPSK formats with NRZ, 33 % RZ and CSRZ are investigated for a single 160 Gbps channel and different dispersion compensation schemes. CD, higher-order CD, nonlinearity and OSNR are considered as well. Results show that RZ-DQPSK enables the longest physical reach; NRZ-DQPSK allows the highest dispersion tolerance and RZ-DPSK offers the highest nonlinearity tolerance. Authors in [86] review 42.7 Gbps DWDM systems with NRZ-OOK, DB, NRZ-DBPSK and RZ-DQPSK formats. The results from simulations show that RZ-DQPSK in a system with LEAF, 50 GHz channel spacing and spectral efficiency of 0.8 bit/s/Hz can provide approximately 50 % improvement in terms of transmission distance over implementations based on other fiber types and modulation formats.

2.3.3 Advanced Modulation Formats

PDM has been demonstrated to potentially double the capacity of transmission systems based on DQPSK [87] as well as other multi-level formats [88]. In PDM, two optical signals are coupled to two orthogonal polarizations being mutually delayed by a symbol period to improve OSNR. The two delayed lines: a coupled resonator and a photonic crystal waveguide are compared by using PDM transmission in [89]. PDM has been applied experimentally in [87] to increase 8 DQPSK channels with 200 GHz DWDM grid from 100 Gbps to 200 Gbps. The data were transmitted through a 1200-km long link with completely compensated CD. However, in their experiment, an automatic polarization control is not implemented and proper polarization should be set manually every tens of minutes. PDM can also double transmission capacity of other modulation formats. Dual-carrier PDM with 16 Quadrature Amplitude Modulation (QAM) occupying two 100 GHz channel slots has been proposed in [73] to transmit data at 1 Tbps over 3200 km with spectral efficiency of 5.2 b/s/Hz. The

proposed DSP algorithm [90] and decoding with soft decision FEC compensates receiver imperfection and mitigates CD.

Similar spectral efficiency can be obtained in data transmission by Coherent Optical Orthogonal Frequency Division Multiplexing (CO-OFDM) [91]-[93] owing to the partially overlapped optical carriers. A construction of CO-OFDM signal with cascaded optical modulators and subsequent coherent detection is described in detail in [76] and [91], respectively. A 1 Tbps CO-OFDM signal with a spectral efficiency of 3.3 b/s/Hz has been generated by using a Recirculating Frequency Shifter that requires a single optical modulator and lower drive voltage on the contrary to the cascaded optical modulators [92]. Optical signals have been detected after transmission over 600 km SSMF without Raman amplification and dispersion compensation. Further OSNR improvement can be obtained using trellis-coded modulation in 1 Tbps CO-OFDM transmission [92].

Another format which benefits from PDM is PDM-QPSK, which has been widely denoted differently either by PDM, polarization multiplexing, dual polarization or orthogonal polarization [74]. Its transmitter is similar to the so denoted earlier format PDM-DQPSK. Innovation in PDM-QPSK stands for the employment of a coherent receiver. The use of DSP requires a large number of components, as well as low-linewidth lasers [94]. Despite the fact that other formats have been designed and some of them are already commercially available, such as PM-OFDM-QPSK; PDM-QPSK proves to work better at 100 Gbps with respect to estimated reach, spectral efficiency, OSNR, CD and DGD tolerances [74].

The main bottleneck of wide-spreading 100 Gbps and higher rate transponders [69][74][95] are their high requirements for power consumption, DSP circuits and analogue to digital converters [96]. Authors in [97], investigate 100 Gbps PDM-QPSK channels for 8 Tbps transmission over a dispersion managed link based on low dispersion fibers. Experiment in [98] compares the system performance of 80 x 112 Gbps long-haul PDM-QPSK DWDM transmission over large-area fiber and SSMF spans. Other formats for 100 Gbps and higher rates are recently under research [74][99], e.g. Dual Polarization Multi-Band OFDM (DP-MB-OFDM). Authors in [100] show that DP-MB-OFDM and PDM-QPSK offer nearly the same results at 100 Gbps after transmission over a 10 x 100 km fiber line. Generally PDM combined with QAM formats seems to currently have the highest attention for transmission rates over 100 Gbps [101][102]. Experiment in [103] shows the suitability of 256 Gbps PM-16QAM and 128 Gbps PM-QPSK modulated signals in long-haul and submarine systems with span lengths over 100 km.

2.3.4 Electronic Dispersion Compensation

Dispersion is one of the key limiting factors which directly affects the transmission rate. In this section I describe techniques of its Electronic Dispersion Compensation (EDC). CD and PMD have a significant role in SMFs. On the other side modal dispersion is present in multi-mode fibers (MMF). Several techniques exist to compensate CD in the optical domain among which is the use of dispersion compensating fibers or Fiber Bragg Grating. PMD is randomly variable, therefore it is not easily predictable, which introduces a potential problem in case of static optical compensation. The cost of dispersion compensation techniques in optical domain and the efficiency in long-haul transmission systems must be considered as well. For these reasons, dispersion compensation in the electrical domain comes into strong consideration as an alternative solution.

a) Feed-Forward Equalization

Adaptive filtering techniques can electronically mitigate modal dispersion using adaptive equalization. The linear time-invariant model approximates the channel response for MMF. The effects of modal dispersion can be modeled using the linear and slowly time-varying model given in (1) [104]:

$$r(t) = \int_{-\infty}^{\infty} h(\tau, t) m(t-\tau) d\tau + w(t) \quad (1)$$

where $m(t) = \sum_n d[n] \cdot p(t - nT)$ is the modulation waveform with pulse shape $p(t)$ transmitted per bit interval T; $h(\tau, t)$ is the equivalent electrical impulse response for the MMF and $w(t)$ is the white Gaussian noise detected at the receiver. If we consider $g(t)$ as the convolution of the transmit pulse with the channel impulse response i.e. $g(t) = h(t) * p(t)$, and $h(t)$ as time-invariant i.e. $h(\tau,t) = h(\tau)$, the function $r(t)$ can be written in terms of the transmitted bit sequence $d[n]$ as expressed in (2):

$$r(t) = \sum_{k=-\infty}^{\infty} d[k] g(t - kT) + w(t) \quad (2)$$

Therefore, the optimal receiver filter is a matched filter to the transmit pulse $g(t)$. Subsequently, the transmitted bit sequence $d[n]$ can be obtained by sampling the output of this filter at intervals $t = nT$. This means that pulses caused by distortion can be suppressed by using adaptive equalizers modelling transmission of the pulses.

The Feed-Forward Equalization (FFE) method is based on Finite Impulse Response filters, whose output can be expressed as shown in (3):

$$y[n] = y(nT) = \sum_{k=0}^{N} c_k r(nT - k\tau) \quad (3)$$

where τ is the delay-line spacing of the N taps in the equalizer and c_k are filter coefficients which can be determined by Least Mean Square (LMS) [105] or Minimum Mean Square Error (MMSE) [106] algorithm. Figure 5 schematically describes how FFE works in reality.

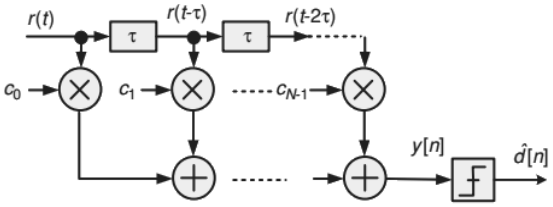

Figure 5: Feed-Forward Equalization [104]

b) Decision Feedback Equalization

While FFE can operate well for linear channels with modest frequency selectivity; they are not particularly well-suited to channels with deep spectral nulls [104]. Decision Feedback Equalizer (DFE) is a natural extension of FFE, which comes as a solution. A DFE typically consists of an FFE with an additional linear (or nonlinear) filter which applies further correction based on the current and previous bits. The idea behind DFE is to start from FFE and correct it by employing a feedback equalizer as shown in Figure 6.

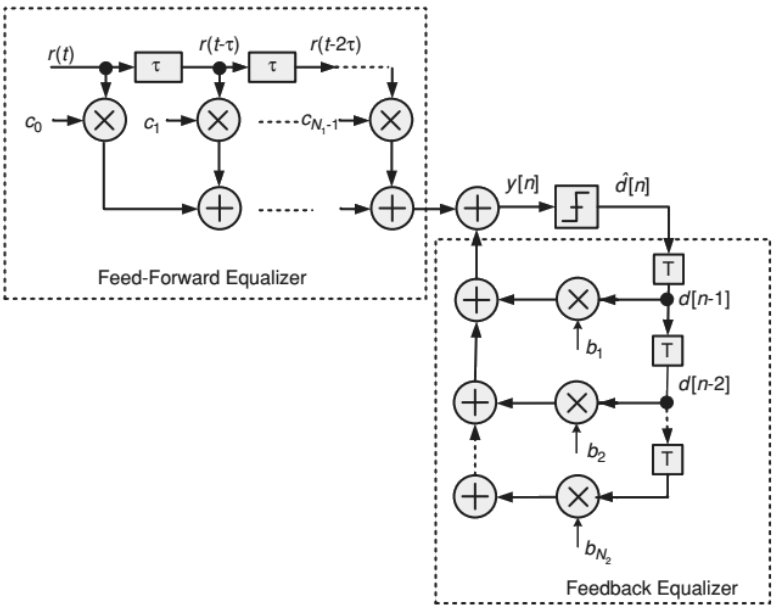

Figure 6: Decision Feedback Equalizer [104]

The output of the DFE with a linear feedback filter can be expressed as shown in (4):

$$y[n] = \sum_{k=0}^{N_1-1} c_k[n] r(nT - k\tau) - \sum_{j=1}^{N_2} b_j[n] \hat{d}[n-j] \quad (4)$$

where LMS coefficient updates are determined by the equations shown in (5) and (6)

$$c_k[n] = c_k[n-1] + \mu r(nT - k\tau) e[n], k = 0,2, \dots, N_1 - 1 \quad (5)$$

$$b_j[n] = b_j[n-1] + \mu \hat{d}[n-j] e[n], j = 1,2, \dots, N_2 \quad (6)$$

The FFE/DFE approach is an appropriate solution for modal dispersion, i.e. for short-reach MMF systems. On the other hand, CD and PMD in longer reach applications were not considered in the above investigated linear and slowly time-varying model. Nevertheless, different studies are related to CD compensation using FFE/DFE such as in [107]-[110].

c) Maximum Likelihood Sequence Estimator

The Maximum Likelihood Sequence Estimation (MLSE) is a nonlinear equalization technique that has performance advantages for correcting CD distortions over other algorithms such as FFE and DFE. Simulations and experimental results have shown that MLSE-based receivers can be capable of supporting uncompensated transmission over SSMF exceeding 1000 km, at transmission rate 10 Gbps for a total accumulated dispersion of over 17000 ps·nm^{-1}. Meanwhile, FFE/DFE-based receivers are mostly limited in the range of 2000 – 4000 ps·nm^{-1}. The SMF channel can be modeled as a nonlinear continuous-time channel with finite memory whose output at the detector can be expressed as shown in (7):

$$r(t) = S(t\,;\, d[n], d[n-1], \dots, d[n-L_c]) + n(t) \quad (7)$$

where $S(t,\dots)$ describes the noise-free state-dependent component of the signal, which is a function of L_c adjacent transmitted symbols, and *n(t)* stands for the optical noise in an amplified link or electrical noise in a unamplified fiber span. A baud-sampled bank of matched filters is used to detect such continuous-time channels with memory. Therefore, for each possible state of the channel, i.e. 2^{Lc} from $S(t,0,\dots,0)$ to $S(t,1,\dots,1)$, one filter is required. For is reason, a bank of 2^{Lc} continuous-time matched filters can be used, each sampled with a perfect symbol synchronization at rate T. The band of the detected electrical signal is mostly limited twice the bandwidth of the optical waveform. An oversampled Analog to Digital Converter (ADC) could comprise a set of sufficient statistics for subsequent data detection. Further data reduction to one sample per bit period can be obtained by filtering in the discrete

time [104]. The maximum a posteriori probability [109] detector is used to optimally detect an optical signal through a non-linear channel with memory in terms of minimizing the BER. The algorithm described in [111] can be used for its computation. MLSE provides a similar performance in terms of minimizing the Sequence Error Rate (SER). The SER-optimal transmitted sequence can be solved recursively with Viterbi algorithm [104]. While designing an MLSE receiver, many issues should be considered, among which the design of a baud-sampled ADC, clock recovery in the presence of dispersion, nonlinear channel estimation in the absence of a training sequence, the design of a high-speed Viterbi equalizer, etc.

d) Other Electronic Dispersion Compensation techniques

FFE-DFE can utilize the Volterra series [112][113], which approximates the response of a non-linear system if the output of this system depends strictly on the input. The main idea is to substitute the linear impulse response with a higher-order impulse response (named as kernel) in the non-linear Volterra term. Authors in [113] show how the second order FFE/DFE can compensate CD as well as non-linear effects. However, PMD tolerance is not significantly improved compared to conventional DFEs. The Volterra series can be also incorporated in MLSE as shown in [114].

Direct compensation at the transmitter can be an alternative to equalization at the receiver side. MZMs can control in this case the amplitude and the phase of the transmitted signal to obtain pre-distorted signals. This would enable compensation of large amounts of dispersion, in addition to fiber nonlinearities. As a result, the majority of CD can be compensated at the transmitter as well as intra-channel nonlinearities, meanwhile equalization of the residual dispersion and rapidly varying impairments such as PMD can be carried out at the receiver as proposed in [115]. The idea behind "Electronic Pre-Distortion" is that the distortion of the transmitted pre-distorted signals is reversed by CD during the signal propagation which results in the desired waveform at the receiver [116].

The Single Side-Band (SSB) can be an alternative solution for greater range. In [117], authors propose the SSB transmitter architecture with a 6-bit digital to analog converters and a dual electrode MZM among others, driven by signals from a Pseudo-Random Binary Sequence (PRBS) generator. In order to generate the two MZ drive signals, the Hilbert transformation is applied on the PRBS digital signal. The effect of dispersion in fibers is modelled by using a transfer function, which takes into consideration the fiber dispersion and length, laser wavelength and the frequency offset from the carrier. The received signal enters to the detector. Subsequently it is sampled and transferred to further digital processing.

Chapter 3

Methods

3.1 Time Domain vs. Frequency Domain Split Step Method

The propagation of an optical signal through a fiber can be expressed as shown in (8):

$$\frac{\delta A(t,z)}{\delta z} = \{L + N\}A(t,z) \tag{8}$$

where $A(t, z)$ is the optical field intensity, L is the operator which considers linear effects such as dispersion, meanwhile N stands for non-linear effects such as FWM [118]. The Split Step method applies separately L and N operators to calculate $A(t, z)$ over small fiber spans δz. Two basic methods are differentiated based on how the operator L is calculated: TDSS [119] and Frequency Domain Split Step (FDSS). N is calculated in the same manner. Simulations, which were built during the research work in OptSim software environment, are based on the TDSS method. TDSS computes L in the time domain from the convolution product in discrete time, as shown in (9):

$$A_L[n] = A[n] * h[n] = \sum_{k=-\infty}^{\infty} A[k]h[n-k] \tag{9}$$

where h is the impulse response of L. On the other hand, FDSS method calculates L in frequency domain by using the Fast Fourier Transform (FFT) algorithm on the signal in sampled time A[n] and on the impulse response in sampled time h[n] as well [118]. The Inverse FFT (IFFT) is subsequently applied on their product as shown in (10):

$$A_L^{'}[n] = A[n] \otimes h[n] = \text{IFFT}\{\text{FFT}(A[n]) \cdot \text{FFT}(h[n])\} \tag{10}$$

TDSS has no constrains on the shape of signal spectra and it has no modelling limits. Although FDSS can be implemented much easier, the circular convolution it applies will introduce aliasing and the error is unavoidable. Thus, TDSS benefits in many features against FDSS at the cost of increased implementation complexity, such as its immunity against aliasing errors, accurate DGDs, full band simulation, etc. The speed of TDSS computation is enhanced with software pipelining as individual components can process one sample and pass it on to the next component without requiring other signal information.

3.2 Monitors

The waveforms of optical signals are distorted when they arrive at the other end of fiber links due to the impact of negative factors such as PMD, CD, noise, non-linear effects, etc. Hence, bit errors are present when the receiver converts the optical signal into electrical domain. For this reason, suitable measurement techniques need to be utilized. I have measured in this thesis signal spectra, power levels, BER, Q-factor, eye diagrams and its related parameters, such as eye opening and jitter [120], among others.

BER is an ultimate indicator for measuring transmission quality. It specifies the ratio of bit errors to the total number of transmitted bits. Therefore, a lower BER indicates a better service delivery. BER is affected by attenuation, noise, dispersion, crosstalk between adjacent channels, nonlinear phenomena, and jitter or by bit synchronization problems. Its numerical value may be improved by launching a stronger signal into the transmission system unless this causes cross-talk and more errors; by choosing a robust modulation format, or by applying channel coding schemes.

The ratio of the net signal power to the net noise power is given by OSNR. This parameter indirectly reflects BER and it can give a warning of potential BER deterioration. The predominant source for its degradation is the amount of noise inserted by OAs. Q-factor on the other hand specifies the minimal required OSNR to obtain a certain value of BER. Therefore, Q-factor provides a qualitative description of the transmission system performance. It can be expressed as shown in (11):

$$Q[-] = \frac{\mu_1 - \mu_0}{\sigma_1 + \sigma_0} \tag{11}$$

where μ_0, μ_1 are the mean binary 0, binary 1 level values, and σ_0, σ_1 are their corresponding standard deviations [120]. Higher Q-factor indicates a better result. Optical systems operating at 10 Gbps per channel, for example, require BER to be below 10^{-12} and for better performance below 10^{-14}. Q-factor and BER are mathematically related as shown in (12) [121]:

$$\mathrm{BER}[-] = \frac{1}{2}\, erfc\left(\frac{Q}{\sqrt{2}}\right) \tag{12}$$

This equation is exact when the noise at the receiver is Gaussian and Inter-Symbol Interference (ISI) is negligible. In general, BER decreases as Q-factor increases. A Q-factor ranging from 6 to 7 [-] is needed to obtain a BER of 10^{-9} down to 10^{-12}. The details of Q-factor and BER measurement techniques in OptSim are described in [118].

The eye diagram graphically represents many cycles of the signal superimposed on top of each other. From its appearance, it is possible to judge the amount of noise, ISI, jitter and signal distortion [122], as shown in Figure 7.

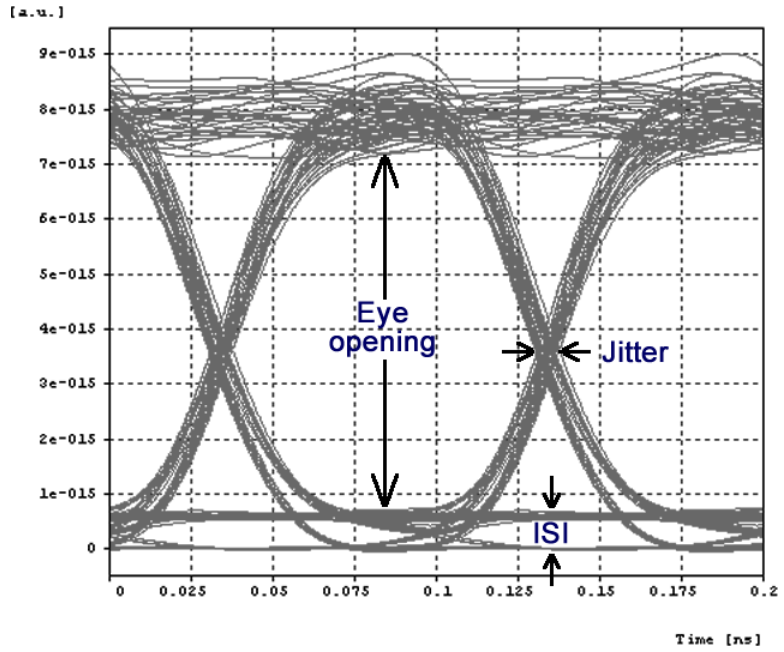

Figure 7: Eye opening, ISI and jitter in a sample eye diagram obtained from a simulation in Optsim software environment

OSNR can be estimated by observing the difference between the lowest level of binary 1 state and the origin. Less noise makes eye diagrams appear smoother as there is less distortion in the signal. The timing variation can be assessed by observing the width at the beginning of the eye. The height of the eye determines the amount of noise that a receiver can tolerate. The larger the size of the eye opening is, the lower the error rate will be [120].

3.3 Estimation of the Attenuation on Optical Links

The predominant part of the total attenuation in an ODN is accumulated from splitters and fibers. The overall attenuation can be decreased by deploying optical fibers with a lower specific attenuation or connectors with low insertion loss; by applying long distances between splices, or by utilizing splitters based on planar technology on behalf of their cost, among others. The estimation of attenuation together with dispersion and noise is discussed in details in [123] and [124]. Figure 8 shows a typical scheme of a tree topology ODN.

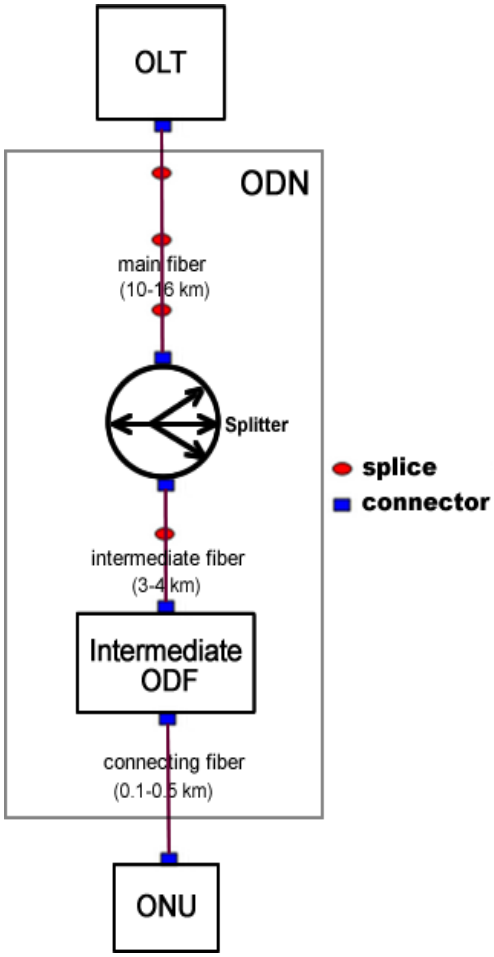

Figure 8: ODN – Evaluation of the attenuation

The total attenuation of this network scheme can be evaluated as shown below in (13):

$$A = m \cdot A_c + A_s + A_{ODF} + A_f + n \cdot A_{splc} + A_t$$

$$= m \cdot A_c + A_s + A_{ODF} + (l_1 + l_2 + l_3) \cdot \alpha + n \cdot A_{splc} + A_t \text{ [dB]} \quad (13)$$

where α [dB·km^{-1}] is the specific attenuation and A_f represents the attenuation of fibers; l_1, l_2 and l_3 are the main, intermediate and connecting fiber lengths; A_{splc} is the attenuation of splices (e.g. 0.05 dB) and n is their total number; A_c is the insertion loss of connectors in OLT and ONU (e.g. 0.2 dB) and m the number of connectors; A_s specifies the insertion loss of the splitter (e.g. 17.3 dB for 1:32 splitter); A_{ODF} stands for the attenuation of the intermediate optical distribution frame (e.g. 0.5 dB) into which are considered connectors and the connecting fiber; and A_t is the attenuation tolerance against material aging, temperature changes, etc. (e.g. 0.5 dB).

3.4 Structural Design Optimization of Optical Splitters

The Y-branch splitters were designed and optimized in OptiBPM photonic tool, based on the beam propagation method, which simulates the light passage through slowly varying optical waveguides. The splitter optimization is discussed in [59][126][127] by the authors Burtscher and Seyringer from the FHV Vorarlberg University of Applied Sciences in Austria, with whom I have cooperated during my doctoral studies. The length-optimized splitters from their research have been investigated in different PON schemes, as it will be described later in this section. The input design parameters are summarized in Table 5.

Table 5: Design parameters for 1x64 branch splitters

Refractive index of the waveguide core, n_c	1.456
Refractive index of the cladding, n_{cl}	1.445
Refractive index contrast, Δn	0.75 %
Operating wavelength, λ	1550 nm

The refractive index contrast is considered 0.75 %, which is a typical value for optical fibers. The structural parameters of the proposed splitter are shown in Figure 9.

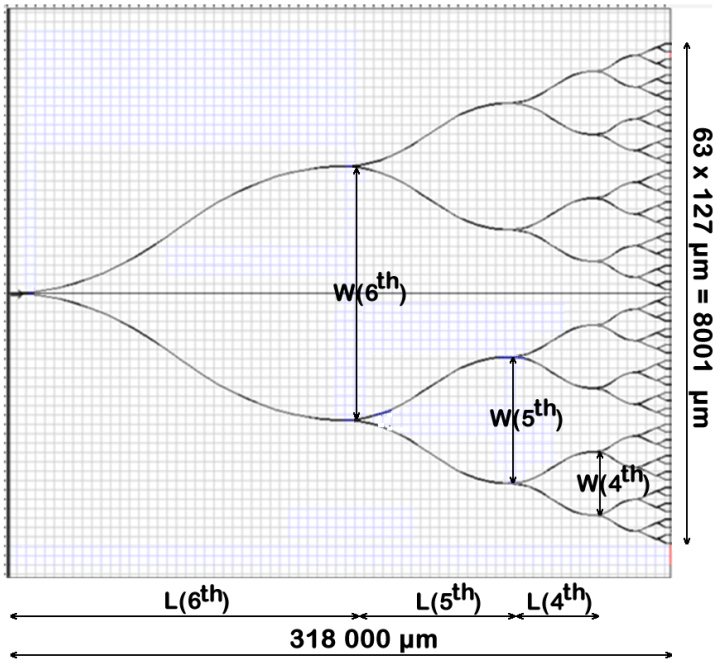

Figure 9: Standard 1x64 Y-branch splitter structure designed using OptiBPM [126]

Simulations in OptiBPM were performed at the operating wavelength of 1550 nm. The s-bend-arc shapes of Y-branches were used, because they offer the lowest losses [125]. The 63 branches that are required for 64 linear outputs are distributed into 6 branch layers. W(1^{st})

specifies the port pitch of output branches, where fibers are connected. This parameter is set to 127 µm. Based on this value, the length of the 1st branch layer L(1st) is set to 5000 µm. The remaining lengths and widths of branch layers are given in Table 6. These two parameters are doubled from one layer to another to keep a constant bending shape. As a result, the total length of this standard 1x64 splitter reaches 318000 µm and its width is 8001 µm, while considering that the input and output port lengths are 1000 µm.

Table 6: Widths and lengths of branch layers in the standard 1x64 splitter structure

Widths of branch layers	$W(1^{st})$	127 µm
	$W(2^{nd})$	254 µm
	$W(3^{rd})$	508 µm
	$W(4^{th})$	1016 µm
	$W(5^{th})$	2032 µm
	$W(6^{th})$	4064 µm
Lengths of branch layers	$L(1^{st})$	5000 µm
	$L(2^{nd})$	10000 µm
	$L(3^{rd})$	20000 µm
	$L(4^{th})$	40000 µm
	$L(5^{th})$	80000 µm
	$L(6^{th})$	160000 µm

The optimization of its length has been achieved as described in [126]. Individual widths and lengths of branch layers of this length optimized splitter are shown in Table 7.

Table 7: Widths and lengths of branch layers in the length optimized 1x64 Y-branch splitter structure

Widths of branch layers	$W(1^{st})$	127 µm
	$W(2^{nd})$	254 µm
	$W(3^{rd})$	508 µm
	$W(4^{th})$	1016 µm
	$W(5^{th})$	2032 µm
	$W(6^{th})$	4064 µm
Lengths of branch layers	$L(1^{st})$	5000 µm
	$L(2^{nd})$	10000 µm
	$L(3^{rd})$	17000 µm
	$L(4^{th})$	17000 µm
	$L(5^{th})$	34000 µm
	$L(6^{th})$	34000 µm

As it can be seen from Table 7, widths remain the same as in the standard Y-branch splitter. The layout of the length optimized 1x64 Y-branch optical splitter is given in Figure 10. The overall splitter length has been reduced from 318000 μm to 120000 μm.

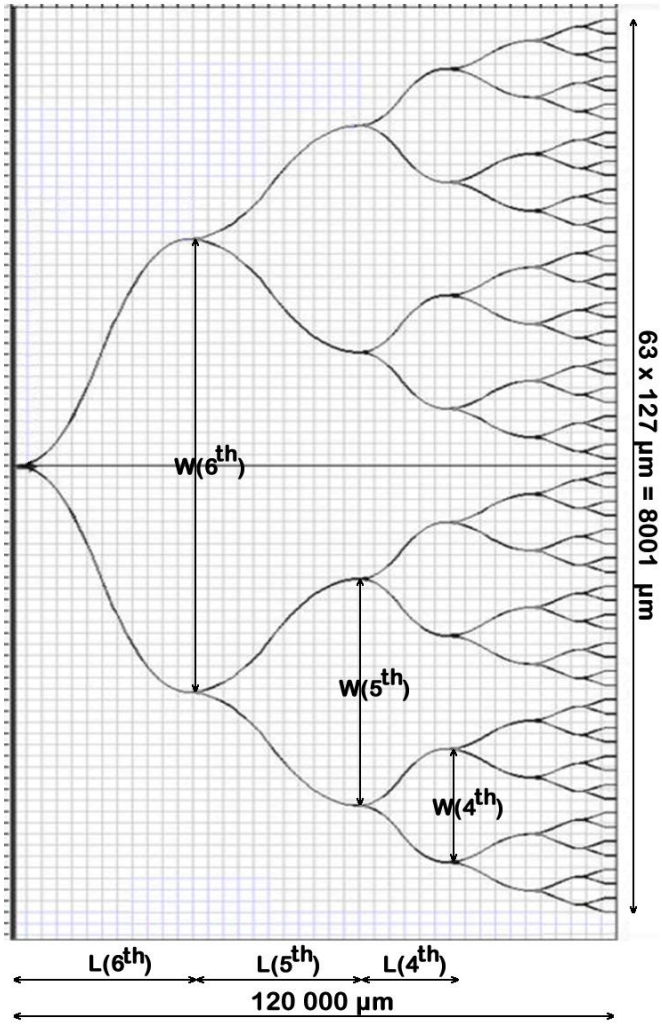

Figure 10: Layout of the low-loss length-optimized 1x64 Y-branch splitter [126]

Simulation results showed that a key factor, which affects the non-uniformity of the splitter, is the presence of the first mode. This phenomenon can be suppressed by reducing the waveguide core size from 6 μm x 6 μm to 5.5 μm x 5.5 μm and keeping constant the size of the Y-branch splitter structures [127].

Both proposed splitter designs were deployed in a PON and investigated in terms of physical reach, Q-factor and BER. Simulation scheme is shown in Figure 11. I focus on the downstream traffic, which does not restrict the generality of the problem. Scheme consists of three parts: OLT, ODN and ONU. Both GPON (2.5 Gbps downstream) and XG-PON (10 Gbps downstream) are simulated.

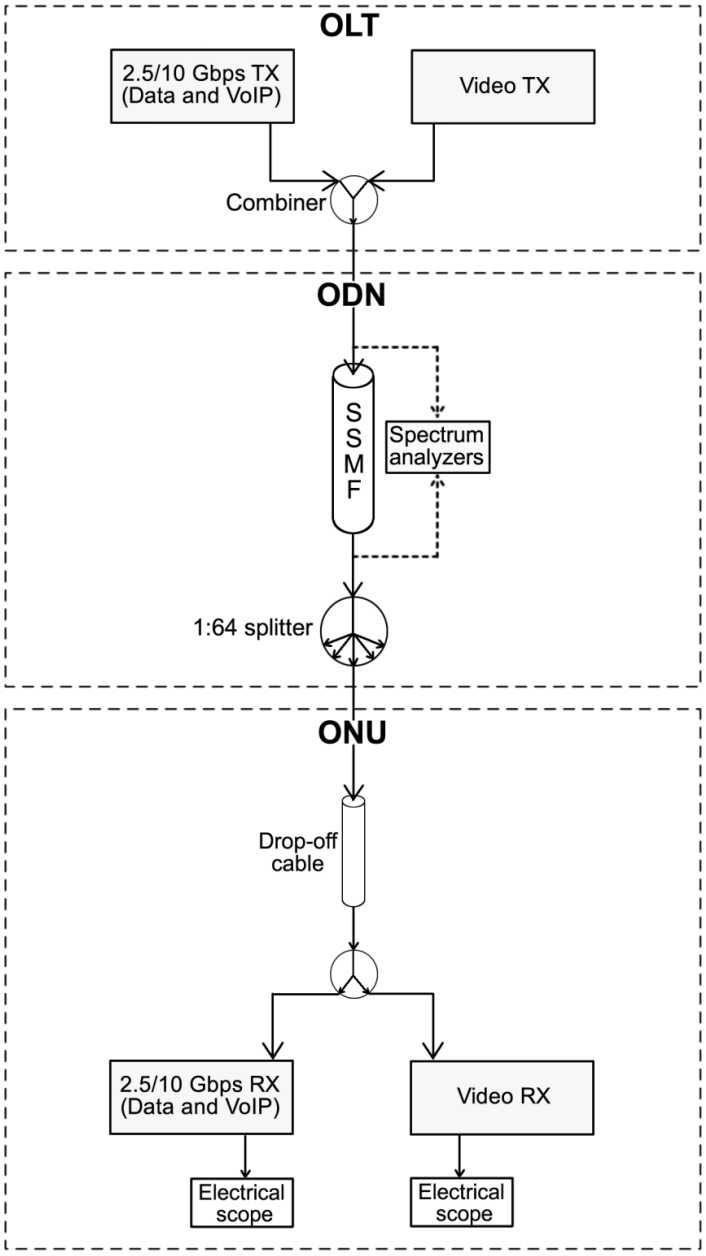

Figure 11: GPON/XG-PON simulation schemes with triple-play services employing the designed 1x64 splitters

Voice transmitter is considered as a Voice over Internet Protocol (VoIP) service due to its current applications and wide deployments globally as an alternative solution to traditional public switched telephone network with plain old telephone service at the customer's end. Data and VoIP transmitters generate NRZ modulated signals, which are multiplexed together with the video component by applying CWDM technique. A detailed description on the design of all transmitters which were used during the research is given in section 3.7. The 800 Mbps video stream was generated via a 16-QAM modulation. The data, voice and video transmitter's output power was set to -3 dBm, since this is a commonly used value. ODN

consists of a 20 km long SSMF with an attenuation factor of 0.2 dB·km^{-1}, and the 1x64 splitter to be analyzed. The drop-off cable is several meters long. It was included in this simulation to consider the fiber patch cables at the customer promises. The main goal of this simulation was to find out the practical benefits of the length optimized splitter in OANs. The results are discussed in Chapter 4.

3.5 Transmission Network Transparency and Potential Convergence at the Physical Layer

The coexistence of GPON, XG-PON and video services is simulated in hybrid PONs to find out potential bandwidth utilization improvements. The idea behind this novel simulation setup is to show the benefits of convergence of multiple access network solutions in hybrid TDM/WDM-PONs, which I strongly recommend for next generation PONs. I focus on the downstream traffic for simplification purposes and due to the software limitations of the simulation tool that has been used; however it does not restrict the final goal of this investigation. The proposed TDM/WDM-PON can be realized by stacking a TDM-PON on top of a WDM structure, as shown schematically in Figure 12.

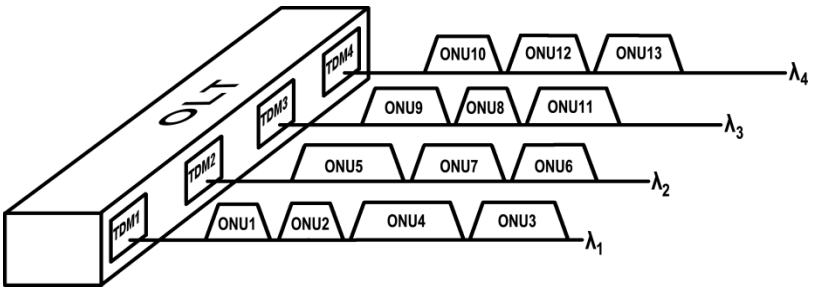

Figure 12: Hybrid PON channel allocation in TDM and WDM domains

Each of the wavelengths has its own independent TDM domain. As a result, system capacity can be expanded by increasing the wavelengths, leading in the ideal case to TDM/DWDM-PON systems. The simulation scheme that I have built in OptSim environment is shown in Figure 13. I consider GPON/XG-PON recommendations from ITU-T for the TDM-PON domain to allow triple-play service delivery up to 64 subscribers. Figure 26 is divided in three parts: OLT, which contains the data/voice/video transmitters; ODN, which includes the transmission path components; and ONU, which represents end user equipment.

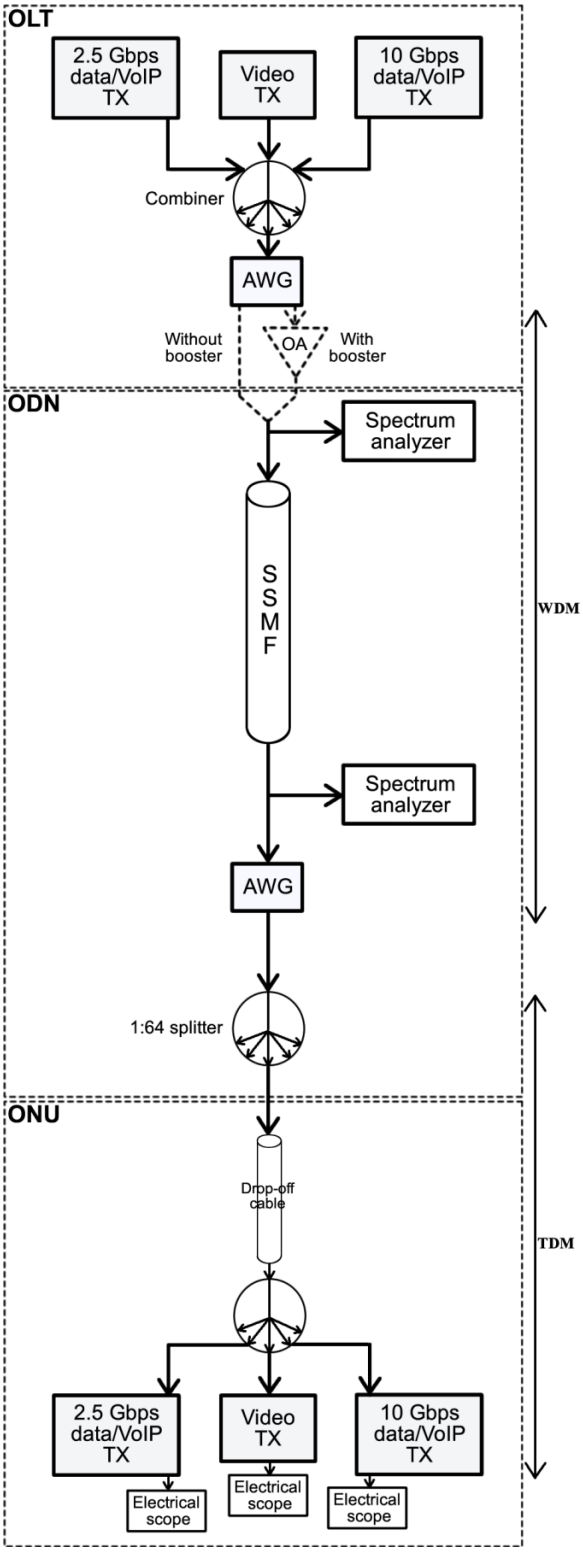

Figure 13: FTTH TDM/WDM-PON system with GPON/XG-PON and video access architecture

An Arrayed Waveguide Grating (AWG) is used to multiplex the optical channels in the WDM domain. The TDM part is built based on a common TDM-PON architecture. The Internet component is represented by a data link with a download speed of 2.5 Gbps for

GPON and 10 Gbps for XG-PON. Data transmitters produce NRZ modulated signals. Further details on the transceiver construction are described in section 3.7.

The voice component can serve VoIP services. CWDM technique has been applied to transmit the data/voice stream together with the video signal, which runs within the wavelength range 1550-1560 nm, in accordance with ITU-T recommendations [21], as shown previously in Figure 4. For simplification purposes, a 16-QAM SubCarrier Multiplexed system is used to generate the video signal, although other Quadrature Amplitude Modulation (QAM) formats are more typical. The 800 Mbps video stream is launched into the modulator, where the QAM modulated electrical signal is generated. This electrical signal is subsequently processed by an optical modulator, which is driven by a laser, similarly as in the data/voice transmitter. The output power of each transmitter is set to 0 dBm. Transmission media consists of an SSMF with 0.2 dB/km attenuation, an optical splitter for signal distribution among 64 subscribers and a drop-off cable of several meters. The signal of each optical channel is filtered at the corresponding receiver and the obtain electrical signals are measured in terms of eye diagram, Q-factor and BER. This scenario is also simulated for an AON by deploying a single booster, as schematically shown in Figure 26. The purpose of this simulation is to figure out the benefits of introducing an OA. Different transceiver designs from modulation perspective are considered as well to find out which of the network schemes offers the most enhanced system performance. The results are discussed in Chapter 4.

3.6 Practical Implementations of EDC

a. Ideal EDC

Different schemes of deploying EDC have been simulated in this thesis to determine the advantages of each application. Firstly, an ideal EDC is used to detect the signal of a PDM-QPSK modulated signal, which will be further discussed in section 3.7. The compensator has four electrical inputs and four electrical outputs. The four input signals represent the in-phase and quadrature components on the two polarizations of the received optical field and derived from a coherent homodyne receiver [118]. This ideal EDC applies the same amount of compensation on the signals. The two parameters which can be set in this compensator are the total amount of CD to compensate [ps/nm], or the total amount of CD slope to compensate [ps/nm^2]. The numerical results discussed in Chapter 4 will show that the measured pre-FEC BER value at the PDM-QPSK receiver is within the acceptable threshold, even after hundreds of km in a long-distance transmission system.

b. Implementation of EDC Using MMSE-based FFE and DFE

In this section, an application scheme of the EDC using MMSE-based FFE and DFE is shown. For this purpose, a 10 Gbps NRZ signal transmision is simulated over an 80 km SSMF, as illustrated in Figure 14.

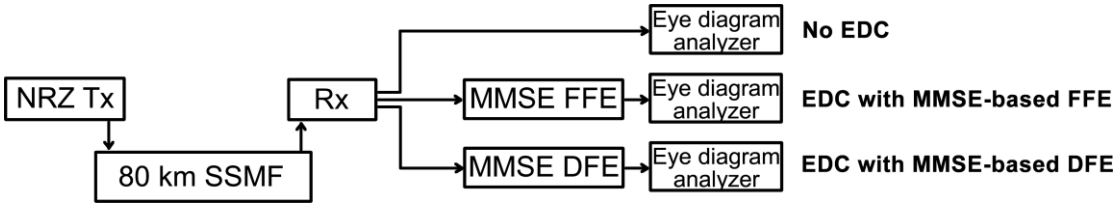

Figure 14: EDC using MMSE-based FFE and DFE

The benefits from this EDC technique with FFE and DFE, both optimized based on the MMSE algorithm, are given in Chapter 4 together with the corresponding received eye diagrams.

c. Implementation of EDC FFE in a Multimode Link

Another application of EDC FFE can be in multimode links. Figure 15 shows a design scheme of such implementation, where a 10 Gbps multimode link is considered for simulation purposes.

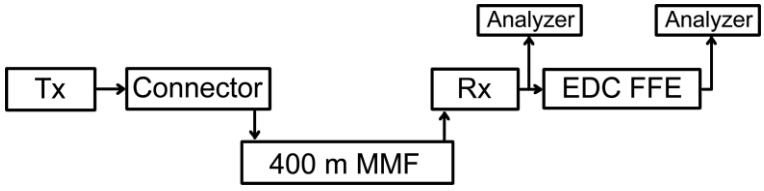

Figure 15: EDC FFE in a multimode link

The graded-index OM4 MMF, which is used in this simulation scheme, is 400 m long with a 50 μm core diameter. Common fiber manufacturing imperfections are considered by using the fiber refractive index profile with a dip defect in the centre of the core. The connector between transmitter and MMF adds 10 micron offset from the fiber core center. This results in a distorted eye diagram. FFE is applied in the electrical signal after the first receiver to improve the results, and the parameters of equalization filter are optimized for the given

offset of laser-fiber alignment [118]. The FFE parameters were set to: 3 taps, tap delay of $½T_B$, and taps coefficients {-0.3, 1.0, -0.3}. The results are discussed in Chapter 4.

d. Implementation of a MLSE Receiver

The aim of the following simulation is to design and test direct-detection systems deploying MLSE-based receivers. The simulation scheme is shown in Figure 16. The simulated 10 Gbps transmission system includes a 500 km SSMF with dispersion equal to 16 $ps \cdot nm^{-1} \cdot km^{-1}$. The transmitter generates an amplitude modulated signal at 1550 nm using a single arm MZM with $\sin^2$ electrical shaped input-output P-V characteristic. The signal is then amplified so its output power level is at 0 dBm and subsequently it is noise loaded.

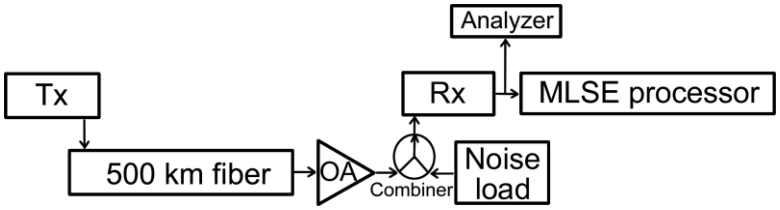

Figure 16: Investigation of an MLSE-based receiver in an uncompensated transmission system

The receiver consists of an optical filter, an ideal photo-detector and an electrical filter. The MLSE Viterbi processor is configured in such a way that it is sufficient to compensate the total amount of the accumulated dispersion, i.e. 16 $ps \cdot nm^{-1} \cdot km^{-1} \cdot 500$ km, with a -3 dB OSNR penalty. It employs 8192 states, 4 samples per bit, an analog to digital decoder with infinite resolution and a delay of 3N bits (where N is the number of states) before making a bitwise decision [118]. BER is obtained as a function of OSNR by using a Monte-Carlo error counting approach. The simulation results are discussed in Chapter 4.

3.7 Modulations formats

This section explains the design of all transceivers used in this thesis, together with the simulation schemes in which they are applied, either single channel or DWDM. The transmitters of intensity modulation formats NRZ, RZ and CSRZ are shown in Figure 17. The simplest transmitter is that of NRZ format. It consists of a Continuous Wave (CW) laser, an amplitude modulator, a PRBS generator and an NRZ raised cosine electrical driver. Bit rate, CW laser frequency and output power of the laser are defined as input parameters, among

others. Figure 17 shows that RZ transmitter is identical to that of NRZ, except of the driver type. In CSRZ, a second modulator is deployed to achieve the carrier-suppression effect. The frequency of sinusoidal signal generator is set to half of the bit rate to obtain a π phase shift between any two adjacent bits.

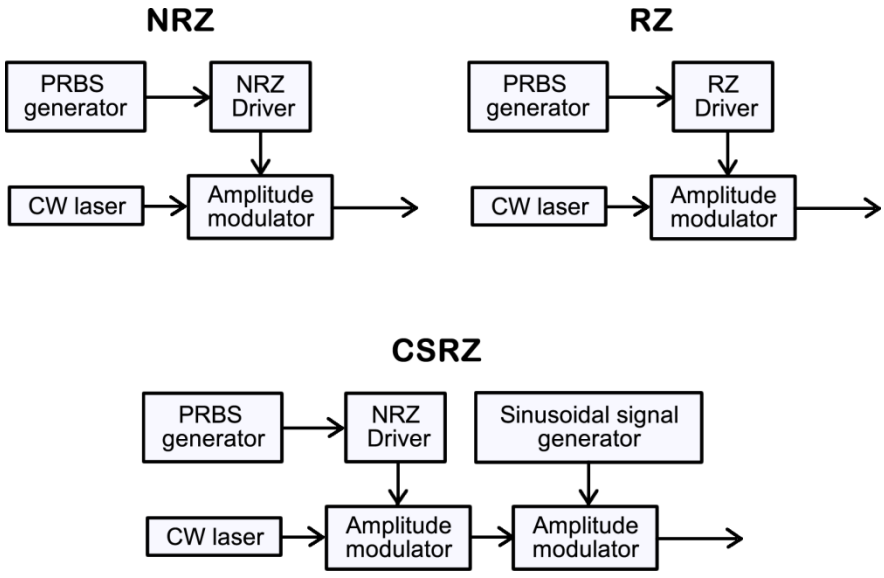

Figure 17: Transmitter design of NRZ, RZ and CSRZ

The design of DB transmitter is given in Figure 18. The amplitude dual-arm MZM is one of its key components. The binary sequence of one of the 'arms' is inverted by using a NOT gate. Low-Pass Filters (LPF in Figure 18) are included in the scheme to consider the impact of a non-ideal binary-to-electrical signal conversion.

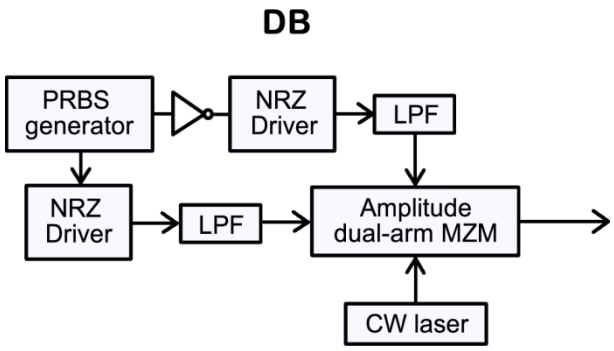

Figure 18: Transmitter design of DB format

Intensity formats are detected and measured at the receiver side with optical band-pass filters, PIN photodiodes and electrical scopes. The corresponding bandwidth of optical filters has been optimized by running a recursive scan with varied values to find out for which bandwidth we can achieve the lowest BER for a given modulation format.

Moving on to phase-based formats, the transmitter's complexity increases. The transmitters of NRZ-DPSK and RZ-DPSK are shown in Figure 19.

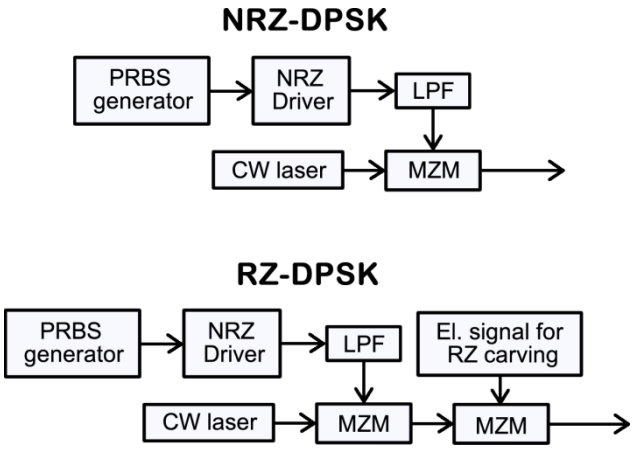

Figure 19: Transmitter design of NRZ-DPSK and RZ-DPSK

MZM plays a key role in DPSK transmitters, because it generates the required phase-modulated signal. The driver must be carefully set up with proper maximum and minimum values of electrical signal. RZ-DPSK transmitter contains in addition a second MZM driven by an electrical signal to generate RZ pulses.

The design of DPSK is relatively simple compared to NRZ-DPQSK, RZ-DQPSK and CSRZ-DQPSK formats, which are shown in Figure 20. DQPSK deals with both in-phase and quadrature components, therefore it is necessary to work with each of them separately. Both binary signals for in-phase and quadrature parts are firstly encoded, so that signals at the receiver side will match the transmitted ones. Subsequently, their corresponding electrical signals are generated through the use of drivers to control MZMs, one per each component. An additional phase shift of 90° needs to be applied to one of the optical outputs for the quadrature component. This can be achieved by deploying a phase modulator, driven by a bias wave generator with correct settings. The output from the phase modulator is then combined with in-phase component to create a single NRZ-DQPSK modulated signal. Similarly as in RZ-DPSK transmitters, RZ-DQPSK contains in addition to NRZ-DQPSK

another MZM to generate the desired RZ output pulses. CSRZ-DQPSK transmitter is similar to the conventional DQPSK. The carving of signal is obtained via the use of an amplitude modulator, which is inserted between the laser source and DQPSK modulator. The effect of carrier suppression is achieved by driving the modulator between $V_{off} - V_{\pi}$ and $V_{off} + V_{\pi}$.

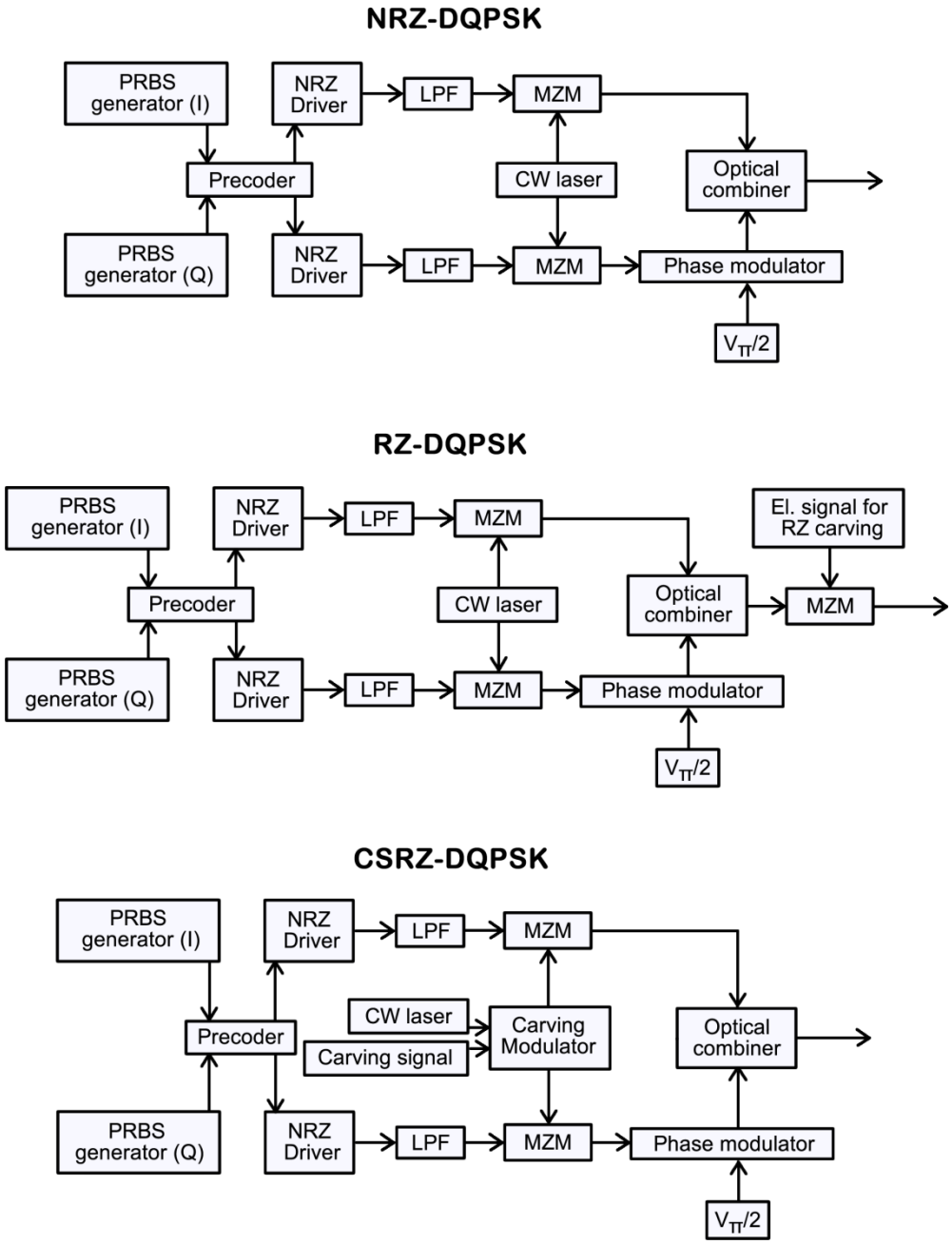

Figure 20: NRZ-DQPSK, RZ-DQPSK and CSRZ-DQPSK transmitters

In order to detect phase modulated signals, the receivers require a different design compared to intensity formats. The core component of a DPSK receiver is a balanced 2DPSK

block which consists of a tuneable MZI followed by two optical paths, delayed to each other by one bit time duration. Each of these optical outputs is detected by a PIN photodiode. The output electrical signal of 2DPSK receiver is determined by the difference between the measured currents [118]. Two 2DPSK receivers are used in case of DQPSK format; one for in-phase and one for quadrature component. Similarly as for intensity formats, optical filters with optimized bandwidth settings are included in the input of phase-based receivers.

Moving on to PDM-QPSK format, the implementation requirements significantly increase for both transmitter and receiver parts due to the combination of PDM and phase modulation, as shown in Figure 21. Four data sources are used to generate a single PDM-QPSK signal. The first part of the transceiver generates the phase-based modulated components, which are subsequently incorporated into PDM by rotating the polarization of one branch.

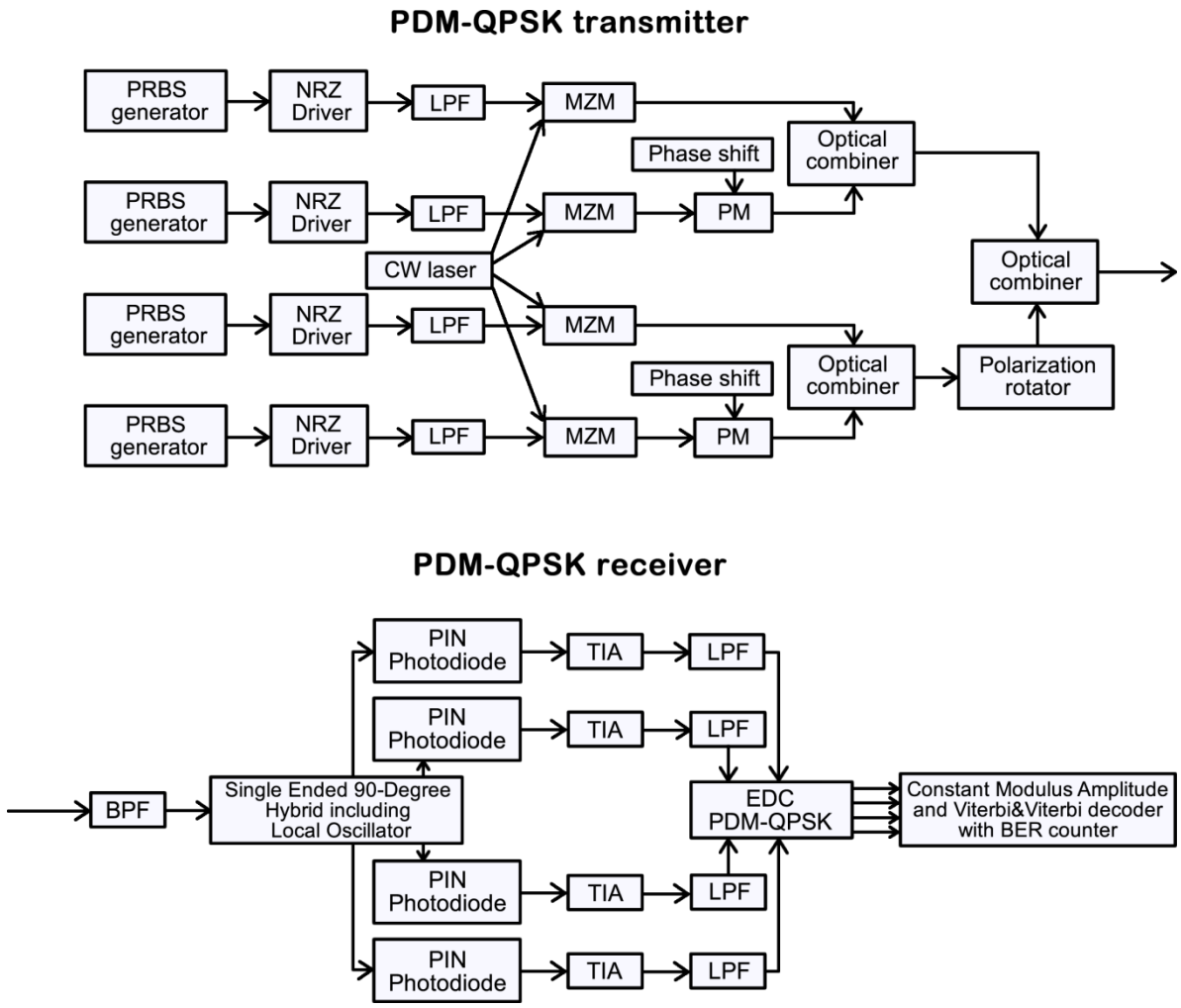

Figure 21: Transceiver design of PDM-QPSK

At the receiver, a single ended 90° hybrid with local oscillator and four PIN photodiodes in its four output interfaces enable the coherent detection. Subsequently, signals travel through Trans-Impedance Amplifiers (TIA in Figure 21), electrical filters and then through an ideal EDC with four electrical input signals and four electrical output signals. An error counting is then applied on the four signals. The EDC block implements an ideal electronic dispersion compensator, which applies the same amount of compensation on all signals, and it takes into account the number of fiber spans, dispersion and fiber lengths. The final block in the PDM-QPSK receiver consists of a memoryless blind receiver, which separates orthogonal polarizations as well as in-phase and quadrature signals by applying the Constant Modulus and Viterbi & Viterbi algorithms [118].

PDM can be applied also on other formats, such as QAM. Based on similar design principles, which were described previously for PDM-QPSK, I have built in the OptSim environment a PDM-16QAM transceiver. The numerical results from simulations, which will be discussed in Chapter 4, prove the suitability of this format for terabit transmission over long distances and its ability to double the spectral efficiency of PDM-QPSK.

Single-channel and DWDM simulation schemes are created in OptSim to investigate various aspects of the network performance for each modulation format, such as transmission rate, BER, Q-factor, optical reach, channel spacing, spectral efficiency, network topology. The simulation scheme, which is given in Figure 22, is used for the single-channel scenarios, where no OAs are deployed and no dispersion compensation technique is applied.

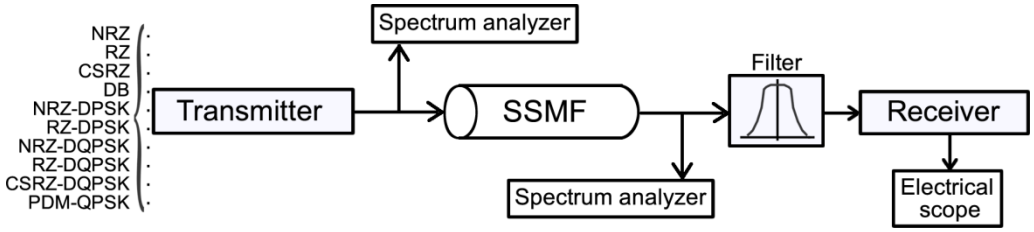

Figure 22: Single-channel simulation scheme for comparison of optical modulation formats in OptSim software environment

The optical path consists of an SSMF with 0.2 dB/km loss. The output power of transmitters is set to 0 dBm for comparison purposes, and the operating wavelength is set to 1550 nm. Many measuring devices such as signal and spectrum analyzers, BER testers, eye diagram analyzers, optical power meters, etc., are used to investigate the modulation formats and find out not only their general efficiency, but also their performance at certain points of

transmission path and their main limiting factors. Optical and electrical noises are considered as well. The results from simulations in Chapter 4 will show that the overall system performance of a certain modulation format is degraded after a certain point and its deployment in a DWDM network starts to become quite inefficient without applying dispersion compensation schemes, optical amplification or further improvements of transceiver design, among others. Despite such enhancements, some formats cannot operate well at higher bit rates due to their physical limitations, therefore they have been excluded from the comparison after a certain bit rate to figure out the most appropriate format for a given network topology and transmission rate.

Two different DWDM network topologies are used. The first one is based on a single fiber, as shown in Figure 23. One of the goals of this scheme is to find out the maximum physical reach in point-to-point links.

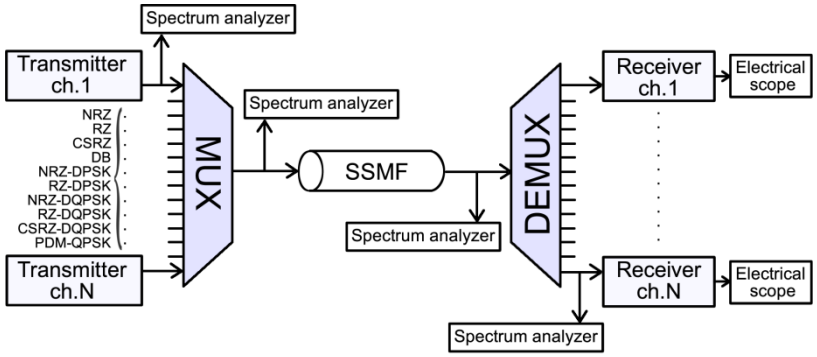

Figure 23: DWDM passive optical network to investigate formats at 10, 40 and 100 Gbps

The second considered DWDM scenario is based on a tree topology, as shown in Figure 24. The purpose of this scheme is to find out how formats operate in a typical OAN scheme.

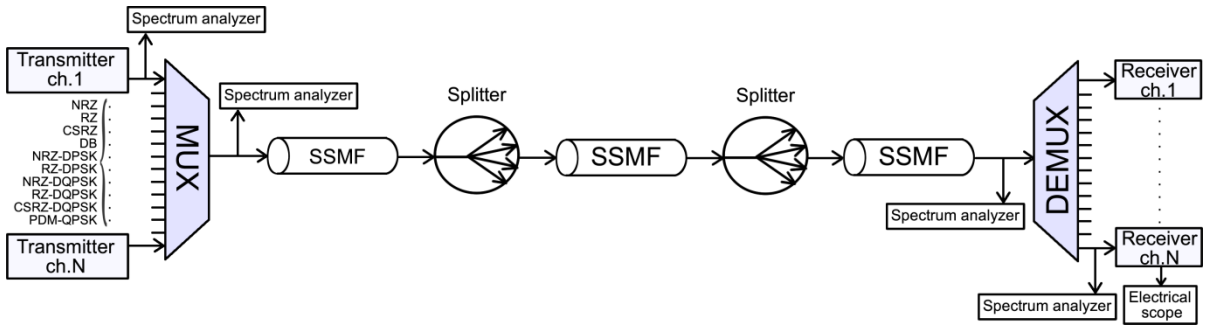

Figure 24: Tree topology for 10, 40 and 100 Gbps DWDM systems

In both DWDM network schemes, the output power of each transmitter is set to 0 dBm for comparison purposes. SSMFs have an attenuation of 0.2 dB/km. WDM multiplexers and demultiplexers are modelled as a set of filters, whose parameters have been optimized based on the modulation type to obtain the best results, i.e. the lowest BER, respectively the highest Q-factor value. This has been achieved by running a sequence of simulations with a variable parameter, such as the bandwidth and transfer function of filters. The final goal is to achieve as higher spectral efficiency as possible.

Another simulation scheme is introduced in addition in case of PDM-QPSK and PDM-16QAM formats, as shown in Figure 25. The optical dispersion compensation is applied by using Non-Zero DSFs with 0.2 dB/km loss and CD 4 ps/nm/km at the considered band to avoid FWM.

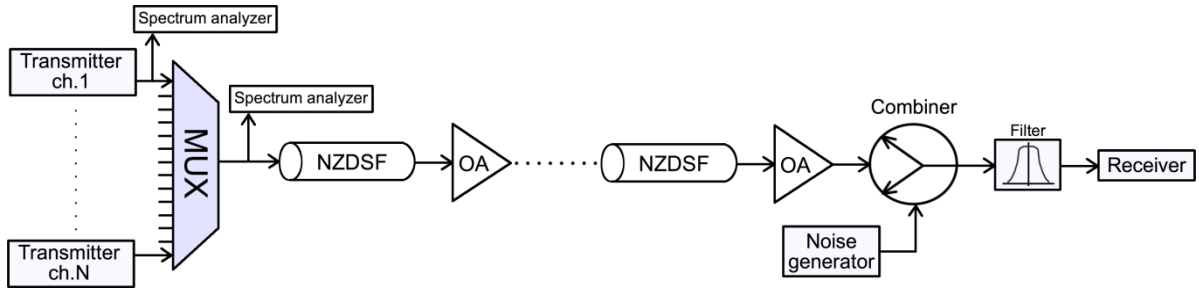

Figure 25: Simulation scheme for PDM-QPSK and PDM-16QAM DWDM systems

The purpose of this simulation setup is to figure out the efficiency of PDM-QPSK and PDM-16QAM in long haul transmission systems, consisting of hundreds of kilometres. The optical signal is noise loaded to extract BER as the function of OSNR [128]. Each of the fiber spans is 100 km long and separated from each other by OAs with a fixed gain around 20 dB. I also consider in the transmitters a 7 % bit rate overhead for FEC, and 0 dBm of transmitted power. PDM-QPSK and PDM-16QAM formats are deployed at systems with 50 GHz channel grid and baud rate of 32 Gbps, which results in a per channel bit rate of 128 Gbps in case of PDM-QPSK and 256 Gbps in case of PDM-16QAM, including FEC overheads. The results are discussed in the next chapter.

Chapter 4

Results and Discussion

4.1 Optimization of Optical Network Capacity

In this chapter, I summarize research accomplishments and describe the scientific progress, which was done in terms of network capacity and transmission rate. Techniques such as optimization of optical splitters, coexistence of different OAN solutions at the physical layer and introduction of hybrid PONs are proposed to optimize the utilization of network capacity. These solutions enable improved scalability and enhanced bandwidth efficiency.

Table 8 shows the main results from simulating the standard 6 μm × 6 μm and low-loss length-optimized 5.5 μm x 5.5 μm 1x64 Y-branch splitters, which were discussed in Chapter 3. Four different parameters are compared, specifically: insertion loss uniformity (non-uniformity) *ILu*, insertion loss *IL*, maximum background noise BX and chip size.

Table 8: Comparison of the main parameters of standard and low-loss length-optimized 1x64 Y-branch splitters

	Standard waveguide core size 6 μm × 6 μm	**Optimized waveguide core size 5.5 μm × 5.5 μm**
Non-uniformity, *ILu*	2.67 dB	1.98 dB
Insertion loss, *IL*	-19.89 dB	-19.93 dB
Max. background noise, *BX*	-42.24 dB	-41.85 dB
Chip size	318 000 μm	120 000 μm

From Table 8, it can be seen that the most significant enhancement in splitter design is related to non-uniformity. The individual values of insertion losses per each output port have been calculated and the results are given in Figure 26. The scale of y axis in the figure has been adjusted to distinguish better the deviations from the mean attenuation value and to compare both optical splitter designs. Figure 26 clearly proves that the non-uniformity has been significantly improved while using the low-loss length-optimized 1x64 optical splitter with the 5.5 μm × 5.5 μm waveguide core size. This is very beneficial especially for PONs with triple-play services as the provider can offer similar signal quality to individual users, and therefore it can maintain more efficiently the same Service Level Agreement (SLA) to each of the customers.

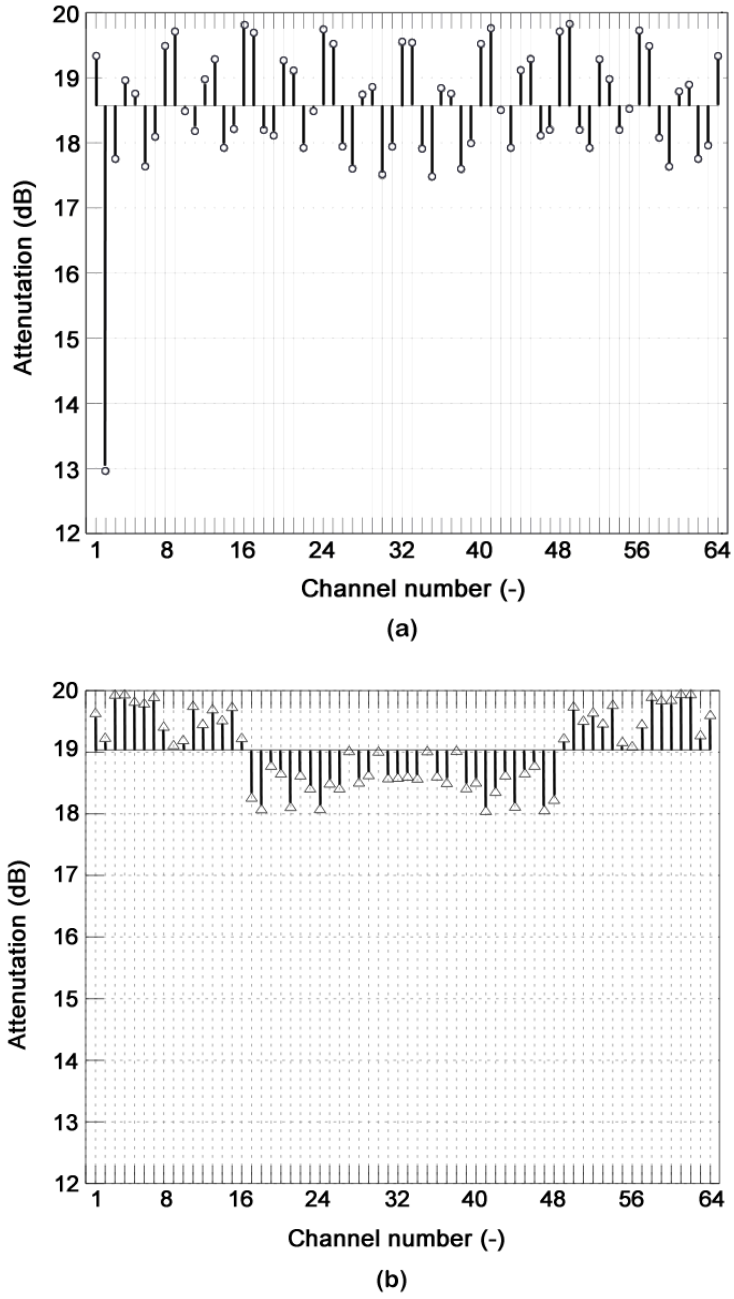

Figure 26: (a) Attenuation and deviations from the mean value for each of the output ports for both: conventional and (b) low-loss length optimized (triangles) 1x64 Y-branch splitters

Both splitters, the conventional and the optimized one, are deployed in GPON and XG-PON systems. Figure 27 and 28 show the results for data and voice services. As no changes were applied to video signals, the video service delivery remained the same under acceptable thresholds in both cases; hence it is not taken into account for comparison. The minimum and maximum values achieved by Q-factor and BER are displayed in Figure 27 and 28 with dashed lines.

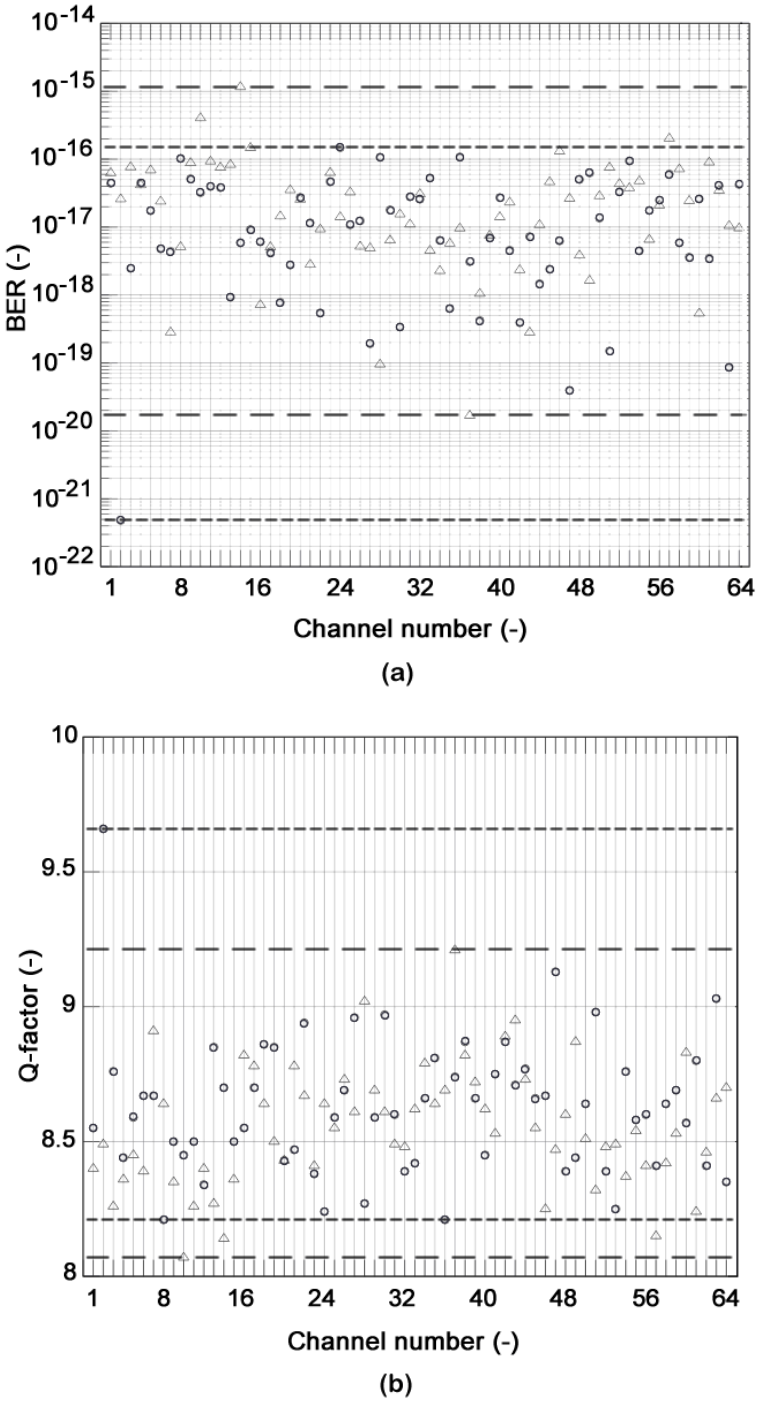

Figure 27: (a) BER and (b) Q-factor values for GPON with triple-play services (circles - standard splitter; triangles- optimized splitter)

Figure 27 shows that splitting uniformity was just slightly improved in case of GPON scenario, mainly because all BER values were too low, respectively Q-factor too high, at the receivers. As a result, small changes in attenuation of output ports of the splitters deployed in GPON were not noticeably influencing the overall service quality to end users. The minimum

and maximum achieved BER values differ by a factor of 10^6 when the standard splitter is used, and by a factor of 10^5 in case of the optimized splitter. For higher speed rates, like that of XG-PON and beyond, the optical signal quality significantly decreases if other network parameters are not properly tuned. The results for XG-PON systems are given in Figure 28.

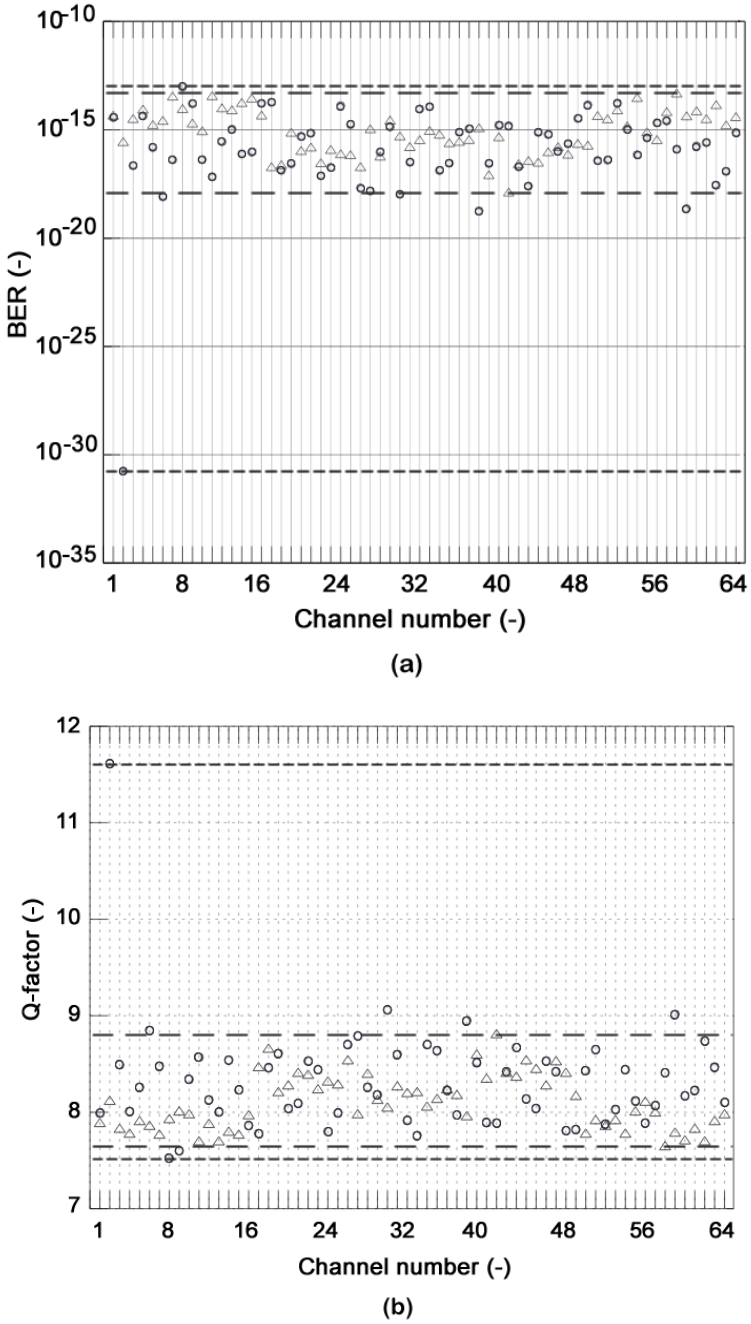

Figure 28: (a) BER and (b) Q-factor values for XG-PON with triple-play services (circles - standard splitter; triangles - optimized splitter)

Figure 28 shows that the minimum and maximum BER values, which were measured in XG-PON scenario, vary by a factor of 10^{17} in case of the standard splitter deployment and by only 10^{4} when the optimized optical splitter is deployed within the ODN. These simulation results clearly prove that the power split over all output ports becomes a crucial parameter for higher transmission rates to maintain similar customer SLAs and the proposed length-optimized splitter performs much better.

Besides splitter optimization, other design aspects are considered to enhance the network capacity starting from transceivers that combine simultaneously TDM and WDM techniques, which leads to hybrid PONs, and those who combine different OAN solutions at the physical layer to utilize more efficiency the available bandwidth. The main benefit from the coexistence of OAN solutions is the cost-efficiency and flexibility. Figure 29 shows the optical spectra of GPON/XG-PON data and voice components, and the video signal for downstream traffic, towards 64 subscribers.

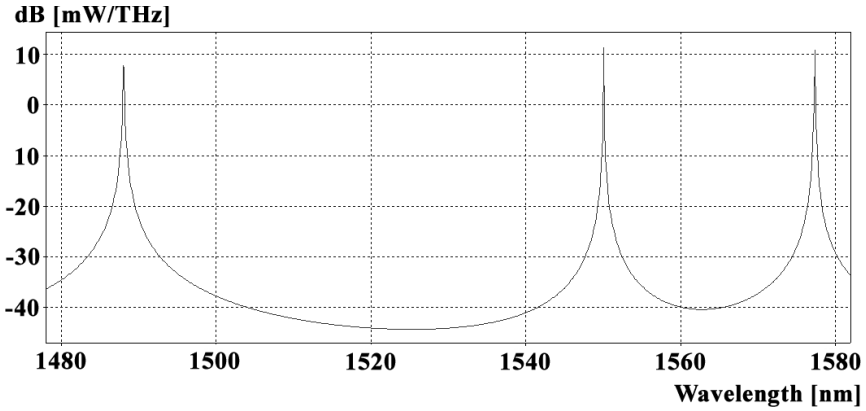

Figure 29: Optical spectrum for triple-play services and coexistence of GPON/XG-PON in a TDM-PON architecture

The allocation of optical channels avoids the cross-talk between GPON, XG-PON and video signals. The simulation results proved that this system could work with BER values lower than 10^{-10} up to 20 km. Over this system, I implement a WDM platform to model the hybrid TDM/WDM-PON as per the simulation setup described in section 3.5, Figure 13. The maximum number of allowed wavelength channels within the GPON/XG-PON bandwidth ranges as per ITU-T is determined from simulations. The 50 GHz spacing between GPON/XG-PON channels has been found out as acceptable. The overall optical spectrum of this system is shown in Figure 30.

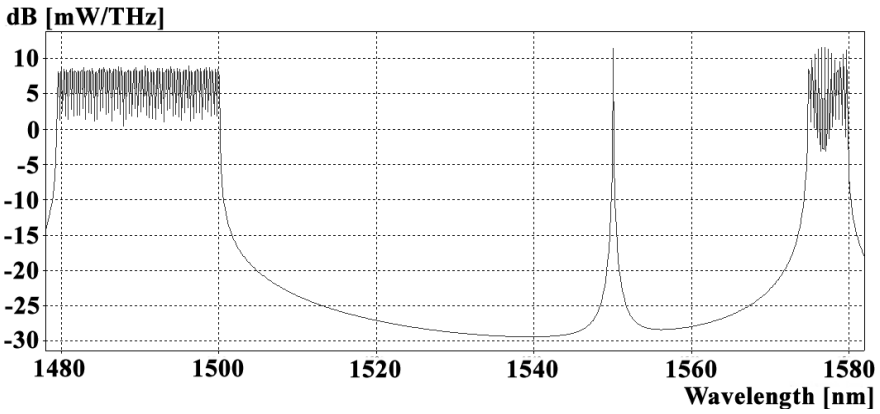

Figure 30: Spectrum for triple-play services and coexistence of multiple GPON/XG-PON channels in a TDM/WDM-PON

The simulation results showed that it is possible to fit up to 50 GPON wavelength channels and 12 XG-PON channels for the download traffic with BER less than 10^{-10}, or Q-factor higher than 6.3 respectively. This means that hybrid PONs based on this WDM scenario would allow triple-play service distribution up to 50x64 subscribers for GPON and 12x64 subscribers for XG-PON in the time domain.

The main advantages of PONs are their lower and simpler requirements on deployment and maintenance. On the other side, AONs can be a long-term investment for triple-play service delivery. Installation of a single amplifier can significantly extend the physical reach of PONs, including hybrid solutions. Therefore, installation of an optical amplifier has been investigated as well. Few options come into consideration while using optical amplification as per the simulation scheme discussed previously in section 3.5, in Figure 13. An amplifier can be deployed as a booster after the AWG at the OLT side; or before the AWG near the ONU side; or it can be used as an in-line amplifier. Deployment outside of this segment would be not efficient, since the amplification will have to be done separately on a wavelength basis. The use of an in-line amplifier would not be efficient as well from the cost and implementation perspective, as the provider will have to introduce an active NE in the middle of transmission path. I have reviewed the remaining two options in terms of BER, Q-factor and optical reach. A 10 dB amplifier was selected for reference purposes. The results showed that physical reach could be extended to 35 km while using a booster, meanwhile the deployment of an OA at the ONU side can enable a physical reach of 31 km.

NRZ is the recommended modulation format by the ITU-T for GPON/XG-PON systems. However, other intensity formats have been considered as well to search for any significant improvement in this research area. For this reason, NRZ, RZ and CSRZ formats have been simulated and compared to each other. The results showed that RZ is not beneficial for hybrid PONs mainly due to its wider spectrum, which introduces higher interference between adjacent channels in the wavelength domain. The CSRZ signalling brought just a slight improvement compared to NRZ due to its central peak suppression at the carrier frequency, which makes this reduced power to be distributed in other areas of the spectrum where real data traffic is carried. Nevertheless, due to its insignificant improvement and higher design requirements, I propose to keep NRZ and deploy the hybrid PON scenario with a booster. The final results from hybrid TDM/WDM-PONs based on GPON in the time domain are shown in Figure 31.

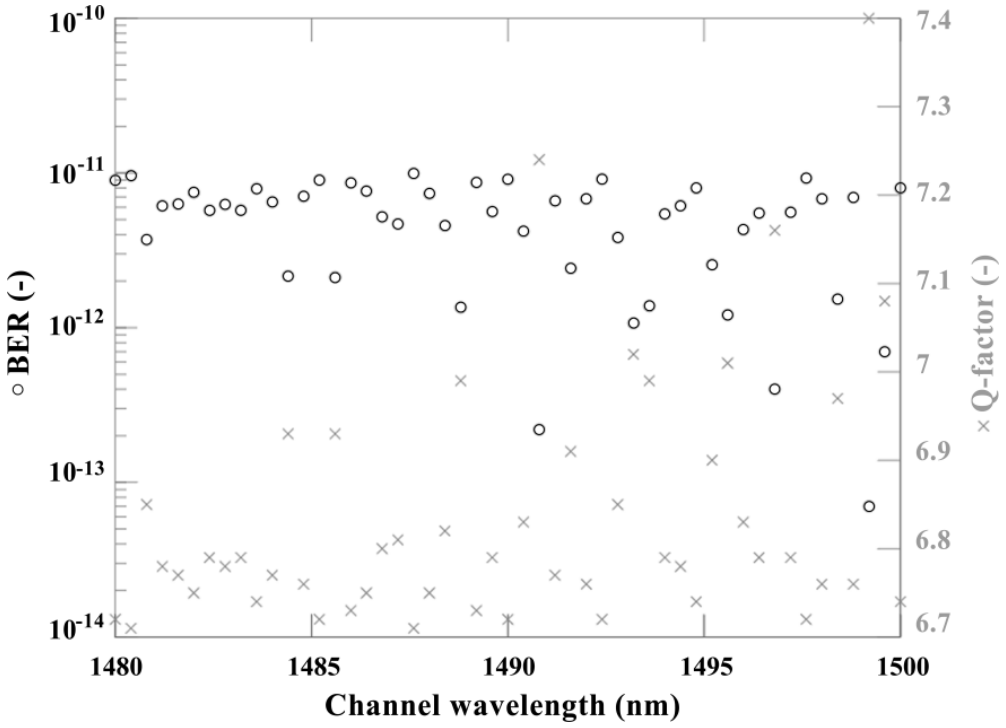

Figure 31: Q-factor (crosses) and BER (circles) for GPON downstream channels in hybrid TDM/WDM-PON

Similar results are drawn in Figure 32 for hybrid PONs based on XG-PON in the time domain. As it can be seen from these graphs, the proposed hybrid TDM/WDM-PON with a booster and 35 km long SSMF proves to have acceptable BER, respectively Q-factor values, for each of the channels, either for GPON or XG-PON TDM based.

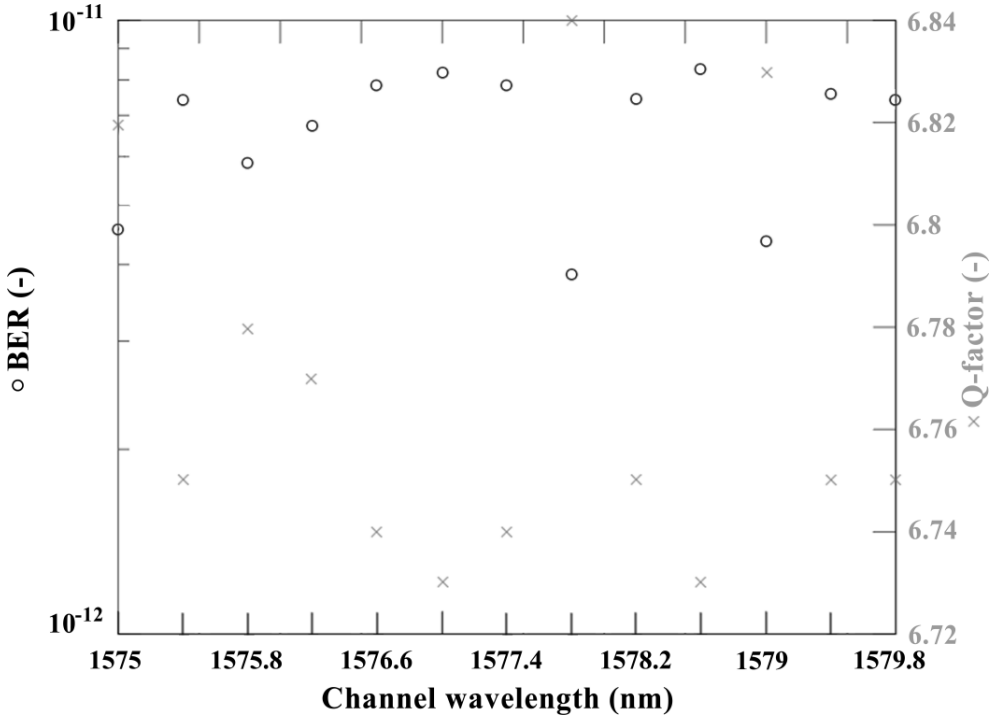

Figure 32: Q-factor (crosses) and BER (circles) for XG-PON downstream channels in hybrid TDM/WDM-PON

The combination of FTTH TDM/WDM-PON system with GPON/XG-PON, video access architecture and a booster proves to be the best solution for scalable and future-proof network systems as it combines together all benefits of TDM, WDM and AONs. I highly recommend this solution for the next generation of OANs not only because of the physical reach, capacity and amount of users that it can handle, but also due to the fact that it doesn't introduce any changes in the ODN, which makes the migration from the current network infrastructure easier, and its deployment and maintenance more efficient.

4.2 Optimization of Transmission Rate

This section summarizes the results from simulation schemes, which were proposed in Chapter 3 regarding the optimization of transmission rate in optical systems, such as the implementation of EDC and advanced modulation formats.

Firstly, the implementation of EDC using FFE and DFE is discussed based on the simulation scheme described previously in section 3.6, Figure 14. DFE was applied with 14 feed-forward and 5 feedback taps. The tap weights were optimized using the MMSE criterion. The receiver noise was considered as well. OptSim software environment doesn’t offer an FFE block by itself, however equalization has been set up as feed-forward by setting to zero

the number of taps of the Feed-Back Finite Impulse Filter in DFE block [118]. The received eye diagram without any dispersion compensation was distorted. Figure 33 shows the improvement which is done in terms of eye diagram, when EDC using MMSE-based FFE or DFE is applied.

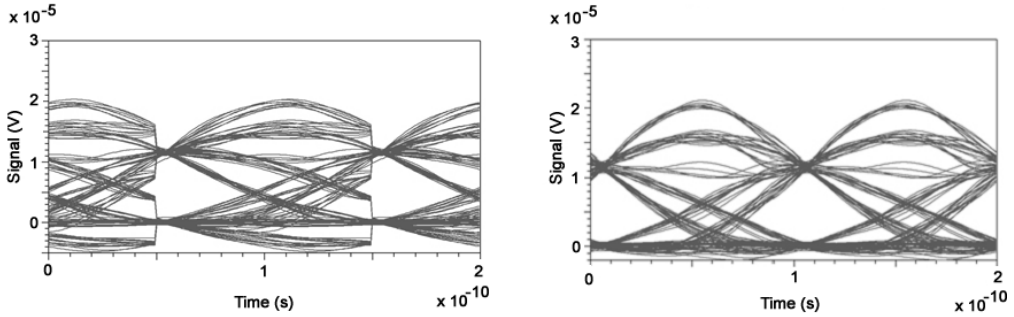

Figure 33: The received eye diagrams from EDC using MMSE-based DFE (left) and FFE (right)

Simple upgrade of multimode links from 1 Gbps to 10 Gbps without applying EDC leads to potential signal degradation due to the higher modal dispersion penalties. One of the proposed solution is the implementation of EDC based on FFE as per the simulation scheme which was described in Figure 15, section 3.6. The eye diagrams have been measured again and they are given in Figure 34.

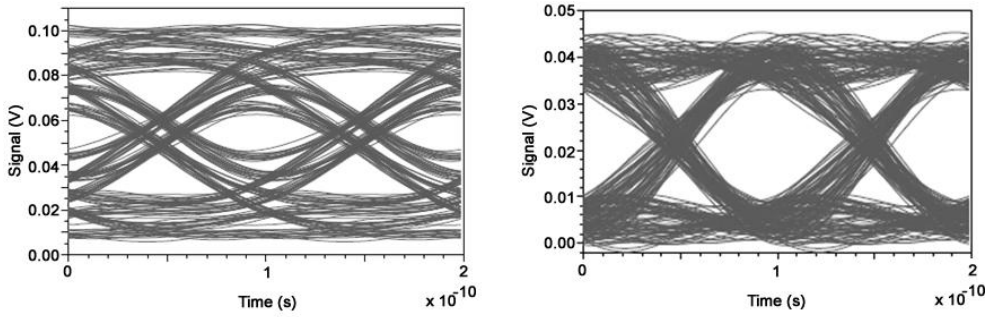

Figure 34: The eye diagrams before (left) and after (right) EDC in a multimode link

Figure 34 shows the significant enhancement when EDC is applied. The achieved BER value is on the order of 10^{-12}. This solution can be a sample implementation of the IEEE standard for 10 Gigabit Ethernet long reach multi-mode (10GBASE-LRM), which is based on the application of EDC at the receiver side.

In conclusion of EDC implementations, the design of direct-detection systems by deploying MLSE-based receivers is discussed. The results are obtained from the simulation scheme explained previously in section 3.6, Figure 16. The received eye diagram was found to be entirely closed. Figure 35 shows BER as a function of OSNR, obtained with a Monte-Carlo error counting approach [118].

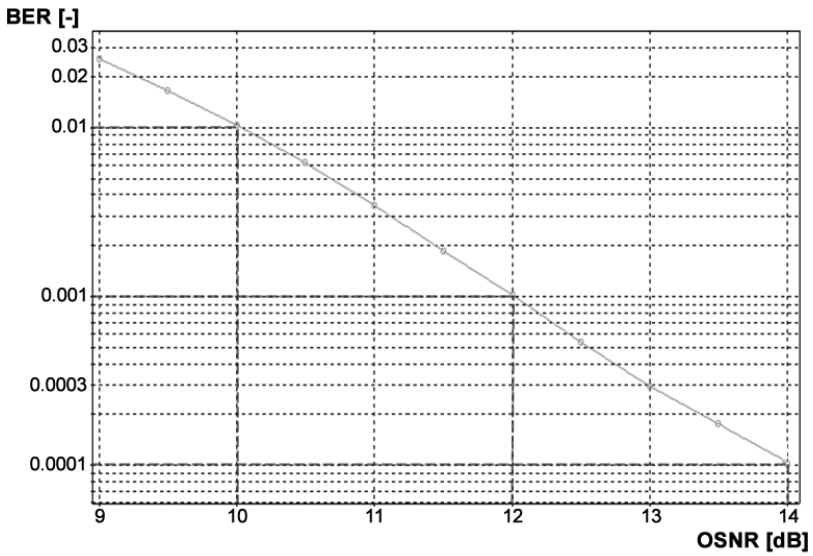

Figure 35: BER as a function of OSNR for an uncompensated transmission system with a MLSE-based receiver

As it can be seen from this graph, a BER of 10^{-4} is achieved for an OSNR equal to 14 dB. EDC is a suitable method for transmission systems up to 10 Gbps in terms of operations and cost efficiency. However, for higher transmission rates, the system can be too expensive, even for simple implementations. In addition, for very long traces in the order of hundreds of km, the standard optical dispersion compensation methods become necessary. Nevertheless, EDC can compensate non-linear effects unlike the optical domain approach. Furthermore, EDC is more resistant to PMD. This means that the best service delivery of an optical system can be achieved by properly combining electrical and optical methods, i.e. EDC for nonlinear effects and optical dispersion compensation for CD.

The selection of modulation formats represents the most significant part while designing optical systems and optimizing their transmission rate. I was focused not only on enhancing the system performance of well-known formats in practice, but also of the new proposed solutions which can be promising for future use. One-channel systems with well-known formats are investigated at 10 Gbps and 40 Gbps in terms of BER and Q-factor, as per the scheme described in section 3.7, Figure 22. The main results are summarized in Figure 36.

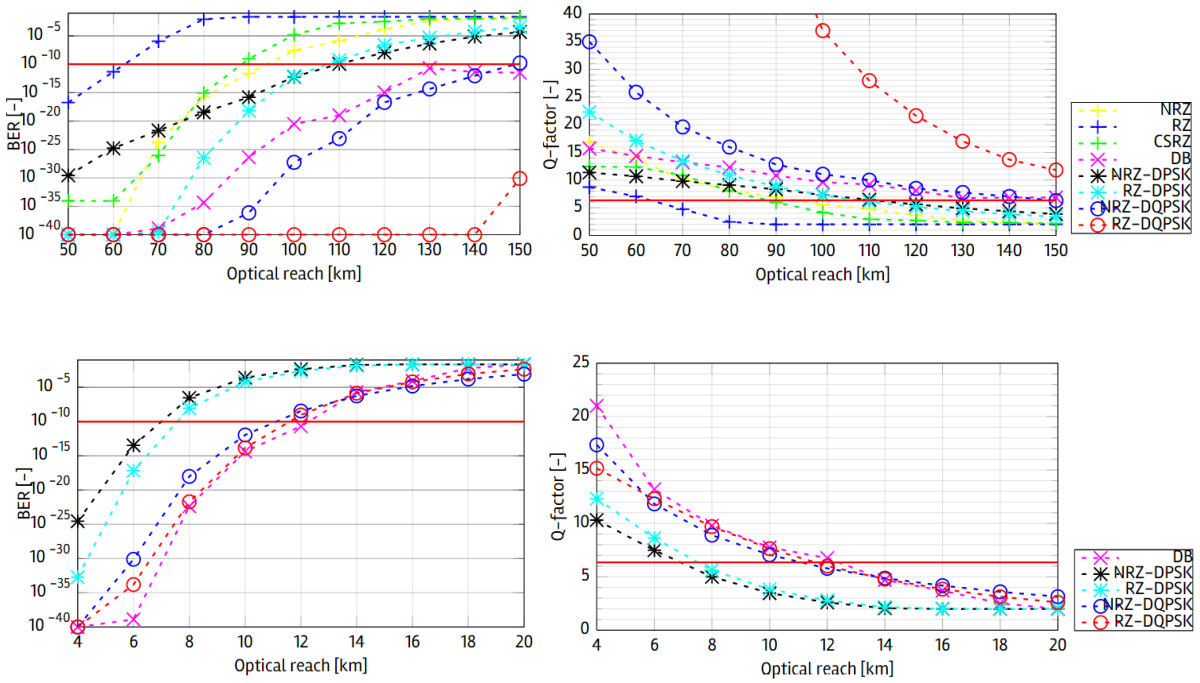

Figure 36: BERs and their corresponding Q-factor values of the investigated modulation formats in 10 Gbps (above) and 40 Gbps (below) transmission systems for different fiber lengths [3].

Although OptSim can predict very high Q-factor values, the maximum value of y-axis has been limited due to the fact that the required measurement time duration in such cases would be unfeasible. As it can be seen from the graphs, RZ-DQPSK offers at 10 Gbps the lowest BER, respectively the highest Q-factor for any fiber length. DB operates more efficiently among the intensity formats. A red horizontal line in each graph indicates the threshold values of either BER equal to 10^{-10} or its corresponding Q-factor of approx. 6.36. Figure 36 shows that only DB, NRZ-DQPSK and RZ-DQPSK meet this threshold requirement up to 150 km of fiber length. Meanwhile, all OOK formats do not perform well at 40 Gbps. For this reason, I include in the bottom graphs of Figure 36 only DB, DPSK and DQPSK formats to distinguish better their limitations on physical reach. DB, NRZ-DQPSK and RZ-DQPSK do not differ much. Up to a certain fiber length, DB can operate even better than other formats, however as the fiber length increases, DPQSK starts to take over and it offers a lower BER value.

These results however do not explain the essential physical key factors, which directly contribute in the overall system performance of a modulation format. I go deeper into the analysis and investigate each channel from the optical spectrum point of view at the operating wavelength of 1550 nm. The optical spectra of NRZ, RZ and CSRZ are given in Figure 37.

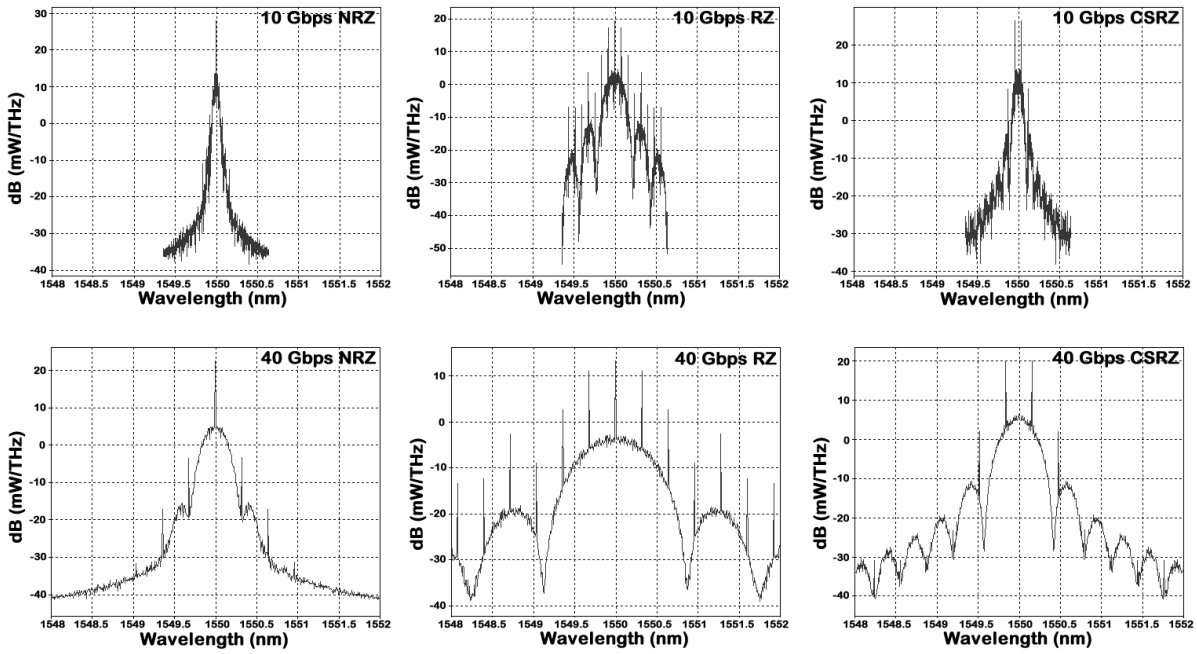

Figure 37: Optical spectra of intensity modulation formats at 10 and 40 Gbps [5]

The scale of the x axis has been unified for comparison purposes. Figure 37 shows that NRZ format has the narrowest main lobe. One can observe the spectrum broadening of RZ, which can result in an ineffective bandwidth utilization and it can significantly limit its implementation in DWDM transmission systems. CSRZ modulated signal introduces a π phase shift between adjacent bits resulting in carrier suppression, which can potentially reduce the interference between adjacent pulses.

Modulation formats have been deployed in DWDM PONs as per the simulation schemes specified previously in section 3.7. The results showed that the acceptable DWDM grid in point-to-point links for each format is 25 GHz, as per the simulation scheme given in Figure 23. In this context, NRZ and CSRZ could allow in 10 Gbps systems with 25 GHz channel spacing a maximum BER of 10^{-10} up to 80 km with a proper use of optical filters. RZ did not work well primarily due to its broader spectrum. Tree topologies have been investigated as well due to their extensive usage in access networks to deliver efficiently triple-play services among end users. I refer to the scheme shown in Figure 24. The attenuation of splitters is considered also in simulations. The results for the tree topology are analogous, while comparing them to the previous point-to-point scenario. NRZ and CSRZ could enable up to 24 km of physical reach, consisting of three fiber spans: 12 km, 8 km and 4 km, and separated by 1:8 and 1:32 splitters. Nevertheless, there was seen a slight improvement in terms of BER by CSRZ format. The transition to higher transmission rates emphasis the shortcomings of

each format, as it can be expected for the spectra shown in Figure 37. At 40 Gbps and beyond, all these formats did not achieve adequate results due to their significant increased crosstalk penalties, resulting in a highly deteriorated signal quality at the receiver. The only intensity format which benefits in higher spectral efficiencies is DB. The results from spectrum analysers are shown in Figure 38 for a DB modulated signal at 10 and 40 Gbps.

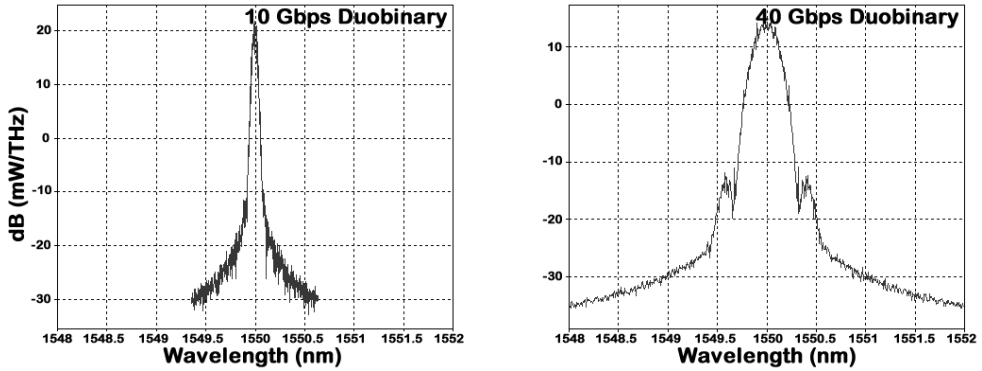

Figure 38: Optical spectra of DB at 10 and 40 Gbps [5]

At 10 Gbps, the smallest acceptable channel spacing was found to be 12.5 GHz and this combination of parameters could offer an optical reach up to 110 km. Furthermore, a DWDM grid of 25 GHz could improve 27 % more the maximum physical reach. In a tree topology, DB has been efficiently implemented at these SSMF lengths: 25 km, 15 km, 5 km, separated by 1:8 and 1:32 splitters, referring to the scheme given in Figure 24. DB's immunity to nonlinear effects is not that different from the previously mentioned binary modulation formats, especially at higher transmission rates. At 40 Gbps and 100 GHz grid, DB could grant up to 15 km of physical reach. Better results can be achieved if the dispersion map optimization is considered, among others.

Moving on to phase-based formats, new spectral features are introduced. I show in Figure 39 the optical spectra of NRZ-DPSK and RZ-DPSK. Both formats at 40 Gbps start to have much wider spectra, which extensively decreases their efficiency at this transmission rate and makes them unsuitable for higher ones. The limit acceptable grid at 10 Gbps was found to be 25 GHz. In this system, NRZ-DPSK modulated signals could travel up to 105 km and meet the maximum allowed BER requirement at the receiver side. On the other hand, RZ-DPSK offered 6 % less in terms of physical reach, primarily due to its wider spectrum which produces higher interference between adjacent channels. The simulation results in a tree topology were close as well.

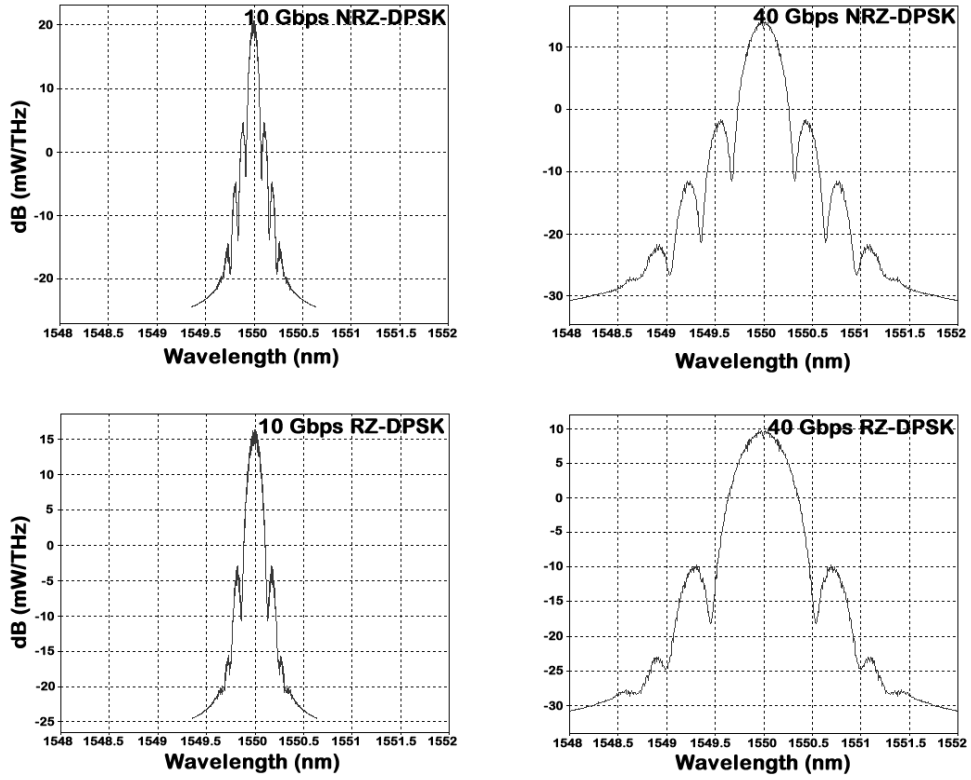

Figure 39: Optical spectra of NRZ-DPSK and RZ-DPSK at 10 and 40 Gbps [5]

At 40 Gbps, the grid limitation is 100 GHz, but the system performance of formats was significantly decreased. Simulations showed that the usage of SSMF is in this case not effective. Therefore, I tried to replace them by the world's most widely deployed Non-Zero DSF, i.e. Corning LEAF. With this fiber replacement, NRZ-DPSK could enable a physical reach up to 26 km and RZ-DPSK about 8 % more, to maintain a BER lower than 10^{-10}.

Unlike DPSK, DQPSK format introduces a compression in frequency, as shown in Figure 40. This enables higher spectral efficiency primarily at 10 Gbps, as well as increased tolerance to CD and PMD due to its longer symbol length. DQPSK can double the bit rate for a given bandwidth, or it can halve the required bandwidth for a given bit rate. The numerical results showed that NRZ-DQPSK allows a maximum optical reach of 100 km after optimizing the simulation parameters, without using any active component in the optical path in a 10 Gbps transmission system with 12.5 GHz channel spacing. Larger channel spacing significantly decreases the inter-channel interference. In case of NRZ-DQPSK, a channel spacing of 25 GHz could improve the numerical results up to 40 % in terms of physical reach. Meanwhile, RZ-DQPSK could enable up to 130 km of physical reach in a system with 12.5 GHz channel spacing and about 45 % more when the 25 GHz grid was considered. The tree

topology has been also simulated. The best outcome was achieved by a 10 Gbps RZ-DQPSK system with 25 GHz spacing, and fiber spans 110 km, 60 km and 10 km, separated by 1:8 and 1:32 splitters, according to the scheme in Figure 24.

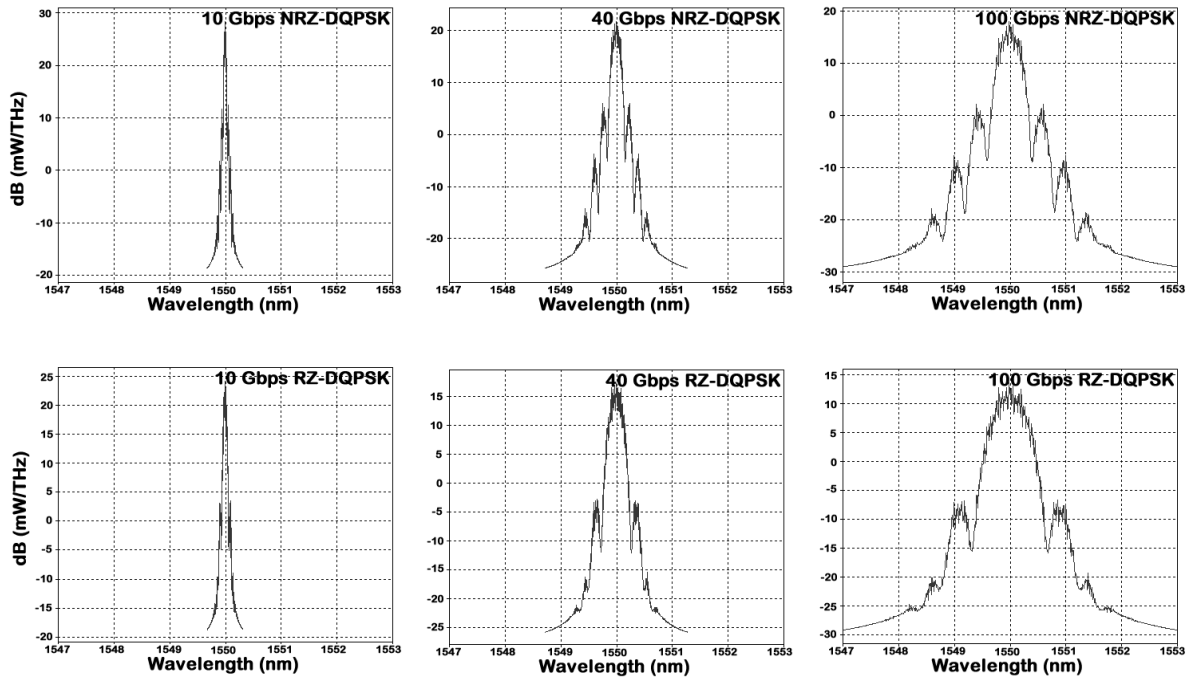

Figure 40: Spectra of NRZ-DQPSK and RZ-DQPSK at 10, 40 and 100 Gbps [5]

Similarly as DPSK, the results in terms of optical reach were poor for 40 Gbps DQPSK systems with SSMFs. After replacing SSMFs with LEAFs, the transmission path could reach up to 35 km for a 50 GHz DWDM grid, which was found to be the threshold channel spacing. RZ-DQPSK's results were 10 % lower, primarily due to its wider main lobe. As it can be also expected from Figure 40, simulations showed that optical transmission of a 100 Gbps NRZ-DQPSK DWDM system based on LEAF is not efficient without further improvements in transceivers and deployment of optical amplifiers. The maximum reach did not exceed 10 km and the maximum allowed spacing was found to be 100 GHz.

PDM-QPSK is a promising format for transmission rates 100 Gbps and beyond. This format was not simulated for lower rates that 100 Gbps, because the other simpler formats, that have been mentioned earlier, can operate well at lower transmission rates and fulfil the contemporary infrastructure needs. The higher spectral efficiency of PDM-QPSK at 100 Gbps can be noticed at first glance from its optical spectrum in Figure 41. Its coherent detection

provides high sensitivity receivers. I could find that the minimum acceptable channel spacing at 100 Gbps is 50 GHz.

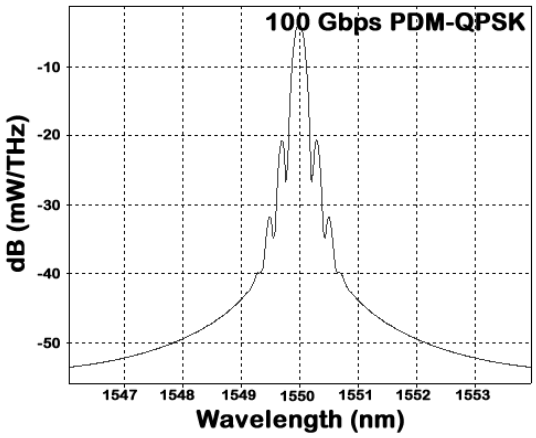

Figure 41: Optical spectrum of a 100 Gbps PDM-QPSK modulated signal [5]

By properly tuning the typical transceiver parameters, including those of optical filters, PDM-QPSK could successfully transmit optical signals up to 2000 km. I refer to the transmission scheme in Figure 25, which consisted of 20 fiber spans, 100 km each, and separated by inline amplifiers with fixed gains 20 dB. The total measured pre-FEC value for all four signals was in the order of 10^{-4} for 20 dB of span loss, which demonstrates the suitability of this format in long transmission systems.

The results from research on modulations were related till now to single-channel systems and their individual analysis in DWDM networks. Subsequently, I deploy all formats in DWDM networks, and investigate them under the same simulation parameters, topology, transmission rate and DWDM grids, as per the scheme given in Figure 23. For simplification purposes, only nine channels in C-band with central frequency at 1550 nm are shown in the results. Modulation formats were firstly deployed in a 10 Gbps transmission system with 25 GHz channel spacing, for three different fiber lengths: 70, 100 and 130 km. PDM-QPSK was not included in the results, because currently there is no acute need and cost benefit to deploy at lower speeds such complex formats, which are primarily designed for 100 Gbps and beyond. The results are shown in Figure 42. As previously mentioned, the red lines in graphs are related to the threshold values, i.e. Q-factor of approx. 6.36 and BER of 10^{-10}. The y-axis has been limited up to a Q-factor of 7, which corresponds to a BER of approximately 10^{-12}. Referring to the limitation of OOK formats, a 25 GHz DWDM grid is considered in the graphs of Figure 42. At 10 Gbps, all formats worked well in a 70 km SSMF transmission system, except of RZ, which is mainly affected by its wider spectrum.

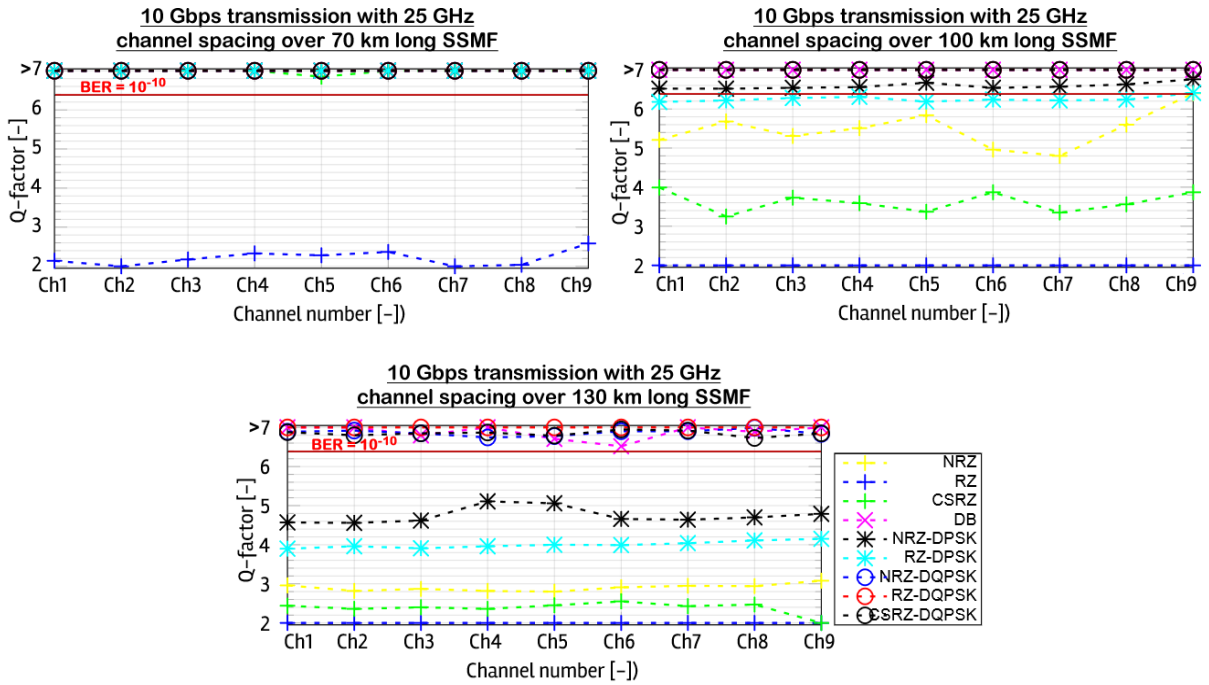

Figure 42: 10 Gbps DWDM systems with 25 GHz channel spacing and fiber length 70, 100 and 130 km [4].

As the fiber length increases, the difference between formats becomes more clear. At 100 km, all OOK formats do not meet the threshold BER requirement, although NRZ worked a little better. Meanwhile, the results of DPSK formats are close to threshold values. The slight difference between NRZ-DPSK and RZ-DPSK is primarily related to the wider spectrum of RZ-DPSK. DB is the only intensity format, which is still stable even for a 130 km long transmission and its system functionality is quite similar to that of DQPSK. Furthermore, DB's narrow bandwidth could manage together with DQPSK also a 12.5 GHz grid. The outcome from this channel spacing over a 100 km long transmission is shown in Figure 43.

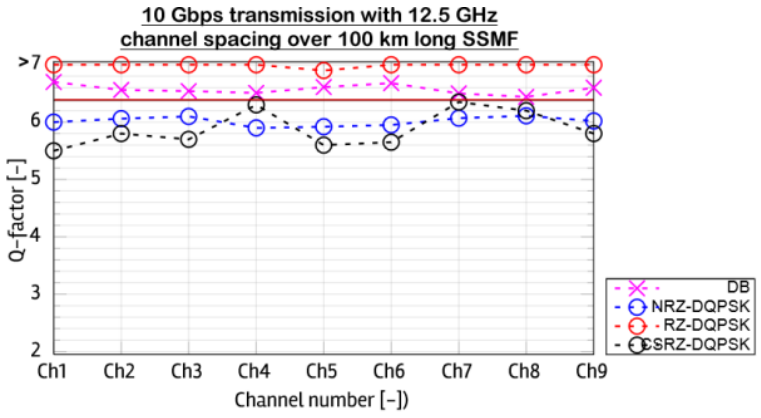

Figure 43: 10 Gbps DWDM system with 12.5 GHz channel spacing and 100 km long SSMF [4].

The highest Q-factor for each optical channel was achieved by RZ-DQPSK among DQPSK formats. DB proves again to be a stable format, which can be even more efficient than NRZ-DQPSK and CSRZ-DQPSK in terms of transmitter design complexity.

All formats are subsequently deployed in a 40 Gbps system. The fiber length is set to 12 km to distinguish better the performance between individual formats. OOK's efficiency significantly decreases at this rate, therefore they have been excluded from the results in Figure 44.

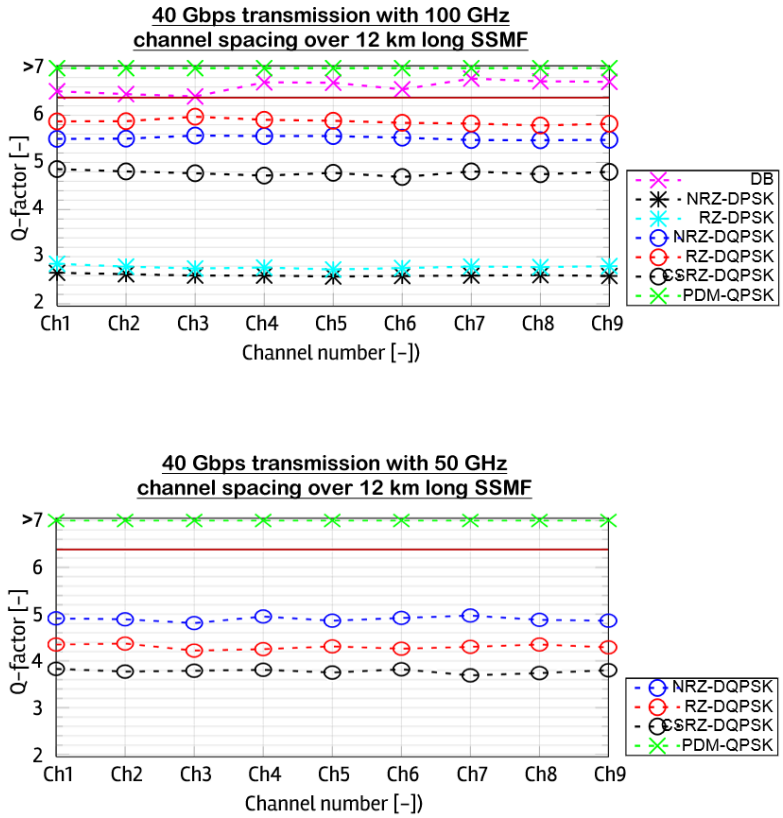

Figure 44: 40 Gbps DWDM systems with 12 km long SSMF [4].

The results are shown for two different DWDM grids. The first selected grid is 100 GHz, which is the minimum acceptable channel spacing for DB and DPSK. The second grid is 50 GHz, which is related to the grid limitations of DQPSK and PDM-QPSK formats. From the first graph of Figure 44, it can be seen the overall system improvement in terms of Q-factor of DQPSK compared to DPSK for each optical channel. Although being an intensity format, DB proves its superiority in this scenario over phase-based formats. Nevertheless, DB's boundary DWDM grid at 40 Gbps is 100 GHz and the only two formats which could handle a channel spacing of 50 GHz are DPQSK and PDM-QPSK. PDM-QPSK operates way better than

DPQSK and furthermore, it can also be efficient at 100 Gbps with 50 GHz spacing, and as it was earlier shown, it can enable hundreds of km of physical reach by properly applying dispersion compensation techniques and in-line amplification.

Other modulation formats more complex than PDM-QPSK have been studied as well. Nowadays some trials exist mainly in the lab environments, but none of them has been standardized to be massively deployed in practice. The primary reason is their design complexity for massive production so far and operators are often using other simpler solutions such as link aggregation technologies or deployment of more fibers with common transceivers to fulfil the capacity needs in their backbone networks. One of the most promising solutions which might be a standardized solution in the upcoming years for terabit transmissions can be the combination of QAM formats with PDM. The idea behind it, is similar as the combination of QPSK with PDM. I simulate PDM-QPSK and PDM-16QAM formats using the simulation scheme as per Figure 25, with a 50 GHz grid for few optical channels at a baud rate of 32 Gbps. This results in a per channel bit rate of 128 Gbps in case of PDM-QPSK and 256 Gbps in case of PDM-16QAM including FEC overhead. The optical spectrum of PDM-16QAM is given in Figure 45.

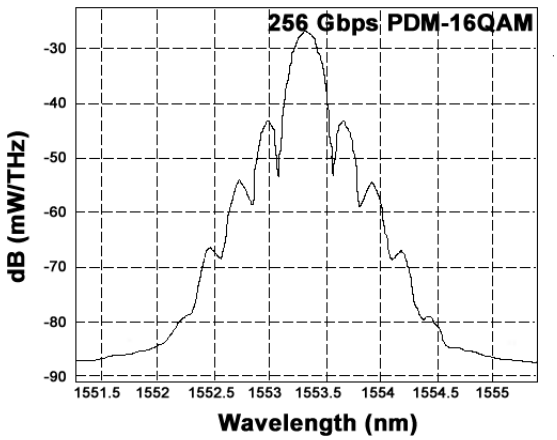

Figure 45: Optical spectrum of a 256 Gbps PDM-16QAM modulated signal

The spectral efficiency for PDM-QPSK is 2.56 bits/Hz (i.e. 128 Gbps / 50 GHz), meanwhile for PDM-16QAM is 5.12 bits/Hz (i.e. 256 Gbps / 50 GHz). This means that PDM-16QAM offers double spectral efficiency compared to PDM-QPSK. However this comes at the cost of higher required OSNR at a given BER. For e.g., the required OSNR for a pre-FEC BER of 10^{-3} is 13.5 dB for PDM-QPSK and 21 dB for PDM-16QAM.

Conclusions

In this thesis I proposed many novel solutions that can be utilized for the optimization of existing optical telecommunication networks and fulfilment of future demands for higher transmission rates and capacities. Among the proposed solutions are: the use of complex modulation formats for transmissions above 100 Gbps per optical channel such as PDM-QPSK and PDM-xQAM; transparency and convergence of access networks at the physical layer including dynamic solutions which can support different bit rates within the same transmission system; optimization of CWDM and DWDM systems and their maximum allowed channel spacing; maximal utilization of the fiber capacity meanwhile minimization of the cost per transmitted date; and deployment of length optimized splitters, among others. Thesis gave a broad set of recommendations on how to systematically design optical networks, either access or backbone, based on the topology, number of channels, most efficient modulation format and highest possible network throughput.

A low-loss length-optimized 1x64 Y-branch splitter has been considered to improve the insertion loss uniformity of casual splitters, so the signal quality from providers' edge to customers is distributed in even quality. This adds additional assurance to providers to maintain the same SLA to each of the customers. Significant improvements were achieved at 10 Gbps systems in terms of BER, Q-factor. I showed that the combination of WDM and TDM is the most efficient PON solution in terms of cost-effectiveness, flexibility and extendibility. The hybrid system based on GPON and XG-PON recommendations in the time domain could theoretically provide simultaneous network connectivity up to four thousands of subscribers over the same optical medium. The same system was optimized further by deploying a booster, which could significantly extend the physical reach. This proposed solution doesn't introduce any changes within ODN and it can serve as a long-term resolution for future data, voice and video demands on access networks. The EDC implementation is one of the ways how to contribute on transmission rate optimization. Implementation of EDCs using MMSE-based FFE and DFE was investigated as well as EDC FFEs in multimode links, and MLSE receivers for uncompensated systems. EDC can compensate non-linear effects and it is more resistant to PMD, unlike the standard optical dispersion compensation methods. However, for higher transmission rates than 10 Gbps, the system can be too expensive even for simple scenarios, hence as a better approach comes the proper

combination of electrical and optical methods, i.e. EDC for nonlinear effects and optical dispersion compensation for CD.

A significant part of the research done for this thesis was also the investigation of modulation formats, since they play the most significant role while designing optical transceivers. In this document I primarily investigated intensity, phase-based and PDM-based modulation formats. The main goal was to find out their limitations in commonly used network topologies, either single-channel or DWDM systems, with respect to transmission rate, BER, Q-factor, OSNR, optical reach, spectral efficiency, transceiver design, hardware limitations, channel spacing, fiber type, among others. Limitations in DWDM networks were figured out for each format and the most suitable solution has been proposed. Many schemes have been recommended to be the ones with the most efficient modulation format based on the number of channels, topology, either point to point or tree topology, channel spacing if more than one channel, transmission rate, fiber type and physical reach. The spectrum of each individual format was analyzed at a reference wavelength and justified why it is an important physical factor, which directly affects the spectral efficiency and the overall system performance. The spectrum broadening of RZ can result in an ineffective fiber capacity utilization, primarily in DWDM systems. Up to 10 Gbps, NRZ and CSRZ operate well even for a channel spacing of 25 GHz. At 40 Gbps, all OOK formats were not suitable due to their significant increased crosstalk penalties, resulting in a highly deteriorated signal quality at the receiver side. Among all intensity formats, DB performed the best.

Phase-based modulation formats introduce new spectral features. DPSK could enable a physical reach above 100 km in 10 Gbps systems with 25 GHz grid, and without any repeaters involved. At 40 Gbps, NRZ-DPSK and RZ-DPSK formats can be beneficial while running over Corning LEAFs and minimum channel spacing of 100 GHz. Nevertheless, DPSK didn't offer significant improvements compared to other phase-based formats. DQPSK format introduces a new enhanced compression in frequency, and it can double the bit rate for a given bandwidth. Among the biggest advantages of this format are: higher spectral efficiency primarily at 10 Gbps, as well as increased tolerance to CD and PMD due to its longer symbol length. At 40 Gbps, DQPSK can be also an attractive solution in DWDM PON systems with 50 GHz grid and LEAFs within the ODN. After comparing all these formats within the same ODN which utilized the DWDM technique, DB proved to be even more efficient at 10 Gbps than DQPSK in terms of transceiver design and implementation complexity. DB proved to perform the best at 40 Gbps as well, however its boundary DWDM grid at this transmission rate is 100 GHz.

The most promising formats for future PONs are the ones that combine phase modulation with PDM, coherent detection and DSP, at the cost of higher design complexity, power consumption and faster circuits. These formats were proved to bring significant benefits at 100 Gbps and beyond. PDM-QPSK has been recommended to be used at 100 Gbps and PDM-16QAM at 256 Gbps in DWDM systems with 50 GHz channel spacing. By proper tuning of the parameters within the transmission system, PDM-QPSK could carry data traffic up to 2000 km of transmission path with the help of dispersion compensation techniques and optical amplification. PDM-QPSK and PDM-16QAM have been investigated in DWDM systems to determine which of them can offer a more significant scientific progress in the area of optical transmitter design. PDM-16QAM was found to offer double spectral efficiency compared to PDM-QPSK, at the cost of higher OSNR for a given BER.

I strongly believe that 400 Gbps or 1 Tbps channels for long-haul transmission systems can be standardized in a near future as well, if the vendors properly combine and utilize the followings: complex constellations, high symbol rates, multiple sub-carriers. This is an open research which might take several more years.

List of Publications:

Journal with Impact Factor

1. Agalliu, R.; Lucki, M., “System Performance and Limits of Optical Modulation Formats in Dense Wavelength Division Multiplexing Systems,” Elektronika IR Elektrotechnika, ISSN 1392-1215, vol.22, no.2, pp.123-129, doi: http://dx.doi.org/10.5755/j01.eie.22.2.9599, April 2016 (50%).

   Cited by 1 document in SCOPUS:

   - Kurbatska, O.; Alsevska, A.; Gegere, L.; Bobrovs, V., "Investigation of influence of mixed configurations on performance of WDM-PON," Elektronika IR Elektrotechnika, ISSN 2029-5731, vol.23, no.2, pp.74-78, doi: http://dx.doi.org/10.5755/j01.eie.23.2.18003, April 2017.

Peer-reviewed Journal

2. Agalliu, R.; Lucki, M., “Benefits and Limits of Modulation Formats for Optical Communications,” Advances in Electrical and Electronic Engineering, vol.12, no.2, pp.160-167, doi: 10.15598/aeee.v12i2.992, June 2014 (50%).

   Cited by 11 documents in SCOPUS:

   - Kurbatska, I.; Spolitis, S.; Bobrovs, V.; Alsevska, A.; Ivanovs, G., “Performance comparison of modulation formats for 10 Gbit/s WDM-PON systems,” Advances in Wireless and Optical Communications, RTUWO, January 2017.
   - Kurbatska, I.; Spolitis, S.; Ivanovs, G.; Bobrovs, V., “Investigation on optimal transmission parameters for different modulation formats in 10 Gbit/s WDM-PON systems,” International Workshop on Fiber Optics in Access Network, FOAN, December 2016.
   - Vitasek, J.; Latal, J.; Bojko, M.; Vanderka, A.; Hajek, L.; Hejduk, S., “Measurement and modelling of thermal turbulence effects on FSO optical beams,” International Conference on Transparent Optical Networks, doi: 10.1109/ICTON.2016.7550484, August 2016.
   - Vitasek, J.; Martinek, R.; Vanderka, A.; Hajek, L.; Latal, J.; Lu, Z.; Li, B., ‘Effects of carbon dioxide on different PSK modulation formats of Optical Wireless Communications using USRP,” International Conference on Transparent Optical Networks, doi: 10.1109/ICTON.2016.7550384, August 2016.
   - Kurbatska, I.; Bobrovs, V.; Spolitis, S.; Gavars, P.; Ivanovs, G.; Parts, R., “Investigation on Maximum Available Reach for Different Modulation Formats in WDM-PON Systems,” Latvian Journal of Physics and Technical Sciences, vol.53, iss.4, pp.66-75, doi: 10.1515/lpts-2016-0030, August 2016.

- Vanderka, A.; Hajek, L.; Bednarek, L.; Latal, J.; Vitasek, J.; Hejduk, S.; Vasinek, V., "Testing FSO WDM communication system in simulation software optiwave OptiSystem in different atmospheric environments," Proceedings of SPIE - The International Society for Optical Engineering, vol.9979, September 2016.
- Litvik, J.; Kuba, M.; Benedikovic, D.; Dubovan, J.; Dado, M., "Numerical Estimation of Spectral Properties of Laser Based on Rate Equations," Mathematical Problems in Engineering, doi: 10.1155/2016/4152895, January 2016.
- Koudelka, P.; Latal, J.; Siska, P.; Vitasek, J.; Liner, A.; Martinek, R.; Vasinek, V., "Indoor visible light communication: Modeling and analysis of multi-state modulation," Proceedings of SPIE - The International Society for Optical Engineering, conference volume 9224, doi: 10.1117/12.2063090, October 2014.
- Vanderka, A.; Hajek, L.; Latal, J.; Vitasek, J.; Hejduk, S.; Vasinek, V., "Testing resistance modulation formats for FSO communication in turbulent environment, with used simulation box," Proceedings of SPIE - The International Society for Optical Engineering, conference volume 9614, doi: 10.1117/12.2180335, September 2015.
- Liner, A.; Papes, M.; Jaros, J.; Koudelka, P.; Latal, J.; Vitasek, J.; Hajek, L.; Vasinek, V., "Software design of optical link for indoor wireless optical communication network used LEDs as source visible light communication," Proceedings of SPIE - The International Society for Optical Engineering, conference volume 9387, doi: 10.1117/12.2087120, February 2015 .
- Vitasek, J.; Siska, P.; Kepak, S.; Cubik, J.; Poboril, R.; Latal, J., "VLC transmitter with plastic optical fibers for indoor free space optic networks," Advances in Electrical and Electronic Engineering, vol.12, iss.6, pp.617-621, doi: 10.15598/aeee.v12i6.1273, 2014.

Conference Proceedings

3. Agalliu, R.; Lucki, M., "System improvements in dense wavelength division multiplexing networks by using advanced optical modulation formats," 17th International Conference on Transparent Optical Networks (ICTON), doi: 10.1109/ICTON.2015.7193511, July 2015 (50%).

Cited by 2 documents in SCOPUS:

- Kurbatska, I.; Alsevska, A.; Gegere, L.; Bobrovs, V., "Comparison of modulation formats for use in the next generation passive optical networks," Progress In Electromagnetics Research Symposium, PIERS, November 2016.
- Kurbatska, I.; Bobrovs, V.; Spolitis, S.; Gavars, P.; Ivanovs, G.; Parts, R., "Investigation on Maximum Available Reach for Different Modulation Formats in WDM-PON Systems," Latvian Journal of Physics and Technical Sciences, vol.53, iss.4, pp.66-75, doi: 10.1515/lpts-2016-0030, August 2016.

4. Lucki, M.; Agalliu, R.; Zeleny, R., “Limits of advanced modulations formats for transition in fiber optical telecommunication systems to increase speeds from 10, 40, 100 Gbps to higher bit rates,” Proc. SPIE 9131, Optical Modeling and Design III, doi:10.1117/12.2054279, May 2014 (33.33%).

5. Agalliu, R., “Comparison of Modulation Formats in Fiber-Optic Transmission Systems,” 19th International Student Conference on Electrical Engineering (Poster CVUT), May 2015.

Under Peer Review:

6. Agalliu, R.; Burtscher, C.; Lucki, M.; Seyringer, D., “Optical splitter design for application in telecommunication access networks with triple-play services,” Elektronika IR Elektrotechnika (25%).

7. Agalliu, R.; Lucki, M., "Achieving transmission rate of 100 Gbps and beyond by using polarization division multiplexing, coherent detection and digital signal processing," Advances in Electrical and Electronic Engineering (50%).

8. Agalliu, R.; Lucki, M., “Transmission network transparency and potential convergence of optical access network solutions at the physical layer,” Optical Engineering (50%).

References

[1] Lucki, M.; Agalliu, R.; Zeleny, R., “Limits of advanced modulations formats for transition in fiber optical telecommunication systems to increase speeds from 10, 40, 100 Gbps to higher bit rates,” Proc. SPIE 9131, Optical Modelling and Design III, doi:10.1117/12.2054279.May 2014.

[2] Agalliu, R.; Lucki, M., “Benefits and Limits of Modulation Formats for Optical Communications,” Advances in Electrical and Electronic Engineering, vol.12, no.2, pp.160-167, doi: 10.15598/aeee.v12i2.992, June 2014.

[3] Agalliu, R., “Comparison of Modulation Formats in Fiber-Optic Transmission Systems,” 19th International Student Conference on Electrical Engineering (Poster CVUT), May 2015.

[4] Agalliu, R.; Lucki, M., “System improvements in dense wavelength division multiplexing networks by using advanced optical modulation formats,” 17thInternational Conference on Transparent Optical Networks (ICTON), doi: 10.1109/ICTON.2015.7193511, July 2015.

[5] Agalliu, R.; Lucki, M., “System Performance and Limits of Optical Modulation Formats in Dense Wavelength Division Multiplexing Systems,” Elektronika IR Elektrotechnika, ISSN 1392-1215, vol.22, no.2, pp.123-129, doi: http://dx.doi.org/10.5755/j01.eie.22.2.9599, April 2016,

[6] ITU-T Recommendation G.982, “Optical access networks to support services up to the ISDN primary rate or equivalent bit rates,” available from: <http://www.itu.int/rec/T-REC-G.982-199611-I/en>, November 1996.

[7] Schlitter, P., “Optické prístupové site,” available from: <http://access.feld.cvut.cz/view.php?cisloclanku=2004072807>, July 2004 [Cited 10 February 2016].

[8] Steenbergen, A R. “Everything You Always Wanted to Know About Optical Networking – But Were Afraid to Ask,” 57th meeting of the North American Network Operators' Group (NANOG), February 2013.

[9] ITU-T Recommendation G.694.2,“Spectral grids for WDM applications: CWDM wavelength grid,” available from <http://www.itu.int/rec/T-REC-G.694.2>, December 2003.

[10] Fiberstore, “Research work of transmission systems-CWDM VS DWDM,” available

from: <http://www.fiberstore.com/Research-work-of-transmission-systems-CWDM-VS-DWDM-aid-63.html>, June 2013 [Cited 15 March 2016].

[11] Udunuwara, A., "An Introduction to Optical Backbone Networks," available from: <http://www.slideshare.net/udunuwara/introduction-to-optical-backbone-networks>,April 2014 [Cited 20 January 2016].

[12] ITU-T Recommendation G.694.1, "Spectral grids for WDM applications: DWDM frequency grid," available from: <http://www.itu.int/rec/T-REC-G.694.1/>, February 2012.

[13] Brobe, K.; Elbers, J., "PON Evolution from TDMA to WDM-PON," Optical Fiber communication/National Fiber Optic Engineers Conference (OFC/NFOEC), doi: 10.1109/OFC.2008.4528293, May 2008.

[14] Wey, J. Sh., "Advances in Next Generation FTTH: Ultra Dense WDM-PON Utilizing Coherent Detection," Nokia Siemens Networks, December 2010.

[15] Seyringer, D., "Arrayed Waveguide Gratings: tiny structures for big ideas," FHV Research Centre for Microtechnology, Application Note, May 2010.

[16] Dixit, S.,"IP over WDM: Building the Next-Generation Optical Internet," ISBN: 978-0471212485, January 2004.

[17] Agata, A.; Nishimura, K., "Suboptimal PON Network Designing Algorithm for Minimizing Deployment Cost of Optical Fiber Cables," 16th International Conference on Optical Network Design and Modelling (ONDM), doi: 10.1109/ONDM.2012.6210195, June 2012.

[18] Prat, J.; Lazaro, J.; Chanclou, P.; Soila, R.; Velanas, P.; Texeira, A.; Beleffi, G.; Tomkos, I.; Klonidis, D., "Hybrid Ring-Tree WDM/TDM-PON Optical Distribution Network". 11th International Conference on Transparent Optical Networks (ICTON), doi: 10.1109/ICTON.2009.5185328, July 2009.

[19] Vodrazka, J., "Optické prístupové síte EPON a CWDM", available from: <http://access.feld.cvut.cz/view.php?nazevclanku=opticke-pristupove-site-epon-a-cwdm&cisloclanku=2005070401, July 2005 [Cited 25 November 2015].

[20] IEEE Standard 802.3av, "Telecommunications and information exchange between systems; Local and metropolitan area networks; Specific requirements. Part 3: Carrier Sense Multiple Access with Collision Detection (CSMA/CD) Access Method and Physical Layer Specifications. Amendment: Physical Layer Specifications and Management Parameters for 10 Gb/s Passive Optical Networks," available from: <http://ieeexplore.ieee.org/servlet/opac?punumber=4816156>, April 2009.

[21] ITU-T Recommendation G.987.1, “10-Gigabit-capable passive optical networks (XG-PON): General requirements,” available from: <http://www.itu.int/rec/T-REC-G.987.1/en>, March 2016.

[22] ITU-T Recommendation G.983.1, “Broadband optical access systems based on Passive Optical Networks (PON),” available from: <http://www.itu.int/rec/T-REC-G.983.1/en>, January 2005.

[23] ITU-T Recommendation G.984.1, “Gigabit-capable passive optical networks (GPON): General characteristics,” available from: <http://www.itu.int/rec/T-REC-G.984.1/en>, March 2008.

[24] ITU-T Recommendation G.984.5, “Gigabit-capable Passive Optical Networks (G-PON): Enhancement band,” available from: <http://www.itu.int/rec/T-REC-G.984.5/en>, May 2014.

[25] Sima, J., “GPON site a jak dal? Site FTTx v roce 2013,” RLC Praha a.s., available from: <http://www.profiber.eu/files/14.3.2013_A5_Jaromir_Sima_A5_-_GPON_site_a_jak_dal.pdf>, March 2013.

[26] Trost, J., “An Overview of GPON in the An Overview of GPON in the Access Network,” Ericsson AB, November 2008.

[27] IEEE Standard 802.3ah, “Telecommunications and information exchange between system; Local and metropolitan area networks; Specific requirements. Part 3: Carrier Sense Multiple Access with Collision Detection (CSMA/CD) Access Method and Physical Layer Specifications. Amendment: Media Access Control Parameters, Physical Layers, and Management Parameters for Subscriber Access Networks,” available from: <http://www.ieee802.org/21/doctree/2006_Meeting_Docs/2006-11_meeting_docs/802.3ah-2004.pdf>, September 2004.

[28] Jain, S.; Effenberger, F.; Szabo, A.; Feng, Zh.; Forcucci, A.; Guo, W.; Luo, Y.; Mapes, R.; Zhang, Y.; O’Byrne, V., "World's First XG-PON Field Trial," Journal of Lightwave Technology, vol.29, no.4, pp.524-528, doi: 10.1109/JLT.2010.2104313, January 2011.

[29] Novotny, K.; Martan, T.; Sistek, J., “Systémy pro optické komunikace,“ ISBN: 80-01-02810-0, 2007.

[30] Novotny, K.,“Optická komunikační technika,” ISBN: 978-80-01-03920-5, 2002.

[31] ITU-T Recommendation G.984.2 Amendment 1, “Gigabit-capable Passive Optical Networks (G-PON): Physical Media Dependent (PMD) layer specification, Amendment 1: New Appendix III – Industry best practice for 2.488 Gbit/s downstream, 1.244 Gbit/s upstream G-PON,” available from:

<http://www.itu.int/rec/T-REC-G.984.2-200602-I!Amd1/en>, February 2006.

[32] ITU-T Recommendation G.984.2 Amendment 2, “Gigabit-capable Passive Optical Networks (G-PON): Physical Media Dependent (PMD) layer specification, Amendment 2,” available from: <http://www.itu.int/rec/T-REC-G.984.2-200803-I!Amd2/en>, March 2008.

[33] ITU-T Recommendation G.984.6, “Gigabit-capable passive optical networks (GPON): Reach extension,” available from: <http://www.itu.int/rec/T-REC-G.984.6/en>, March 2008.

[34] ITU-T recommendation G.984.7, “Gigabit-capable passive optical networks (GPON): Long reach,” available from: <http://www.itu.int/rec/T-REC-G.984.7/en>, July 2010.

[35] Hood, D.; Lu, L., "Current and future ITU-T PON systems and standards," 17th Opto-Electronics and Communications Conference (OECC), pp.125,doi: 10.1109/OECC.2012.6276402, July 2012.

[36] Boriboon, B.; Worasucheep, D.; Shimizu, S.; Wada, N., "Computation and experiments of 10 Gb/s optical access network with long reach and a large number of subscribers," 12th International Conference on Electrical Engineering/Electronics, Computer, Telecommunications and Information Technology (ECTI-CON), pp.1-6, doi: 10.1109/ECTICon.2015.7206934, June 2015.

[37] Kaur, A.; Singh, M.L; Sheetal, A., "Comparison of RZ and NRZ data formats for co-existing GPON and XG-PON system," International Conference on Advanced Nanomaterials and Emerging Engineering Technologies (ICANMEET), pp.666-669, doi: 10.1109/ICANMEET.2013.6609379, July 2013.

[38] Elbers, J.-P.; Grobe, K., "Optical access solutions beyond 10G-EPON/XG-PON," Conference on Optical Fiber Communication (OFC/NFOEC), collocated National Fiber Optic Engineers Conference, pp.1-3, May 2010.

[39] Lei, J., “Architecture Analysis of Hybrid TDM/WDM PON,” IEEE meeting, Huawei Technologies, available from: <http://www.ieee802.org/3/ad_hoc/ngepon/public/jul14/lei_ngepon_01_0714.pdf>, July 2014.

[40] Abdalla, M.E.; Idrus, S.M.; Mohammad, A.B., "Hybrid TDM-WDM 10G-PON for high scalability next generation PON," 8th IEEE Conference on Industrial Electronics and Applications (ICIEA), pp.1448-1450, doi: 10.1109/ICANMEET.2013.6609379, July 2013.

[41] Wong, E., "Next-Generation Broadband Access Networks and Technologies," Journal

of Lightwave Technology, vol.30, no.4, pp.597-608, February 2012.

[42] ITU-T recommendationG.989, “40-Gigabit-Capable Passive Optical Network (NG-PON2): Definitions, abbreviations and acronyms,” available from: <https://www.itu.int/rec/T-REC-G.989/en>, October 2015.

[43] Lin, R., “Next Generation PON in Emerging Networks,” Conference on Optical Fiber communication/National Fiber Optic Engineers (OFC/NFOEC), doi: 10.1109/OFC.2008.4528701, February 2008.

[44] Hulsermann, R.; Grobe, K.; Breuer, D., “Cost and Performance Evaluation of WDM-Based Access Networks,” Conference on Optical Fiber communication/National Fiber Optic Engineers (OFC/NFOEC), doi: https://doi.org/10.1364/NFOEC.2013.NTh3F.4, March, 2013.

[45] Hatt, A.K.; Zetteberg, O.; Ahl, K.; Bosshart, D.; Montagne, R.; Chaillou, V.; “Creating a Brighter Future,” FTTH Council Europe Press Conference, available from: <http://www.ftthcouncil.eu/documents/Presentations/20140219PressConfStockholm.pdf>, February 2014.

[46] Machuca, C.; Krauss, S.; Kind, M., “Migration from GPON to Hybrid PON: Complete Cost Evaluation,” ITG Symposium Proceedings - Photonic Networks, pp.1–6, May 2013.

[47] Wang, K.; Gavler, A.; Machuca, C.M.; Wosinska, L.; Brunnström, K.; Chen, J., “Migration Strategies for FTTx Solutions Based on Active Optical Networks”, IEEE Communications Magazine, vol.54, iss.2, pp.78-85, doi: 10.1109/MCOM.2016.7402265, February 2016.

[48] Emsia, A.; Le, Q.T.; Malekizandi, M.; Briggmann, D.; Djordjevic, I.B.; Küppers, F., “WDM–TDM NG-PON Power Budget Extension by Utilizing SOA in the Remote Node,” IEEE Photonics Journal, vol.6, iss.2, doi: 10.1109/JPHOT.2014.2314108, April 2014.

[49] Chandru, B.; Rajini, J.H.; TamilSelvi, S., “Performance analysis of downstream transmission of 10Gbps WDM PON using single and hybrid optical amplifiers,” International Conference on Advanced Communication Control and Computing Technologies (ICACCCT), doi: 10.1109/ICACCCT.2014.7019208, May 2014.

[50] Latal, J.; Koudelka, P.; Siska, P.; Vitasek, J.; Vasinek, V., "WDM-PON network simulation with different implementation of optical amplifier in the line," Proc. SPIE 9193, Novel Optical Systems Design and Optimization XVII, doi:10.1117/12.2060112, September 2014.

[51] Mullerova, J.; Korcek, D.; Dado, M., "On wavelength blocking for XG-PON coexistence with GPON and WDM-PON networks," 14th International Conference on Transparent Optical Networks (ICTON), pp.1-4, doi: 10.1109/ICTON.2012.6253748, July 2012.

[52] Benedikovic, D.; Litvik, J.; Kuba, M.; Dado, M.; Dubovan, J., "Influence of nonlinear effects in WDM system with non-equidistant channel spacing using different types of high-order PSK and QAM modulation formats," Proc. SPIE 8429, Optical Modelling and Design II, doi: 10.1117/12.921836, June 2012.

[53] Markovic, G.Z., "Wavelength Converters Placement in Optical Networks Using Bee Colony Optimization," Advances in Electrical and Computer Engineering, vol.16, no.1, pp.3-10, doi: 10.4316/AECE.2016.01001, January 2016.

[54] Perecar, F.; Marcinka, O.; Bednarek, L.; Lucki, M.; Liner, A.; Hajek, L.; Papes, M.; Jaros, J.; Vasinek, V., "The impacts of ageing effects due to radiation burden on optical fiber couplers," Proc. SPIE 9586, Photonic Fiber and Crystal Devices: Advances in Materials and Innovations in Device Applications IX, doi: 10.1117/12.2187517, August 2015.

[55] Grobe, K.; Elbers, J.P., "PON Evolution from TDMA to WDM-PON," Conference on Optical Fiber communication/National Fiber Optic Engineers (OFC/NFOEC). pp.1-7, 24-28, doi: 10.1109/OFC.2008.4528293, February 2008.

[56] Wong, E.; "Next-Generation Broadband Access Networks and Technologies," in Journal of Lightwave Technology, vol.30, iss.4, pp.597-608, doi: 10.1109/JLT.2011.2177960, February 2012.

[57] Segarra, J.; Sales, V.; Polo, V.; Prat, J., "Dimensioning OLT Architectures for UDWDM-PONs Employing Coherent Transceivers," 17th International Conference on Transparent Optical Networks (ICTON), pp.1-6, doi: 10.1109/ICTON.2015.7193367, August 2015.

[58] Prat, J.; Cano, I.; Presi, M.; Tomkos, I.; Klonidis, D.; Vall-llosera, G.; Brenot, R.; Pous, R.; Papastergiou, G.; Rafel, A.; Ciaramella, E., "Technologies for Cost-Effective udWDM-PONs," Journal of Lightwave Technology, vol.34, no.2, pp.783-791, doi: 10.1109/JLT.2015.2499381, January 2016.

[59] Burtscher, C.; Seyringer, D., "Influence of waveguide structure on Y-branch splitting ratio," in Proc. SPIE 9133, Silicon Photonics and Photonic Integrated Circuits IV, doi: 10.1117/12.2050846, May 2014.

[60] Shahpari, A.; Ziaie, S.; Reis, J.D.; Vujicic, Z.; Lima, M.; Teixeira, A., "Impact of

splitter configuration strategies on power consumption in PON," in OptoElectronics and Communications Conference held jointly with International Conference on Photonics in Switching (OECC/PS), pp.1-2., July 2013.

[61] Rentao, G.; Xiaoxu, L.; Hui, L.; Lin, B., "Evolutional algorithm based cascade long reach passive optical networks planning," in China Communications, vol.10, iss.4, pp.59-69, doi: 10.1109/CC.2013.6506931, April 2013.

[62] Zukowski, C.; Payne, D.B.; Ruffini, M., "Optical splitters configuration for long-reach passive optical network deployment," 18th European Conference on Network and Optical Communications (NOC) and 8th Conference on Optical Cabling and Infrastructure (OC&i), pp.185-190, doi: 10.1109/NOC-OCI.2013.6582888, July 2013.

[63] Pal, S.; Zukowski, C.; Nag, A.; Payne, D.B.; Ruffini, M., "Cable length minimisation in long-reach-PON planning for sparsely populated areas," International Conference on Optical Network Design and Modelling, pp.234-239, May 2014.

[64] Raghuwanshi, S.K.; Kumar, V.; Chack, D.; Kumar, S., "Propagation Study of Y-Junction Optical Splitter Using BPM," International Conference on Communication Systems and Network Technologies (CSNT), pp.625-629, doi: 10.1109/CSNT.2012.140, May 2012.

[65] Piehler, D., "Long-reach and High Split Ratio Passive Optical Networks," Asia Optical Fiber Communication and Optoelectronic Exposition and Conference, doi: 10.1364/AOE.2008.FF3, November 20098.

[66] Li, C.; Li, X.; Qiu, X.; Xi, Y., "A Novel Planar Waveguide Super-Multiple-Channel Optical Power Splitter," Journal of Lightwave Technology, vol.33, no.24, pp.5019-5024, doi: 10.1109/JLT.2015.2497719, November 2015.

[67] Wang, L.; An, J.; Wu, Y.; Zhang, J.; Wang, Y.; Li, J.; Wang, H.; Zhang, X.; Pan, P.; Zhong, F.; Zha, Q.; Hu, X.; Zhao, D., "Design and Fabrication of Novel Symmetric Low-Loss 1 × 24 Optical Power Splitter," Journal of Lightwave Technology, vol.32, no.18, pp.3112-3118,doi: 10.1109/JLT.2014.2337301,July 2014.

[68] Shuchang, Y.; Songnian, F.; Hantao, W.; Ming, T.; Shum, P.; Deming, L., "Performance comparison for NRZ, RZ, and CSRZ modulation formats in RS-DBS Nyquist WDM system," Journal of Optical Communications and Networking (IEEE/OSA), vol.6, no.4, pp.355-361, April 2014.

[69] Winzer, P.J., "High-Spectral-Efficiency Optical Modulation Formats," Journal of Lightwave Technology, vol.30, no.24, pp.3824-3835, December 2012.

[70] Da Silveira, C.R.; De Lacerda Rocha, M.; Romero, M.A.; Pataca, D.M., "Performance

analysis of modulation formats for 40 Gb/s optical transmission," 2nd National Conference on Telecommunications (CONATEL), pp.1-5, doi: 10.1109/CONATEL.2011.5958670, May 2011.

[71] Hui, R.; Zhang, S.; Zhu, B.; Huang, R.; Allen, C.; Demarest, D., “Advanced Optical Modulation Formats and Their Comparison in Fiber-Optic Systems,” Sprint, January 2004.

[72] Winzer, P.J.; Essiambre, R.-J., "Advanced Modulation Formats for High-Capacity Optical Transport Networks," Journal of Lightwave Technology, vol.24, no.12, pp.4711-4728, December 2006.

[73] Benedikovic, D.; Litvik, J.; Dado, M., "Modelling of single-channel optical transmission systems with high-order ASK and PSK modulation formats," ELEKTRO, pp.22-25, May 2012.

[74] Lach, E.; Idler W., “Modulation formats for 100G and beyond,” Optical Fiber Technology 17, pp.377-386, August 2011.

[75] Tan, A.; Pincemin, E., "Performance Comparison of Duobinary Formats for 40-Gb/s and Mixed 10/40-Gb/s Long-Haul WDM Transmission on SSMF and LEAF Fibers," Journal of Lightwave Technology, vol.27, no.4, pp.396-408, February 2009.

[76] Ip, E.; Lau, A.; Barros, D.; Kahn, J., “Coherent detection in optical fiber systems,” Optics Express vol.16, iss.2, pp.753-791, January 2008.

[77] Winzer, P.J.; Essiambre, R., "Advanced Optical Modulation Formats," Proceedings of the IEEE, vol.94, no.5, pp.952-985, doi: 10.1109/JPROC.2006.873438, May 2006.

[78] Cai, J.-X.; Davidson, C.R.; Foursa, D.G.; Liu, L.; Cai, Y.; Bakhshi, B.; Mohs, G.; Patterson, W.W.; Corbett, P.C.; Lucero, A.J.; Anderson, W.; Li, H.; Nissov, M.; Pilipetskii, A.N.; Bergano, Neal S., "Experimental comparison of the RZ-DPSK and NRZ-DPSK modulation formats," Optical Fiber Communication Conference (OFC/NFOEC), vol.4, doi: 10.1109/OFC.2005.192982, March 2005.

[79] Latal, J.; Vitasek, J.; Koudelka, P.; Siska, P.; Poboril, R.; Hajek, L.; Vanderka, A.; Vasinek, V., "Simulation of modulation formats for optical access network based on WDM-PON," 16th International Conference on Transparent Optical Networks (ICTON), doi: 10.1109/ICTON.2014.6876473, July 2014.

[80] Hoon, K.; Essiambre, R., "Transmission of 8 x 20 Gb/s DQPSK signals over 310-km SMF with 0.8-b/s/Hz spectral efficiency," IEEE Photonics Technology Letters, vol.15, iss.5, pp.769-771, doi: 10.1109/LPT.2003.809983, May 2003.

[81] Bruno, G.; Mongiardini, E.; Riccardi, E.; Rossaro, A., "40 Gb/s upgrade of a 1614 km

link over TrueWave-RS fiber with live 10G OOK traffic," Optical Fiber Communication Conference and Exposition and the National Fiber Optic Engineers Conference(OFC/NFOEC), March 2011.

[82] Poboril, R.; Latal, J.; Koudelka, P.; Vitasek, J.; Siska, P.; Skapa, J.; Vasinek, V., “A Concept of a Hybrid WDM/TDM Topology Using the Fabry-Perot Laser in the Optiwave Simulation Environment,” Advances in Electrical and Electronic Engineering, vol.9, iss.4, pp.167-178, doi: 10.15598/aeee.v9i4.537, December 2011.

[83] Shinada, S.; Furukawa, H.; Wada, N., "Field demonstration of DWDM/NRZ-DQPSK optical packet switching and buffering," 16th Opto-Electronics and Communications Conference (OECC), pp.780-781, July 2011.

[84] Ket-Urai, V.; Maneekut, R.; Kaewplung, P., "Feasibility of 40-Gbps RZ-DQPSK signal transmission over PON," 17th Opto-Electronics and Communications Conference (OECC), pp.319-320, doi: 10.1109/OECC.2012.6276705, July 2012.

[85] Dong, W.; Dan, L.; Caiyun, L.; Li, H.; Wenke, Y., "Performance comparison of phase modulated formats in 160 Gb/s transmission system," Communications and Photonics Conference and Exhibition, ACP Asia, doi: 10.1117/12.904334, November 2011.

[86] Ghoniemy, S.; George, K.F.; MacEachern, L., "Performance Evaluation and Enhancements of 42.7 Gb/s DWDM Transmission System Using Different Modulation Formats," Communication Networks and Services Research Conference (CNSR), pp.189-194, doi: 10.1109/CNSR.2011.35, May 2011.

[87] Linghao, Ch.; Zhaohui, L.; Yanfu, Y.; Chao, L.; Yuanyuan, F.; Hua, J.; Xiaogeng, X.; Qianjin, X.; Shengqian, Zh.; Zheng, Ch.; Tam, H.Y.; Wai, P.K.A., "8×200-Gbit/s polarization-division multiplexed CS-RZ-DQPSK transmission over 1200 km of SSMF," 14th OptoElectronics and Communications Conference (OECC), doi: 10.1109/OECC.2009.5215659, August 2009.

[88] Raybon, G.; Randel, S.; Adamiecki, A.; Winzer, P.J.; Salamanca, L.; Urbanke, R.; Chandrasekhar, S.; Konczykowska, A.; Jorge, F.; Dupuy, J.; Buhl, L.L.; Draving, S.; Grove, M.; Rush, K., "1-Tb/s dual-carrier 80-GBaud PDM-16QAM WDM transmission at 5.2 b/s/Hz over 3200 km," IEEE Photonics Conference (IPC), doi: 10.1109/IPCon.2012.6359319, September 2012.

[89] Morichetti, F.; Canciamilla, A.; Ferrari, C.; Torregiani, M.; Ferrario, M.; Siano, R.; Boffi, P.; Marazzi, L.; Martelli, P.; Parolari, P.; Martinelli, M.; Samarelli, A.; Sorel, M.; De La Rue, R.M.; O'Faolain, L.; Beggs, D.M.; Krauss, T.F.; Melloni, A., "Controlling the delay of 100 Gb/s polarization division multiplexed signals through

silicon photonics delay lines," 36th European Conference and Exhibition on Optical Communication (ECOC), doi: 10.1109/ECOC.2010.5621202, Sept. 2010.

[90] Randel, S.; Ryf, R.; Sierra, A.; Winzer, P.; Gnauck, A.; Bolle, C.; Essiambre, R.; Peckham, D.; McCurdy, A.; Lingle, R., "6×56-Gb/s mode-division multiplexed transmission over 33-km few-mode fiber enabled by 6×6 MIMO equalization," Optics Express, vol.19, iss.17, pp.16697-16707, August 2011.

[91] Shieh, W.; Yang, Q.; Ma, Y.,"107 Gb/s coherent optical OFDM transmission over 1000-km SSMF fiber using orthogonal band multiplexing," Optics Express, vol.16, iss.9, pp.6378-6386, April 2008.

[92] Ma, Y.; Yang, Q.; Tang, Y.; Chen, S.; Shieh, W., "1-Tb/s Single-Channel Coherent Optical OFDM Transmission With Orthogonal-Band Multiplexing and Subwavelength Bandwidth Access," Journal of Lightwave Technology, vol.28, iss.4, pp.308-315, doi: 10.1109/JLT.2009.2030517, February 2010.

[93] Yang, Q.; Ma, Y.; Shieh, W., "1 Tbit/s single-channel coherent optical OFDM transmission with trellis-coded modulation," Electronics Letters, vol.45, iss.20, pp.1045-1047, doi: 10.1049/el.2009.1123, September 2009.

[94] Sotiropoulos, N.; Koonen, T.; De Waardt, H., "D8PSK/OOK bidirectional transmission over a TDM-PON," 14th International Conference on Transparent Optical Networks (ICTON), doi: 10.1109/ICTON.2012.6253937, July 2012.

[95] Xia, T.J.; Gringeri, S.; Tomizawa, M., "High-capacity optical transport networks," IEEE Communications Magazine, vol.50, iss.11, pp.170-178, doi: 10.1109/MCOM.2012.6353698, November 2012.

[96] Kim, K.; Chung, H.S.; Chang, S.H.; Lee, J.Ch.; Lee, J.H., "Field trial of direct-detection and multi-carrier based 100G transceiver," Optical Fiber Communications Conference and Exhibition (OFC), doi: 10.1364/OFC.2014.Tu2B.5, March 2014.

[97] Renaudier, J.; Bertran-Pardo, O.; Charlet, G.; Salsi, M.; Mardoyan, H.; Tran, P.; Bigo, S., "8 Tb/s long haul transmission over low dispersion fibers using 100 Gb/s PDM-QPSK channels paired with coherent detection," Bell Labs Technical Journal, vol.14, iss.4, pp.27-45, doi: 10.1002/bltj.20402, Winter 2010.

[98] Zhu, B.; Peckham, D.W.; Jiang, X.; Lingle, R., "System performance of Long-Haul 112-Gb/s PDM-QPSK DWDM transmission over large-area fiber and SSMF spans," 39th European Conference and Exhibition on Optical Communication (ECOC 2013), doi: 10.1049/cp.2013.1625, September 2013.

[99] Fischer, J.K.; Nolle, M.; Molle, L.; Schmidtlanghorst, C.; Hilt, J.; Ludwig, R.;

Schubert, C., "Beyond 100G - high-capacity transport technologies for next generation optical core networks," Future Network & Mobile Summit (FutureNetw), July 2012.

[100] Karaki, J.; Pincemin, E.; Grot, D.; Guillossou, T.; Jaouen, Y.; Le Bidan, R.; Le Gall, T., "Dual-polarization multi-band OFDM versus single-carrier DP-QPSK for 100 Gbps long-haul WDM transmission over legacy infrastructure," 38th European Conference and Exhibition on Optical Communications (ECOC), doi: 10.1364/ECEOC.2012.P4.17, September 2012.

[101] Xia, T.J.; Wellbrock, G.A.; Ming-Fang Huang; Shaoliang Zhang; Yue-Kai Huang; Do-il Chang; Burtsev, S.; Pelouch, W.; Zak, E.; de Pedro, H.; Szeto, W.; Fevrier, H., "Transmission of 400G PM-16QAM channels over long-haul distance with commercial all-distributed Raman amplification system and aged standard SMF in field," Optical Fiber Communications Conference and Exhibition (OFC), doi: 10.1364/OFC.2014.Tu2B.1, March 2014.

[102] Zhou, X.; Nelson, L.E.; Magill, P.; Isaac, R.; Benyuan, Zh.; Peckham, D.W.; Borel, P.I.; Carlson, K., "High Spectral Efficiency 400 Gb/s Transmission Using PDM Time-Domain Hybrid 32–64 QAM and Training-Assisted Carrier Recovery," Journal of Lightwave Technology, vol.31, iss.7, pp.999-1005, doi: 10.1109/JLT.2013.2243643, April 2013.

[103] Downie, J.D.; Hurley, J.; Pikula, D., "Transmission of 256 Gb/s PM-16QAM and 128 Gb/s PM-QPSK signals over long-haul and submarine systems with span lengths greater than 100 km," 39th European Conference and Exhibition on Optical Communication (ECOC), doi: 10.1049/cp.2013.1345, September 2013.

[104] Singer, A.C.; Shanbhag, N.R.; Bae, H.M., “Electronic Dispersion Compensation, An overview of optical communications systems,” IEEE Signal Processing Magazine, vol.25, iss.6, pp.110-130, doi: 10.1109/MSP.2008.929230, November 2008.

[105] Shetty, K.K., “A Novel Algorithm for Uplink Interference Suppression Using Smart Antennas in Mobile Communications,” Chapter 6, available from: <http://purl.flvc.org/fsu/fd/FSU_migr_etd-1758>, April 2004.

[106] Johnson, D. “Minimum Mean Squared Error Estimators,” Connexion, November 2004.

[107] Chandramouli, S.; Bien, F.; Kim, H.; Scholz, Ch.; Gebara, E.; Laskar, J., “10-Gb/s Optical Fiber Transmission Using a Fully Analog Electronic Dispersion Compensator (EDC) With Unclocked Decision-Feedback Equalization,” IEEE Transactions on microwave theory and techniques, vol.55, iss.12, pp.2740-2746, doi:

10.1109/TMTT.2007.908546, December 2007.

[108] Bulzacchelli, J.F.; Meghelli, M.; Rylov, S.; Rhee V.W.; Rylyakov, A.V.; Ainspan H.A.; Parker, B.D.; Beakes, M.P.; Chung, A.; Beukema, T.J.; Pepeljugoski, P.K.; Shan, L.; Kwark, Y.H.; Gowda, S.; Friedman, D.J. "A 10-Gb/s 5-tap DFE/4-tap FFE transceiver in 90-nm CMOS technology," IEEE Journal of Solid-State Circuits, vol.41, iss.12, pp.2885-2900, doi: 10.1109/JSSC.2006.884342,December 2006.

[109] Yu, Q., "Electronic Data Processing for Error and Dispersion Compensation," Journal of Lightwave Technology, vol.24, iss.12, pp.4514-4525, doi: 10.1109/JLT.2006.886065, December 2006.

[110] Winters, J.H.; Gitlin R.D. "Electrical Signal Processing Techniques in Long-Haul Fiber-Optic Systems," IEEE Transactions on Communications, vol.38, iss.9, pp.1439-1453, doi: 10.1109/26.61385, September 1990.

[111] Bahl, L.; Cocke, J.; Jelinek, F.; Raviv, J., "Optimal Decoding of Linear Codes for minimizing symbol error rate," IEEE Transactions on Information Theory, vol.20, iss.2, pp.284-287, doi: 10.1109/TIT.1974.1055186, March 1974.

[112] Volterra, V., "Theory of Functionals and of Integrals and Integro-Differential Equations", New York: Dover Publications, 1959.

[113] Lu, L.; Lei, J.; Luo, X.; Bing, L., "Electronic Dispersion Compensation for High Speed Long Haul Transmission with DQPSK Modulation," Proceeding of SPIE, vol.7516, doi: 10.1117/12.843355,August 2009.

[114] Zhu, X.; Kumar, Sh.; Raghavan, S.; Mauro Y.; Lobanov, S., "Nonlinear Electronic Dispersion Compensation Techniques for Fiber-Optic Communication Systems," Optical Fiber communication/National Fiber Optic Engineers Conference (OFC/NFOEC), doi: 10.1109/OFC.2008.4528211, May 2008.

[115] Killey, R., "Dispersion and Nonlinearity Compensation using Electronic Predistortion Techniques," IEE Seminar on Optical Fiber Communications and Electronic Signal Processing, December 2005.

[116] Weber, Ch.; Fischer, J.K.; Bunge, Ch.A.; Petermann K., "Electronic Precompensation of Intrachannel Nonlinearities at 40 Gb/s," IEEE Photonics Technology Letters, vol.18, iss.16, pp.1759-1761, doi: 10.1109/LPT.2006.879945,August 2006.

[117] Watts, P.M.; Mikhailov, V.; Glick, M.; Bayvel, P.; Killey R.I., "Single Sideband Optical Signal Generation and Chromatic Dispersion Compensation using Digital Filters," Electronics Letters, vol.40, iss.15, doi: 10.1049/el:20045225, July 2004.

[118] RSOFT Design Group, "OptSim Application Notes and Examples", "OptSim User

Guide", "OptSim models reference", software manuals, 2010.

[119] Zhu, Y.; Plant, D.V., "Optimal Design of Dispersion Filter for Time-Domain Split-Step Simulation of Pulse Propagation in Optical Fiber," Journal of Lightwave Technology, vol. 30, iss.10, pp.1405-1421, doi: 10.1109/JLT.2012.2187172, May 2012.

[120] Freude, W.; Schmogrow, R.; Nebendahl, B.; Winter, M.; Josten, A.; Hillerkuss, D.; Koenig, S.; Meyer, J.; Dreschmann, M.; Huebner, M.; Koos, C.; Becker, J.; Leuthold, J., "Quality metrics for optical signals: Eye diagram, Q-factor, OSNR, EVM and BER," 14th International Conference on Transparent Optical Networks (ICTON), doi: 10.1109/ICTON.2012.6254380, July 2012.

[121] Nebendahl, B.; Schmogrow, R.; Dennis, T.; Josten, A.; Hillerkuss, D.; Koenig, S.; Meyer, J.; Dreschmann, M.; Winter, M.; Huebner, M.; Freude, W.; KOOS, C.; Leuthold, J., "Quality Metrics in optical modulation analysis: EVM and its relation to Q-factor, OSNR, and BER," Communications and Photonics Conference (ACP), November 2012.

[122] Sackinger, E., "Broadband circuits for optical fiber communication," Hoboken: John Wiley & Sons Inc, May 2005.

[123] Bohac, L.; Lucki, M. "Optické komunikační systémy", ISBN: 978-8001-04484-1, 2010.

[124] Novotny, K.;Martan, T.; Sistek, J., "Systémy pro optické komunikace", ISBN: 80-01-02810-0, 2003.

[125] Kohler, L., "Study of the optical properties of passive optical splitters based on MMI and Y-branch approach", Master Thesis, Vorarlberg University of Applied Science, Austria, 2012.

[126] Burtscher, C.; Seyringer, D.; Uherek, F.; Chovan, J.; Kuzma, A., "Design of low loss 1x64 Y-branch splitter having symmetric splitting ratio and small footprint," 10th International Conference on Advanced Semiconductor Devices & Microsystems (ASDAM), doi: 10.1109/ASDAM.2014.6998686, October 2014.

[127] Burtscher, C.; Seyringer, D., "Influence of waveguide structure on Y-branch splitting ratio," Proc. SPIE 9133, Silicon Photonics and Photonic Integrated Circuits IV, doi: 10.1117/12.2050846, May 2014.

[128] Laperle, C.; Villeneuve, B.; Zhang, Zh.; McGhan, D.; Sun, H.; O'Sullivan, M., "WDM Performance and PMD Tolerance of a Coherent 40-Gbit/s Dual-Polarization QPSK Transceiver," Journal of Lightwave Technology, vol.26, no.1, pp.168-175, doi: 10.1109/JLT.2007.913071,January 2008.